An integrative taxonomic revision of Slug-eating Snakes (Squamata: Pareidae: Pareineae) reveals unprecedented diversity in Indochina

Nikolay A Poyarkov [Corresp., 1, 2] , **Tan Van Nguyen** [3] , **Parinya Pawangkhanant** [4] , **Platon V. Yushchenko** [2] , **Peter Brakels** [5] , **Linh Hoang Nguyen** [6] , **Hung Ngoc Nguyen** [6] , **Chatmongkon Suwannapoom** [4] , **Nikolai Orlov** [7] , **Gernot Vogel** [8]

[1] Laboratory of Tropical Ecology, Joint Russian-Vietnamese Tropical Research and Technological Center, Hanoi, Hanoi, Vietnam

[2] Faculty of Biology, Department of Vertebrate Zoology, Moscow State University, Moscow, Moscow, Russia

[3] Department of Species Conservation, Save Vietnam's Wildlife, Ninh Binh, Ninh Binh, Vietnam

[4] Division of Fishery, School of Agriculture and Natural Resources, University of Phayao, Phayao, Phayao, Thailand

[5] IUCN Laos PDR, Vientiane, Vientiane, Lao PDR

[6] Department of Zoology, Southern Institute of Ecology, Vietnam Academy of Science and Technology, Ho Chi Minh City, Ho Chi Minh City, Vietnam

[7] Department of Herpetology, Zoological Institute, Russian Academy of Sciences, St. Petersburg, St. Petersburg, Russia

[8] Society for Southeast Asian Herpetology, Heidelberg, Germany

Corresponding Author: Nikolay A Poyarkov
Email address: n.poyarkov@gmail.com

Slug-eating snakes of the subfamily Pareinae are an insufficiently studied group of snakes specialized in feeding on terrestrial mollusks. Currently Pareinae encompass three genera with 34 species distributed across the Oriental biogeographic region. Despite the recent significant progress in understanding of Pareinae diversity, the subfamily remains taxonomically challenging. Here we present an updated phylogeny of the subfamily with a comprehensive taxon sampling including 30 currently recognized Pareinae species and several previously unknown candidate species and lineages. Phylogenetic analyses of mtDNA and nuDNA data supported the monophyly of the three genera *Asthenodipsas*, *Aplopeltura*, and *Pareas*. Within both *Asthenodipsas* and *Pareas* our analyses recovered deep differentiation with each genus being represented by two morphologically diagnosable clades, which we treat as subgenera. We further apply an integrative taxonomic approach, including analyses of molecular and morphological data, along with examination of available type materials, to address the longstanding taxonomic questions of the subgenus *Pareas*, and reveal the high level of hidden diversity of these snakes in Indochina. We restrict the distribution of *P. carinatus* to southern Southeast Asia, and recognize two subspecies within it, including one new subspecies proposed for the populations from Thailand and Myanmar. We further revalidate *P. berdmorei*, synonymize *P. menglaensis* with *P. berdmorei*, and recognize three subspecies within this taxon, including the new subspecies erected for the populations from Laos and Vietnam.

Furthermore, we describe two new species of *Pareas* from Vietnam: one belonging to the *P. carinatus* group from southern Vietnam, and a new member of the *P. nuchalis* group from the central Vietnam. We provide new data on *P. temporalis*, and report on a significant range extension for *P. nuchalis*. Our phylogeny, along with molecular clock and ancestral area analyses, reveal a complex diversification pattern of Pareinae involving a high degree of sympatry of widespread and endemic species. Our analyses support the "upstream" colonization hypothesis and, thus, the Pareinae appears to have originated in Sundaland during the middle Eocene and then colonized mainland Asia in early Oligocene. Sundaland and Eastern Indochina appear to have played the key roles as the centers of Pareinae diversification. Our results reveal that both vicariance and dispersal are responsible for current distribution patterns of Pareinae, with tectonic movements, orogeny and paleoclimatic shifts being the probable drivers of diversification. Our study brings the total number of Pareidae species to 41 and further highlights the importance of comprehensive taxonomic revisions not only for the better understanding of biodiversity and its evolution, but also for the elaboration of adequate conservation actions.

1 **An integrative taxonomic revision of Slug-eating Snakes (Squamata: Pareidae: Pareineae)**
2 **reveals unprecedented diversity in Indochina**

4 **Nikolay A. Poyarkov[1,2,*], Tan Van Nguyen[3], Parinya Pawangkhanant[4], Platon V.**
5 **Yushchenko[1], Peter Brakels[5], Linh Hoang Nguyen[6], Hung Ngoc Nguyen[6], Chatmongkon**
6 **Suwannapoom[4], Nikolai Orlov[7], Gernot Vogel[8]**

8 *[1] Faculty of Biology, Department of Vertebrate Zoology, Moscow State University,*
9 *Moscow, Moscow, Russia*
10 *[2] Laboratory of Tropical Ecology, Joint Russian-Vietnamese Tropical Research and*
11 *Technological Center, Hanoi, Hanoi, Vietnam*
12 *[3] Department of Species Conservation, Save Vietnam's Wildlife, Ninh Binh, Ninh Binh,*
13 *Vietnam*
14 *[4] Division of Fishery, School of Agriculture and Natural Resources, University of Phayao,*
15 *Phayao, Phayao, Thailand*
16 *[5] IUCN Laos PDR, Vientiane, Vientiane, Lao PDR*
17 *[6] Department of Zoology, Southern Institute of Ecology, Vietnam Academy of Science and*
18 *Technology, Ho Chi Minh City, Ho Chi Minh City, Vietnam*
19 *[7] Department of Herpetology, Zoological Institute, Russian Academy of Sciences, St.*
20 *Petersburg, St. Petersburg, Russia*
21 *[8] Society for Southeast Asian Herpetology, Heidelberg, Germany*
22 ** Corresponding author: Nikolay A. Poyarkov: n.poyarkov@gmail.com.*

24 **ABSTRACT**

26   Slug-eating snakes of the subfamily Pareinae are an insufficiently studied group of snakes
27 specialized in feeding on terrestrial mollusks. Currently Pareinae encompass three genera with 34
28 species distributed across the Oriental biogeographic region. Despite the recent significant
29 progress in understanding of Pareinae diversity, the subfamily remains taxonomically
30 challenging. Here we present an updated phylogeny of the subfamily with a comprehensive taxon
31 sampling including 30 currently recognized Pareinae species and several previously unknown

32 candidate species and lineages. Phylogenetic analyses of mtDNA and nuDNA data supported the

33 monophyly of the three genera *Asthenodipsas*, *Aplopeltura*, and *Pareas*. Within both

34 *Asthenodipsas* and *Pareas* our analyses recovered deep differentiation with each genus being

35 represented by two morphologically diagnosable clades, which we treat as subgenera. We further

36 apply an integrative taxonomic approach, including analyses of molecular and morphological

37 data, along with examination of available type materials, to address the longstanding taxonomic

38 questions of the subgenus *Pareas*, and reveal the high level of hidden diversity of these snakes in

39 Indochina. We restrict the distribution of *P. carinatus* to southern Southeast Asia, and recognize

40 two subspecies within it, including one new subspecies proposed for the populations from

41 Thailand and Myanmar. We further revalidate *P. berdmorei*, synonymize *P. menglaensis* with *P.*

42 *berdmorei*, and recognize three subspecies within this taxon, including the new subspecies

43 erected for the populations from Laos and Vietnam. Furthermore, we describe two new species

44 of *Pareas* from Vietnam: one belonging to the *P. carinatus* group from southern Vietnam, and a

45 new member of the *P. nuchalis* group from the central Vietnam. We provide new data on *P.*

46 *temporalis*, and report on a significant range extension for *P. nuchalis*. Our phylogeny, along

47 with molecular clock and ancestral area analyses, reveal a complex diversification pattern of

48 Pareinae involving a high degree of sympatry of widespread and endemic species. Our analyses

49 support the "upstream" colonization hypothesis and, thus, the Pareinae appears to have originated

50 in Sundaland during the middle Eocene and then colonized mainland Asia in early Oligocene.

51 Sundaland and Eastern Indochina appear to have played the key roles as the centers of Pareinae

52 diversification. Our results reveal that both vicariance and dispersal are responsible for current

53 distribution patterns of Pareinae, with tectonic movements, orogeny and paleoclimatic shifts

54 being the probable drivers of diversification. Our study brings the total number of Pareidae

55 species to 41 and further highlights the importance of comprehensive taxonomic revisions not

56 only for the better understanding of biodiversity and its evolution, but also for the elaboration of

57 adequate conservation actions.

59 **Subjects**: Biodiversity, Biogeography, Evolutionary Studies, Taxonomy, Zoology

61 **Keywords:** *Pareas*, *Asthenodipsas*, *Aplopeltura*, *Eberhardtia*, *Spondylodipsas*, molecular

62 phylogeny, biogeography, Southeast Asia, Sundaland, cryptic species

INTRODUCTION

66   The snakes of the family Pareidae Romer, 1956 (Squamata, Serpentes) currently (as of

67 December 1st, 2021) encompassing 39 species inhabiting the Oriental biogeographic region are

68 divided into two subfamilies: Pareinae Romer, 1956 in Southeast Asia and Xylophiinae Deepak,

69 Ruane & Gower, 2019 in southern India (*Deepak et al., 2019*; *Uetz, Freed & Hošek, 2021*). Slug-

70 eating snakes (or snail-eating snakes) of the subfamily Pareinae are widely distributed throughout

71 the tropical and subtropical areas of Southeast and East Asia. Its members are mainly small-

72 sized, arboreal, nocturnal snakes, and are regarded as dietary specialists of terrestrial pulmonates

73 i.e., slugs and snails (*You, Poyarkov & Lin, 2015*; *Cundall & Greene, 2000*). Snail-eating species

74 of Pareinae are unique among terrestrial vertebrates in having asymmetric lower jaws, with more

75 teeth on the right mandible than on the left (*Hoso et al., 2007*, *2010*). Due to the specialized

76 feeding habit and foraging behaviour, the evolutionary biology of *Pareas* has received much

77 attention in recent years (*Götz, 2002*; *Hoso & Hori, 2006, 2008*; *Hoso, 2007*; *Hoso et al., 2007,*

78 *2010*; *You, Poyarkov & Lin, 2015*; *Danaisawadi et al., 2015, 2016*; *Kojima et al., 2020*; *Chang et*

79 *al., 2021*).

80   The subfamily Pareinae had a turbulent taxonomic history (*David & Vogel, 1996*; *Rao &*

81 *Yang, 1992*) with recent works (*Grossmann & Tillack, 2003*; *Guo et al., 2011*; *Ding et al., 2020*;

82 *Vogel et al., 2020, 2021*) recognizing three genera: *Pareas* Wagler, 1830 with 24 species (type

83 species: *Pareas carinatus* Wagler, 1830); *Asthenodipsas* Peters, 1864 with nine species (type

84 species: *Asthenodipsas malaccana* [Peters, 1864]), and a monotypic genus *Aplopeltura* Duméril,

85 1853 (type species: *Aplopeltura boa* [Boie, 1828]). Two genus-level nomens, namely

86 *Eberhardtia* Angel, 1920 (type species: *Eberhardtia tonkinensis* Angel, 1920, regarded as a

87 synonym of *Pareas formosensis* [Van Denburgh, 1909] by *Ding et al., 2020*) and *Internatus*

88 Yang & Rao, 1992 (type species: *Asthenodipsas leavis* [Boie, 1827]) are presently considered

89 junior synonyms of the genera *Pareas* and *Asthenodipsas*, respectively (see *Grosmann & Tillack,*

90 *2003*; *Wallach, Williams & Boundi, 2014*; *Ding et al., 2020*; *Vogel et al., 2020, 2021*). Several

91 recent phylogenetic studies suggested that the genus *Pareas* consists of two highly divergent

92 major clades and is paraphyletic with respect to *Aplopeltura* or *Asthenodipsas* (*Guo et al., 2011*;

93 *Pyron et al., 2011*; *Wang et al., 2020*). At the same time, other multilocus studies recovered

94   *Pareas* as a monophyletic group though with moderate or low node support values, and

95   suggested the genus *Aplopeltura* as its sister taxon (*Pyron, Burbrink & Wiens, 2013*; *You,*

96   *Poyarkov & Lin, 2015*; *Figueroa et al., 2016*; *Deepak et al., 2019*; *Zaher et al., 2019*). The genus

97   *Asthenodipsas* was also shown to include two major lineages (*Loredo et al., 2013*; *Figueroa et*

98   *al., 2016*; *Deepak et al., 2019*; *Wang et al., 2020*), though its monophyly got only moderate

99   support based on the concatenated analysis of mitochondrial and nuclear DNA markers (*Wang et*

100   *al., 2020*; *Ding et al., 2020*; *Vogel et al., 2021*). Therefore, despite the recent significant progress

101   in evolutionary studies on Pareinae, the phylogenetic relationship among the major genus-level

102   lineages of the subfamily still remain debated and unclear.

103   Several recent taxonomic studies have demonstrated that the species diversity of Pareinae

104   is still underestimated (e.g., *Vogel, 2015*; *Hauser, 2017*; *Quah et al., 2019, 2020, 2021*; *Le et al.,*

105   *2021*). The high degree of morphological similarity among closely related taxa of Pareinae often

106   makes species delineation in slug snakes quite challenging (*Guo & Deng, 2009*; *Vogel, 2015*;

107   *Yang et al., 2021*), suggesting that the molecular data represent an effective tool to help untangle

108   taxonomic controversies when morphological analyses yield inconsistent results (*You, Poyarkov*

109   *& Lin, 2015*; *Loredo et al., 2013*; *Vogel et al., 2020, 2021*; *Bhosale et al., 2020*; *Wang et al.,*

110   *2020*; *Ding et al., 2020*; *Liu & Rao, 2021*; *Yang et al., 2021*). Application of the integrative

111   taxonomic approach combining evidence from morphological and molecular data resulted in the

112   discovery of several previously unnoticed taxa and allowed to revise several species complexes,

113   including the *Pareas hamptoni* complex (*You, Poyarkov & Lin, 2015*; *Bhosale et al., 2020*; *Ding*

114   *et al., 2020*; *Liu & Rao, 2021*; *Yang et al., 2021*), the *P. margaritophorus* complex (*Vogel et al.,*

115   *2020*; *Suntrarachun et al., 2020*), and the *P. monticola* complex (*Vogel et al., 2021*).

116   On the other hand, the Keeled slug snake, *Pareas carinatus*, has received comparatively

117   little attention in most recent revisions. This species was originally described by *Wagler (1830)*

118   from Java, Indonesia, and was later reported to be widely distributed throughout Southeast Asia,

119   from southern China, southern Myanmar, Laos, south-western and eastern Cambodia, Vietnam,

120   Thailand, southwards to Peninsular Malaysia, and islands of Borneo, Sumatra, Java and Bali

121   (*Wallach, Williams & Boundi, 2014*). However, since geographic variation of this species has

122   never been examined across the different regions, its taxonomic status remained controversial

123   and a number of misidentifications were made in the past (e.g., see discussion in *Das, 2012,*

124   *2018*). Recently, *Wang et al.* (2020) demonstrated *P. nuchalis* (Boulenger, 1900) to be closely

125 related to *P. carinatus* complex, and divided the latter by describing *P. menglaensis* Wang, Che,

126 Liu, Li, Jin, Jiang, Shi & Guo, 2020, as a sister species of *P. carinatus* sensu stricto. However, in

127 this revision the authors did not examine type specimens of *P. carinatus*, and also have neglected

128 to re-evaluate the status of two available species names currently considered as junior synonyms

129 of *P. carinatus*: *Pareas berdmorei* Theobald, 1868, and *Amblycephalus carinatus unicolor*

130 Bourret, 1934 (see *Nguyen, Ho & Nguyen, 2009*; *Wallach, Williams & Boundi, 2014*; *Uetz,*

131 *Freed & Hošek, 2021*). The most recent addition to the taxonomy of the group is the discovery of

132 a new species from southern Vietnam – *P. temporalis*, which was suggested as a sister species to

133 *P. nuchalis* from Borneo (*Le et al., 2021*); the authors also provided the most complete

134 phylogeny for the genus *Pareas* published up to date, generally concordant with the earlier

135 results (*Wang et al., 2020*; *Vogel et al., 2021*). The taxonomic history of the *P. carinatus* – *P.*

136 *nuchalis* complex is summarized in Table 1. Overall, the taxonomic status of *P. carinatus*, its

137 synonyms, and *P. menglaensis* remains unclear pending an integrative study combining data on

138 molecular and morphological variation of this group throughout its range.

139   In the present study, we provide an updated phylogeny for the subfamily Pareinae based on

140 the analysis of mitochondrial and nuclear DNA markers, and re-assess the genus-level taxonomy

141 of the group. Based on an extensive sampling we also report on a previously unrecognized

142 diversity of the genus *Pareas* in Indochina. We examine name-bearing types and re-assess

143 taxonomy of the *P. carinatus* complex using an integrative taxonomic approach, combining

144 morphological and molecular data from the newly collected and older specimens preserved in

145 herpetological collections. We also provide an updated identification key for the members of the

146 subfamily Pareinae and species of the *P. carinatus* complex. Finally, we conduct a divergence

147 time estimation analysis for the subfamily Pareinae and discuss evolution and the historical

148 biogeography of this peculiar group of snakes.

150 **MATERIALS AND METHODS**

151

152   **Species concept**

153   In the present study, we follow the General Lineage Concept (GLC: *De Queiroz, 2007*)

154 which suggests that a species constitutes a population of organisms independently evolving from

155 other such populations owing to a lack of gene flow (*Barraclough et al., 2003*; *De Queiroz,*

156   *2007*). Numerous recent integrative taxonomic studies, rather than relying solely on traditional

157   taxonomic procedure increasingly, use a wide range of empirical data to delimit species

158   boundaries (reviewed in *Coyne & Orr, 1998*; *Knowles & Carstens, 2007*; *Fontaneto et al., 2007*).

159   We herein follow the framework of integrative taxonomy (*Padial et al., 2010*; *Vences et al.,*

160   *2013*) which relies on independent multiple lines of evidence to assess the taxonomic status of

161   the lineages. To infer species boundaries we use the DNA-based molecular phylogenies, while to

162   describe those boundaries we rely on univariate (ANOVA) and multivariate (PCA)

163   morphological analyses (e.g. *Okamiya et al., 2018*).

164

165   **Nomenclatural acts**

166   The electronic version of this article in Portable Document Format (PDF) will represent a

167   published work according to the International Commission on Zoological Nomenclature

168   (ICZN), and hence the new names contained in the electronic version are effectively published

169   under that Code from the electronic edition alone (see Articles 8.5–8.6 of the Code). This

170   published work and the nomenclatural acts it contains have been registered in ZooBank, the

171   online registration system for the ICZN. The ZooBank Life Science Identifiers (LSIDs) can be

172   resolved and the associated information can be viewed through any standard web browser by

173   appending the LSID to the prefix http://zoobank.org/.

174   The LSID for this publication is as follows: urn:lsid:zoobank.org:pub:192CDD83-E08C-

175   40B1-92EB-3DB2C3E63CFA. The online version of this work is archived and available from

176   the following digital repositories: PeerJ, PubMed Central and CLOCKSS.

177

178   **Taxon sampling**

179   We used tissues from the herpetological collections of Zoological Museum of Moscow

180   University (ZMMU; Moscow, Russia); **California Academy of Sciences Museum (CAS;**

181   **California, USA); Southern Institute of Ecology Zoological Collection (SIEZC; Ho Chi**

182   **Minh City, Vietnam);** School of Agriculture and Natural Resources, University of Phayao

183   (AUP; Phayao, Thailand); and National Museum of Natural Science (NMNS, Taichung, Taiwan)

184   (summarized in Supplementary Table S1 and Appendix I). For alcohol-preserved voucher

185   specimens stored in museum collections, we removed a small sub-sample of muscle, preserved it

186   in 96% ethanol, and stored samples at −70 °C. Altogether, we analyzed 48 tissue samples

187 representing 20 nominal taxa of the genus *Pareas*. Geographic location of sampled populations

188 of the members of the subgenus *Pareas* is presented in Fig. 1.

189   Permissions to conduct fieldwork and collect specimens were granted by the Department of

190 Forestry, Ministry of Agriculture and Rural Development of Vietnam (permit numbers

191 #547/TCLN-BTTN; #432/TCLN-BTTN; #822/TCLN-BTTN; #142/SNgV-VP; #1539/TCLN-

192 DDPH, #1700/UBND.VX); the Forest Protection Departments of the Peoples' Committees of

193 Gia Lai Province (permit numbers #530/UBND-NC; #1951/UBND-NV), Phu Yen Province

194 (permit number #05/UBND-KT); Phu Tho Province (permit number #2394/UBND-TH3); Thanh

195 Hoa Province (permit number #3532/UBND-THKH); and Quang Nam Province (permit number

196 #308/SNgV-LS), Vietnam; by the Biotechnology and Ecology Institute Ministry of Science and

197 Technology, Lao PDR (permit no. 299); and by the Institute of Animals for Scientific Purpose

198 Development (IAD), Bangkok, Thailand (permit numbers U1-01205-2558 and UP-AE59-01-04-

199 0022). Specimen collection protocols and animal operations followed the Institutional Ethical

200 Committee of Animal Experimentation of University of Phayao (permit number 610104022).

201

202   **DNA isolation, PCR, and sequencing**

203   To infer the phylogenetic relationships among the Pareinae we obtained partial sequence

204 data of cytochrome *b* (cyt *b*) and NADH dehydrogenase subunit 4 (*ND4*) mtDNA genes, as well

205 as two nuclear genes: oocyte maturation factor mos (*c-mos*) and recombination activating gene 1

206 (*RAG1*). These genetic markers have been widely applied in studies of Pareidae diversity and

207 phylogenetic relationships (e.g., *Guo et al., 2011*; *You, Poyarkov & Lin, 2015*; *Deepak et al.,*

208 *2019*; *Wang et al., 2020*; *Vogel et al., 2020, 2021*; *Ding et al., 2020*). Total genomic DNA was

209 extracted from muscle or liver tissue samples preserved in 95% ethanol using standard phenol-

210 chloroform-proteinase K (final concentration 1 mg/ml) extraction procedures with consequent

211 isopropanol precipitation (protocols followed *Russell & Sambrook, 2001*). DNA amplification

212 was performed in 20 ml reactions using ca. 50 ng genomic DNA, 10 nmol of each primer, 15

213 nmol of each dNTP, 50 nmol of additional $MgCl_2$, Taq PCR buffer (10 mM of Tris–HCl, pH 8.3,

214 50 mM of KCl, 1.1 mM of $MgCl_2$, and 0.01% gelatine) and 1 U of Taq DNA polymerase.

215 Primers used for PCR and sequencing are summarized in Supplementary Table S2. PCRs were

216 run on a Bio-Rad T100TM Thermal Cycler. PCR protocols for cyt *b* and *ND4* gene fragments

217 followed *De Queiroz et al. (2002)* and *Salvi et al. (2013)*, respectively; the cycling parameters for

218 *c-mos* gene were identical to those described in *Slowinski & Lawson (2002)*, and for *RAG1* to

219 those described in *Groth & Barrowclough (1999)* and *Chiari et al. (2004)*. Sequence data

220 collection and visualization were performed on an ABI 3730xl automated sequencer (Applied

221 Biosystems, Foster City, CA, USA). PCR purification and cycle sequencing were done

222 commercially through Evrogen Inc. (Moscow, Russia).

223

224 **Phylogenetic analyses**

225 Sequences were managed and edited manually using Seqman in Lasergene. v7.1

226 (DNASTAR Inc., Madison, WI, USA), MEGA 7 (*Kumar, Stecher & Tamura, 2016*), and BioEdit

227 v7.0.5.2 (*Hall, 1999*). For individuals which were detected to be heterozygous in nuclear gene

228 sequences, they were phased using the software program PHASE with default sets of iterations,

229 burn-in, and threshold (*Stephens et al., 2001*), on the web-server interface SEQPHASE (*Flot,*

230 *2010*). One of the phased copies was selected at random to represent each individual in

231 subsequent analyses. All sequences were deposited in GenBank (see Supplementary Table S1 for

232 accession numbers).

233 To reconstruct the phylogenetic relationships within the Pareinae, we aligned the newly

234 obtained cyt *b*, *ND4*, *c-mos*, and *RAG1* sequences together with representative sequences from 32

235 specimens of approximately 16 nominal *Pareas* species and seven other Pareinae representatives,

236 retrieved from GenBank (see Supplementary Table S1). Two species of the genus *Xylophis*

237 (Pareidae: Xylophinae) were added to the alignment and used as outgroups for rooting the

238 phylogenetic tree following the phylogenetic data of *Deepak et al. (2019, 2020)*. In total, we

239 obtained molecular genetic data for 81 samples representing 38 taxa of Pareinae, including all

240 currently recognized species of the genus *Pareas*, five species of *Asthenodipsas*, and the single

241 species of the genus *Aplopeltura* (*A. boa*). Details on taxonomy, localities, GenBank accession

242 numbers, and associated references for all examined specimens are summarized in

243 Supplementary Table S1.

244 The nucleotide sequences were initially aligned in MAFFT v.6 (*Katoh et al., 2002*) with

245 default parameters; the alignment was subsequently checked by eye in BioEdit 7.0.5.2 (*Hall,*

246 *1999*) and slightly adjusted. The mean uncorrected genetic *p*-distances between sequences were

247 calculated with MEGA 7 (*Kumar, Stecher & Tamura, 2016*). Phylogenetic trees were estimated

248 for the combined mitochondrial DNA fragments (cyt *b* and *ND4*) and nuclear gene (*c-mos* and

249 *RAG1*) datasets. The total evidence analysis was performed as the approximately unbiased tree-
250 selection test (AU-test; *Shimodaira, 2002*) conducted using Treefinder v.March 2011 (*Jobb,*
251 *2011*) did not reveal statistically significant differences between mtDNA and nuDNA topologies.

252   Phylogenetic relationships of Pareinae were inferred using Bayesian Inference (BI) and
253 Maximum Likelihood (ML) approaches. The optimum partitioning schemes for alignments were
254 identified with PartitionFinder 2.1.1 (*Lanfear et al., 2012*) using the greedy search algorithm
255 under an AIC criterion, and are presented in Supplementary Table S3. When the same model was
256 proposed to different codon positions of a given gene, they were treated as a single partition.

257   BI was performed in MrBayes v3.1.2 (*Ronquist & Huelsenbeck, 2003*) with two
258 simultaneous runs, each with one cold chain and three heated chains for 200 million generations.
259 Two independent Metropolis-coupled Markov chain Monte Carlo (MCMCMC) runs were
260 performed and checked for the effective sample sizes (ESS) were all above 200 by exploring the
261 likelihood plots using TRACER v1.6 (*Rambaut & Drummond, 2007*). We discarded the initial
262 10% of trees as burn-in. Confidence in tree topology was assessed by posterior probability for
263 Bayesian analysis (BI PP) (*Huelsenbeck & Ronquist, 2001*). Nodes with BI PP values of 0.95 and
264 above were considered strongly supported, nodes with values of 0.90–0.94 were considered as
265 well-supported, and the BI PP values below 0.90 were regarded as no support (*Wilcox et al.,*
266 *2002*).

267   A Maximum Likelihood (ML) analysis was implemented using the IQ-TREE webserver
268 (*Nguyen et al., 2015*; *Trifinopoulos et al., 2016*). One-thousand bootstrap pseudoreplicates via
269 the ultrafast bootstrap (ML UB; *Hoang et al., 2018*) approximation algorithm were employed,
270 and nodes having ML UB values of 95% and above were considered strongly supported, while
271 nodes with values of 90%–94% we regarded as well-supported, and the ML UB node values
272 below 90% were considered as no support (*Minh et al., 2013*).

273

274   **Divergence times estimation**
275   The time-calibrated Bayesian Inference analysis was implemented in the program Bayesian
276 Evolutionary Analysis Utility (BEAUti) version 2.4.7 and run on BEAST v1.8.4 (*Drummond et*
277 *al., 2012*), including the concatenated mtDNA + nuDNA dataset. We used hierarchical likelihood
278 ratio tests in PAML v4.7 (*Yang, 2007*) to test molecular clock assumptions separately for
279 mtDNA and nuDNA markers. Based on PAML results, which indicated that there was very little

280   rate variation among the sites of mtDNA markers and so a strict clock model was used for the

281   final analysis employing unlinked site and linked tree models for the nuDNA, and an

282   uncorrelated lognormal relaxed clock for mtDNA genes. We also used these models and

283   partitioning schemes from the ML analysis with empirical frequencies estimated so as to fix them

284   to the proportions observed in the data. A coalescent exponential population prior was employed

285   as the tree prior because intraspecific relationships among many individuals were being assessed

286   and it was not known *a priori* which individuals would be grouped as species. Under the

287   coalescent model, the default priors for population growth (Laplace Distribution) and size (1/X)

288   were left unchanged because these parameters were not being estimated. We conducted two runs

289   of 100 million generations each in BEAST v1.8.4. We also assumed parameter convergence in

290   Tracer and discarded the first 10% of generations as burn-in. We used TreeAnnotator v1.8.0 (in

291   BEAST) to create our maximum credibility clades. Since no paleontological data for the Pareidae

292   are known to exist, we relied on four recently estimated calibration priors for this family obtained

293   from recent large-scale phylogeny of the group (*Deepak et al., 2019*) as primary calibration

294   points. Calibration points and priors are summarized in Supplementary Table S4.

295

296   **Biogeographic analyses**

297   The biogeographic range evolution history of Pareinae was reconstructed by a model-

298   testing approach in a common ML framework to find the best statistical fit using AIC in RASP

299   v3.2 (*Ree et al., 2005*; *Ree & Smith, 2008*; *Yu et al., 2015*). The models allow testing alternative

300   biogeographic hypotheses, such as dispersal, vicariance, and extinction. Six areas were defined

301   that are covered by our ingroup sample (see Fig. 2A): (A) Mainland East Asia; (B) Eastern

302   Indochina; (C) Western Indochina; (D) Indo-Burma, including eastern Himalaya and the Arakan

303   Mountains of Myanmar; (E) Sundaland; and (F) East Asian islands (Taiwan + the Ryukyus)

304   following *Gorin et al. (2020)*, *Chen et al. (2018)*, and *Nguyen et al. (2020a)*. This coding scheme

305   reflects the complex palaeogeographic history of Southeast Asia, because Borneo, Java, Sumatra

306   and the Thai-Malay Peninsula constituted the connected landmass of Sundaland until recently

307   (*Hall, 2012*; *Morley, 2018*). Maximum areas per species were set to three, as no extant species

308   occurs in more than three biogeographical regions. Matrices of modern distributions of species

309   across the areas are presented in Supplementary Table S5; transition matrices between

310   biogeographic regions are given in Supplementary Table S6. Discrete state transitions for ranges

311   were estimated using ML framework on branches as functions of time, suggesting the best fit

312   model for ancestral ranges at the times of cladogenesis using the Akaike Information Criterion

313   (AIC) and Akaike weights (*Ree & Smith, 2008*; *Matzke, 2013*). Two models were compared:

314   Langrange Dispersal-Extinction-Cladogenesis (DEC; *Ree & Smith, 2008*), and the ML version of

315   Statistical Dispersal-Vicariance Analysis (S-DIVA; *Ronquist, 1997*).

316

317   **Morphological characteristics and analyses**

318   For this study, a total of 270 preserved specimens of the subfamily Pareinae, including 82

319   specimens of the subgenus *Pareas*, were examined for their external morphological characters

320   (see Supplementary Table 11, Appendix II).

321   A total of 46 morphological and chromatic characters were recorded for each specimen

322   (following *Vogel, 2015*). Morphological measurements (all in mm) included: snout-vent length

323   (SVL); tail length (TaL); total length (TL); relative tail length (TaL/TL); horizontal eye diameter

324   (ED); distance from the anterior edge of orbit to nostril (Eye-nos); minimal distance from the

325   ventral edge of orbit to the edge of upper lip (Eye-mouth); head length from snout tip to jaw

326   angles (HL); maximal head width (HW). Meristic characters evaluated were the number of dorsal

327   scale rows counted at one head length behind head (ASR), at mid-body (MSR), namely at

328   SVL/2, and at one head length before vent (PSR); number of enlarged vertebral scale rows

329   (VSE); presence of keeled dorsal scale rows (DORkeel); number of keeled dorsal scale rows at

330   midbody (KMD); number of ventral scales (VEN); number of preventral scales (preVEN);

331   number of subcaudal scales (SC); number of cloacal (anal) plates (AN); number of supralabials

332   (SL); number of supralabials touching the orbit (SL-eye); number of supralabials touching

333   subocular (SL-suboc); number of infralabials (IL); numbers of infralabials touching each other

334   (IL-touch); number of nasals (NAS); number of anterior temporals (At); number of posterior

335   temporals (Pt); number of loreals (LOR); loreal touching the orbit or not (LOR-eye); number of

336   preoculars (Preoc); number of presuboculars (Presuboc); prefrontal touching the orbit or not

337   (Prefr-eye); number of suboculars (SoO); subocular fused with postocular or not (SoO-PoO);

338   number of postoculars (PoO). Coloration and pattern characters evaluated were the background

339   body dorsal coloration; presence or absence of ornamentation on neck; presence or absence of

340   dark blotches or chevron on neck and nuchal areas; coloration of head dorsal surface; presence

341   and number of postorbital stripes; presence or absence of a dark blotch on 7th supralabial;

342 presence or absence of transverse bands on body; number of transverse bands on body; number

343 of discontinuous dorsal bands comprised of dark dots; presence or absence of body

344 ornamentation others than bands; dorsal bands continue on belly or not; belly pattern (no pattern,

345 banded, mottled or dotted).

346   We took the color notes from living specimens or their digital images prior to preservation

347 following *Vogel (2015)*. We measured body and tail lengths with a measuring tape (to the nearest

348 of 1 mm); all other measurements were taken using a Mitutoyo digital slide-caliper (to the

349 nearest 0.1 mm). We counted the number of ventral scales following *Dowling (1951)*; we

350 regarded the first enlarged shield anterior to the ventrals as a preventral, while half-ventrals were

351 counted as one. We regarded the first scale under the tail contacting its opposite as the first

352 subcaudal. We did not include the terminal tail scute in the number of subcaudals. Supralabial(s)

353 touching the presubocular were included in the SL-suboc count. We regarded as infralabials

354 those shields that were bordering the mouth gap and were placed ventrally than supralabials.

355 Smaller shields located posteriorly than the last enlarged supralabial shield do not border the

356 mouth gap and were excluded in the sublabial scales count. We defined the scale starting

357 between the posterior chin shield and the infralabials and bordering the infralabials as the first

358 sublabial shield. We recorded the values for paired head characters on both sides of the head (in a

359 left / right order). We determined the sex of the specimens by the presence of everted hemipenes

360 or by dissection of the ventral tail base. We described the morphology of hemipenial structures

361 on specimens in which such structures were everted before preservation; description and

362 terminology followed *Keogh (1999)*.

363   An analysis of variance (ANOVA) was performed to ascertain if statistically significant

364 mean differences among meristic characters (p<0.05) existed among the discrete populations

365 delimited in the phylogenetic analyses. ANOVAs having a p-value less than 0.05 indicating that

366 statistical differences existed were subjected to a Tukey HSD test to ascertain which population

367 pairs differed significantly (p<0.05) from each other. We used the Principal Component Analysis

368 (PCA) to determine if populations from different localities occupied unique positions in

369 morphospace, as well as the degree to which their variation coincided with potential species

370 boundaries as predicted by the molecular phylogeny and univariate analyses. Juvenile specimens,

371 as well as the specimens with incomplete or damaged tails were excluded from the PCA.

372 Characters used in the PCA were continuous mensural data from SVL, TaL, TL, ED, Eye-nos,

373   Eye-mouth, HL, and HW, and the discrete meristic data from the scale counts VSE, KMD,

374   DORkeel, VEN, preVEN, SC, SL, SL-eye, IL, At, Pt, LOR, Preoc, Presuboc, Prefr-eye, SoO,

375   SoO-PoO, and PoO. In order to normalize the PCA data distribution and to transform meristic

376   and mensural data into comparable units for analysis, we natural log-transformed all PCA data

377   prior to analysis and scaled it to their standard deviation. To exclude possible overweighting

378   effects, when we found a high correlation between certain pairs of characters, we omitted one of

379   them from the analyses. Statistical analyses were carried out using Statistica 8.0 (Version 8.0;

380   StatSoft, Tulsa, OK, USA).

381   Morphological and coloration characters of the examined specimens were compared in

382   detail to other species of the genus the *Pareas*. The examined comparative material is listed in

383   Appendix II. For comparison with other taxa, we also relied on previously published data (e.g.,

384   *Theobald, 1868b; Bourret, 1934; Pope, 1935; Smith, 1943; Taylor, 1965; Guo & Rao, 2004;*

385   *Guo & Deng, 2009; Stuebing et al., 2014; You, Poyarkov & Lin, 2015, Vogel, 2015; Hauser,*

386   *2017; Wang et al., 2020; Vogel et al., 2020, 2021; Ding et al., 2020; Bhosale et al., 2020; Liu &*

387   *Rao, 2021*; *Le et al., 2021*). Other abbreviations used: Prov.: Province; Mt.: Mountain; N.P.:

388   National Park; N.R. Natural Reserve; Is.: Island; asl: above sea level.

389

390   **RESULTS**

391

392   **Partitions, substitution models, and sequence characteristics**

393   Our combined dataset was composed of 1,804 bp of cyt *b* and *ND4* mtDNA genes, 1,757

394   bp of nuDNA (including 734 bp of *c-mos*, and 1,023 bp of *RAG1*), and 3,561 bp (mtDNA +

395   nuDNA), respectively. The concatenated mtDNA + nuDNA dataset included 81 samples,

396   representing ca. 29 *Pareas* taxa, including all 24 currently recognized species of the genus (*Uetz,*

397   *Freed & Hošek, 2021*), one species of the monotypic genus *Aplopeltura*, five species of the

398   genus *Asthenodipsas* (of nine currently recognized species, 56%), and two outgroup taxa (see

399   Supplementary Table S1). Information on fragment lengths and variability is summarized in

400   Supplementary Table S3. PartitionFinder 2.1.1 proposed the partition schemes and substitution

401   models which resulted in nine partitions in total (Supplementary Table S3).

402

403   **Phylogenetic relationships and distribution**

404   Phylogenetic trees obtained with ML and BI analyses of the three data partitions (mtDNA

405   + nuDNA, mtDNA, nuDNA) are congruent apart from the generally lower resolution of nuDNA

406   trees (see Supplementary Figures S2–S3). Overall, since the mtDNA + nuDNA phylogenetic tree

407   was mostly better resolved and had greater node support than the mtDNA and nuDNA trees, we

408   relied on the combined mtDNA + nuDNA topology for inferring phylogenetic relationships and

409   biogeographic history of Pareinae. The BI tree resulted from the analysis of the concatenated

410   mtDNA + nuDNA data (Fig. 3) inferred the following set of phylogenetic relationships:

411   1) The subfamily Pareinae was subdivided into five major strongly supported, deeply

412   divergent groups, including two groups within the genus *Pareas* sensu lato (clades A

413   and B, see Fig. 3), the genus *Aplopeltura* (clade C, see Fig. 3), and two groups

414   corresponding to the genus *Asthenodipsas* sensu lato (clades D and E, see Fig. 3).

415   2) The monophyly of the genus *Asthenodipsas* got strong support in mtDNA + nuDNA

416   analysis (1.0/100; hereafter node support values are given for BI PP/ML UB,

417   respectively; see Fig. 3), while it was rendered paraphyletic in the analysis of the

418   mtDNA dataset alone, though with no significant node support. The two clades within

419   *Asthenodipsas* correspond to the *A. malaccana* species group (clade E, in our analysis

420   represented by *A. laevis* and *A. borneensis*; 1.0/100), and to the *A. vertebralis* species

421   group (clade D, in our analysis including *A. vertebralis*, *A. tropidonota*, and *A.*

422   *lasgalenensis*; 1.0/100).

423   3) The monophyly of the clade joining *Pareas + Aplopeltura* was strongly supported

424   (1.0/99). The monotypic genus *Aplopeltura* (1.0/100) in our analysis was represented

425   with two samples of *A. boa* from Peninsular Malaysia and Borneo (Sabah, Malaysia),

426   which were assigned into two highly divergent lineages (see Fig. 3).

427   4) The monophyly of the genus *Pareas* sensu lato was strongly supported by all analyses

428   (1.0/99); the genus comprised two reciprocally monophyletic highly supported groups:

429   clade A, including the members of the *P. carinatus – P. nuchalis* complex (1.0/100);

430   and clade B, including the remainder of *Pareas* species (1.0/100) (see Fig. 3).

431   5) Within the clade B, encompassing the majority of the genus *Pareas* diversity, four

432   subclades were recovered corresponding to the following species groups:

433   a. **Pareas hamptoni species group** (subclade B1; 1.0/100) including *P.*

434   *formosensis*, *P. xuelinensis*, *P. geminatus*, *P. hamptoni*, *P. niger*, *P.*

435   *mengziensis*, *P. iwasakii*, *P. atayal*, *P. komaii*, *P. vindumi*, *P. kaduri*, and *P.*

436   *nigriceps*. *Pareas kaduri* and *P. nigriceps* from East Himalaya formed a well-

437   supported monophylum (1.0/99). The three species of *Pareas* from the East

438   Asian Islands also formed a well-supported clade (1.0/100); with *P. komaii*

439   reconstructed as a sister species with respect to *P. atayal* + *P. iwasakii* though

440   with a low nodal support (0.56/88). Phylogenetic position of *P. vindumi* from

441   Myanmar within the subclade B1 remained essentially unresolved (Fig. 3). The

442   remaining species of the subclade B1 formed a well-supported clade,

443   corresponding to the *P. hamptoni* species complex (1.0/100). Within the latter,

444   *P. niger* and *P. mengziensis* from Yunnan Province of China grouped together

445   (1.0/100) and were represented with almost identical haplotypes. *Pareas*

446   *hamptoni* from Myanmar and Northern Indochina was suggested as a sister

447   taxon with respect to the clade joining *P. xuelinensis* from Yunnan and *P.*

448   *geminatus* from Northern Indochina; the latter species was recovered as

449   paraphyletic with respect to *P. xuelinensis* (1.0/100). *Pareas formosensis* was

450   represented in our analysis with five major lineages from Taiwan and Hainan

451   islands, southern mainland China and Eastern Indochina; the sample of topotype

452   *P. tonkinensis* from northern Vietnam was placed within the *P. formosensis*

453   radiation with strong support (0.99/98; see Fig. 3).

454   b. ***Pareas margaritophorus* species group** (subclade B2; 1.0/100) included four

455   species from Indochina and Indo-Burma: *P. andersonii*, *P. modestus*, *P.*

456   *macularius*, and *P. margaritophorus*. *Pareas andersonii* and *P. modestus* from

457   Myanmar and Northeast India formed a well-supported clade (1.0/100), to

458   which *P. macularius* (1.0/100) was recovered as a sister taxon. The latter

459   species was represented in our analysis with two samples from Myanmar and

460   Laos, which were assigned into two highly divergent lineages (see Fig. 3).

461   Subclade B2 was suggested as a sister lineage with respect to subclade B1

462   though with significant nodal support (0.99/89; see Fig. 3).

463   c. ***Pareas chinensis* species group** (subclade B3; 1.0/100) included *P. stanleyi*, *P.*

464   *boulengeri*, and *P. chinensis* from mainland China; the latter two species

465   formed a strongly supported monophyletic group (1.0/100). Subclade B3 was

466   suggested as a sister lineage with respect to the clade joining B1+B2 with strong

467   nodal support (1.0/92; see Fig. 3).

468   d.   ***Pareas monticola* species group** (subclade B4; 1.0/100) included two species

469   from East Himalaya and Indo-Burma: *P. monticola* and *P. victorianus*.

470   Subclade B4 was suggested as a sister taxon with respect to other species

471   groups B1–B3 with strong node support (1.0/100; see Fig. 3).

472   6) Within the remainder of the genus *Pareas* (clade A; Fig. 3), unexpectedly high numbers

473   of divergent evolutionary lineages were detected. Present taxonomy recognizes three

474   species within this group: *P. carinatus*, *P. menglaensis* and *P. nuchalis*. Altogether,

475   nine divergent lineages were distinguished by robust BI PP and ML UB node support in

476   analyses of the combined mtDNA + nuDNA dataset (Fig. 3). Of these lineages, those

477   which are presently assigned to *P. carinatus*, were recovered as paraphyletic with

478   respect to both *P. menglaensis* and *P. nuchalis*. The nine evolutionary lineages revealed

479   within clade A were distributed across two major clades, which we name herein: the *P.*

480   *carinatus* species group (A1, lineages 1–6), and the *P. nuchalis* species group (A2,

481   lineages 7–9; see Fig. 3):

482   a.   ***Pareas carinatus* species group** (subclade A1; 1.0/100) comprised six lineages

483   formerly recognized under the sole combination *P. carinatus*, including the

484   populations from Peninsular Malaysia southwards from the Isthmus of Kra,

485   corresponding to *P. carinatus* sensu stricto (1.0/100; lineage 5, see Fig. 3). Two

486   samples from Tenasserim Mountains in Peninsular Thailand and Myanmar

487   northwards from the Isthmus of Kra formed a monophyletic group (1.0/100;

488   lineage 6, see Fig. 3), which represented the sister clade to the Malayan *P.*

489   *carinatus* sensu stricto (1.0/100). The populations of *P. carinatus* from the

490   mainland Indochina formed a monophyletic group (1.0/100), including three

491   well-supported subgroups: (1) populations from lowlands of southern Vietnam,

492   corresponding to the subspecies *P. carinatus unicolor* (Bourret, 1934) (1.0/100;

493   lineage 1, see Fig. 3); (2) populations from the northern portion of Annamite

494   (Truong Son) Mountains in central Vietnam and Laos (1.0/100; lineage 2, see

495   Fig. 3); (3) populations from montane areas of Western Indochina (1.0/100;

496   lineage 3, see Fig. 3), including the recently described *P. menglaensis* from

497   southern Yunnan (locality 22, samples 39–43), and the topotypic specimen of *P.*

498   *berdmorei* Theobald, 1868 from Mon State, Myanmar (locality 17, sample 45).

499   Finally, a single specimen initially identified as *P.* cf. *carinatus* from Phu Yen

500   Province in southern part of Central Vietnam formed a divergent lineage with

501   sister relationships with all other populations of *P. carinatus* species group

502   members from the mainland Indochina (1.0/94; lineage 4, see Fig. 3).

503   b.   ***Pareas nuchalis* species group** (subclade A2; 0.99/80) got moderate node

504   support level in the ML analysis since *P. nuchalis* from Borneo was only

505   represented in our work by the single partial sequence of ND4 mtDNA gene

506   (lineage 9, see Fig. 3). The two reciprocally monophyletic lineages from

507   montane areas of Vietnam initially identified as *P.* cf. *carinatus* formed a well-

508   supported clade (1.0/100) which is unexpectedly only distantly related to other

509   mainland Southeast Asian members of *Pareas* and supposedly more closely

510   related to *P. nuchalis*: the lineage from Kon Tum – Gia Lai Plateau in Central

511   Annamites (1.0/100; lineage 7, see Fig. 3), and the lineage from Langbian

512   Plateau in Southern Annamites, corresponding to the recently described *P.*

513   *temporalis* (1.0/100; lineage 8, see Fig. 3).

514   Distribution of the phylogenetic lineages within the clade A is presented in Figure 1. Most

515   lineages that cluster together in each of our two major subclades A1 and A2 are allopatrically

516   distributed within the clade (Fig. 1). Two lineages from different subclades are found

517   sympatrically: *P. nuchalis* (lineage 9) occurs in sympatry with *P. carinatus* sensu stricto (lineage

518   5) in Borneo and Sumatra, while *P.* cf. *carinatus* (lineage 1) occurs syntopically with lineage 8 of

519   *P. temporalis* in Langbian Plateau of southern Vietnam (locality 37, Fig. 1). The only case of

520   distribution overlap of lineages belonging to the same species group includes the lineages 3 and 6

521   of *P. carinatus* which are occur sympatrically in Suanphueng area of Ratchaburi Province in

522   western Thailand (locality 14, Fig. 1). However in Suanphueng the co-occurring lineages of

523   *Pareas* have clearly different habitat preferences and are not syntopically distributed: vouchers of

524   lineage 3 were recorded in lowland bamboo forest at 300 m asl., while the voucher of lineage 6

525   was collected in the montane forest at ca. 800–1000 m asl.

526

527   **Sequence divergence**

528   The interspecific uncorrected genetic *p*-distances in cyt *b* and *ND4* mtDNA genes within

529   the genus *Pareas* are summarized in Supplementary Tables S7 and S8, respectively. For cyt *b*

530   gene genetic divergence varied from $p=4.1\%$ (between *P. geminatus* sensu stricto and *P.*

531   *xuelinensis*) to $p=25.2\%$ (between *P. kaduri* and lineage 7 of *P.* cf. *carinatus* from Central

532   Annamites) (Supplementary Table S7). For *ND4* gene *p*-distances varied from $p=5.2\%$ (between

533   lineages 1 and 2 of the *P. carinatus* complex) to $p=23.7\%$ (between *P. nuchalis* and *P. komaii*)

534   (Supplementary Table S8). In several cases the intraspecific distances within *Pareas* species

535   were greater than the minimal interspecific divergence values, which is likely explained with the

536   incompletely known taxonomy of the group: lineage 6 of the *P. carinatus* complex from

537   Tenasserim (5.0/4.2, hereafter values correspond to intraspecific distances for cyt *b*/*ND4* genes),

538   *P. geminatus* sensu lato (7.2/-), *P. macularius* (11.5/10.4), *P. margaritophorus* (5.2/4.9), and *P.*

539   *monticola* (3.7/5.7).

540

541   **Divergence times estimation**

542   The time-calibrated BEAST analysis recovered a phylogeny with well-supported nodes

543   (BPP ≥ 90) throughout the tree, topologically identical to the BI tree (Fig. 2; Supplementary Fig.

544   S1). The phylogeny indicates that the most recent common ancestor (MRCA) of Pareinae

545   originated in late Eocene (Fig. 2). Basal radiation of Pareinae likely happened during the late

546   Eocene at approximately 39.3 mya, the group continued to radiate across Asia up until the

547   Pleistocene (Fig. 2). Diversification of the genera *Asthenodipsas* and *Pareas* started during the

548   early Oligocene (30.0 mya and 31.3 mya, respectively). The major lineages (i.e. species groups)

549   within the genus *Pareas* diversified between approximately 24.0–12.4 mya with species-level

550   radiations evolving up until 5.0–2.0 mya (Fig. 2). Estimated node-ages and the 95% highest

551   posterior density (95% HPD) for the main nodes are summarized in detail in Supplementary

552   Table S9.

553

554   **Biogeography**

555   All the trees generated in RASP analyses generally recovered the same ancestral range for

556   each node, thus converging on the same biogeographical scenario (Fig. 2). Model comparisons

557   showed that the Langrange Dispersal-Extinction-Cladogenesis (DEC) model is the best fit to the

558   data and most likely to infer the correct ancestral range at each node being the it had the highest

559   and lowest log likelihood and AIC scores, respectively. Our analyses unambiguously suggested

560   that the MRCA of Pareinae (node 3; Supplementary Fig. S1; Fig. 2) most likely inhabited

561   Sundaland, which is also reconstructed as an ancestral range for the genera *Asthenodipsas* and

562   *Aplopeltura* (nodes 4 and 9, respectively; Supplementary Fig. S1; Fig. 2). The split between

563   *Pareas* and *Aplopeltura* is likely explained by a vicariant event between Sundaland and West

564   Indochina (Fig. 2). The divergence between the two major clades within the genus *Pareas*

565   coincides with a vicariance between Indo-Burma and Eastern Himalaya (ancestral range for clade

566   A) and West Indochina (ancestral range for clade B) (Fig. 2). Major ancestral nodes within the

567   *Pareas* clade A remained within Indo-Burma and Eastern Himalaya, from where its members at

568   least three times widely dispersed to the mainland East Asia and further southwards to Indochina

569   and independently twice eastwards to Taiwan and the Ryukyus (Fig. 2). *Pareas* clade B

570   expanded its range to East Indochina and at least twice dispersed to Sundaland (see Fig. 2).

571   Overall, our analysis suggests an "upstream" colonization hypothesis for the Pareinae (from

572   island to continent; see *Filardi & Moyle, 2005*; *Jönsson et al., 2011*), and, thus, the subfamily

573   appears to have originated in Sundaland and then colonized the mainland Asia.

574

Morphological differentiation

576   The PCA of the morphological dataset on *P. carinatus – P. nuchalis* complex revealed that

577   the most distant morphospatial separation occurs in *P. nuchalis* (lineage 9), *P. temporalis*

578   (lineage 8), *P.* cf. *carinatus* lineages from Kon Tum – Gia Lai Plateau (lineage 7), from Phu Yen

579   Province (lineage 4), and from Tenasserim (lineage 6); followed with general separation of the *P.*

580   cf. *carinatus* lineage from northern Annamites (lineage 2) and cluster consisting of the lineages

581   of *P. carinatus* sensu stricto from Sundaland (lineage 5), and *P.* cf. *carinatus* from western

582   Indochina and Yunnan (lineage 3) and southern Vietnam (lineage 1) (Fig. 4). PC1 accounted for

583   18.5% of the variation in the data set and loaded most heavily for relative tail length, number of

584   subcaudal scales, number of ventral scales, and number of prefrontals bordering eye (TaL/TL,

585   SC, VEN, and Prefr-eye; Supplementary Table S10). PC2 accounted for 14.8% of the variation

586   in the data set and loaded most heavily for number of keeled dorsal scale rows, total length, head

587   length, and tail length (KMD, TL, HL, and TaL; Supplementary Table S10). The univariate and

588   multivariate morphological analyses further supported results of the molecular analyses by

589   indicating that the lineages within the *P. carinatus – P. nuchalis* complex are well separated from

590   each other in morphospace and bear a number of statistically significant mean differences in
591   varying combinations of meristic and color pattern characters, thus providing reliable diagnostic
592   character differences among the species (Table 2; Supplementary Tables S11–13).
593
594   **Systematics**
595
596   **Genus-level taxonomy of Pareinae**
597   All recent phylogenetic studies on caenophidian snakes agree on the monophyly of
598   Pareidae (*Pyron, Burbrink & Wiens, 2013*; *Figueroa et al., 2016*; *Zaher et al., 2019*) and of the
599   subfamily Pareinae with respect to Xylophiinae (*Deepak et al., 2019*). Most works on
600   phylogenetic relationships of this group agreed that the genus *Apolpeltura* is a sister taxon of
601   *Pareas* sensu lato, however, the monophyly of the genera *Pareas* and *Asthenodipsas* has been
602   questioned for a long time.
603   Several earlier studies demonstrated that the *P. carinatus* complex (including *P. nuchalis*)
604   is phylogenetically distant from other members of the genus, which was recovered as
605   paraphyletic (e.g., *Guo et al., 2011*; *Pyron et al., 2011*). It was noted that these genetic
606   divergence are concordant with differences in a number of external morphology and scalation
607   characters (*Guo et al., 2011*) and scale ultrastructure (*He, 2009*; *Guo et al., 2020*) (see Fig. 5).
608   *Guo et al. (2011, 2020)* suggested that *P. carinatus* and *P. nuchalis* are different from other
609   *Pareas* species in morphological, ultrastructural and molecular characteristics, and therefore,
610   they "might be removed from the genus *Pareas*"; this idea was further supported by *Wang et al.*
611   *(2020)*. However, due to incomplete sampling and insufficient morphological data, *Guo et al.*
612   *(2011, 2020)* and *Wang et al. (2020)* refrained from making a formal taxonomic decision on the
613   division of *Pareas* [Note - *Wang et al. (2020)* applied a new genus name '*Northpareas*' to the
614   clade including all *Pareas* species except *P. carinatus*, *P. nuchalis*, and *P. menglaensis*, however
615   this name is only used in Appendix S3 of their paper and is not used in the text of their
616   manuscript, and thus should be considered a nomen nudum]. At the same time, both *Guo et al.*
617   *(2011, 2020)* and *Wang et al. (2020)* have overlooked two taxonomic issues:
618   1) *Pareas carinatus* Wagler, 1830 is the type species of the genus *Pareas* Wagler, 1830,
619   and hence it cannot be placed to a different genus; in our analyses the name *Pareas*
620   Wagler, 1830 corresponds to the *Pareas* clade A (see Fig. 3).

621   2) *Eberhardtia* Angel, 1920 is an available genus-level name, erected for *Eberhardtia*

622   *tonkinensis* Angel, 1920, which was considered a junior synonym of *Pareas*

623   *formosensis* (Van Denburgh, 1909) by *Ding et al. (2020)*; in our analyses it corresponds

624   to the *Pareas* clade B (see Fig. 3).

625   Our phylogenetic analyses confirmed the existence of two highly divergent reciprocally

626   monophyletic clades within *Pareas* sensu lato, while strongly supporting the monophyly of the

627   genus.

628   The genus *Asthenodipsas* Peters, 1864 (type species – *Asthenodipsas malaccana* Peters,

629   1864) was for the long time considered a junior synonym of *Pareas*. *Rao & Yang (1992)*

630   examined morphological differences and placed the two species *laevis* Boie, 1827, and

631   *malaccana* Peters, 1864 (that time members of the genus *Pareas*) to a newly erected genus

632   *Internatus* Rao & Yang, 1992 (type species – *Amblycephalus laevis* Boie, 1827). Further studies

633   have also added the taxa *tropidonota* van Lidth de Jeude, 1923 and *vertebralis* Boulenger, 1900

634   to this genus (*David & Vogel, 1996*; *Grossmann & Tillack, 2003*). However, *Iskandar & Colijn*

635   *("2001" 2002)* noted that *Rao & Yang (1992)* had clearly overlooked an available name for the

636   taxa assigned to their new genus *Internatus*, i.e., *Asthenodipsas* (*Grossmann & Tillack, 2003*). A

637   number of recent works described five additional species within the genus *Asthenodipsas*,

638   without addressing questions of genus-level taxonomy of the group (*Loredo et al., 2013*; *Quah et*

639   *al., 2019, 2020, 2021*). Several studies demonstrated that *Asthenodipsas* includes two major

640   highly divergent clades, one including *A. laevis* and *A. borneensis* (belonging to the *A.*

641   *malaccana* species complex) (clade E in our analyses, see Fig. 3), and another including *A.*

642   *vertebralis*, *A. tropidonota*, and *A. lasgalenensis* (clade D in our analyses, see Fig. 3). Hence,

643   both names *Asthenodipsas* and *Internatus* are referred to the members of clade E, while clade D

644   has no available genus-level name. In previous phylogenetic studies, monophyly of the genus

645   *Asthenodipsas* sensu lato was not supported (*Guo et al., 2011*) or got only moderate level of node

646   support (*Wang et al., 2020*; *Ding et al., 2020*; *Vogel et al., 2021*). In our analyses, monophyly of

647   *Asthenodipsas* sensu lato was strongly supported in the concatenated analysis of mtDNA +

648   nuDNA data (Fig. 3), while the analysis of mtDNA genes alone suggested paraphyly of the genus

649   with respect to *Pareas + Aplopeltura* (Supplementary Fig. S2). This genetic divergence among

650   two clades of *Asthenodipsas* is concordant with significant differences in taxonomically valuable

651   scalation characters, such as the number of chin shields and the number of infralabials in contact

652 (see Fig. 5).

653   In summary, in the molecular phylogenetic analysis, Pareinae is obviously divided into five

654 major branches: (A) *Pareas carinatus* + *P. nuchalis* complex, (B) other species of *Pareas*, (C)

655 *Aplopeltura*, (D) *Asthenodipsas vertebralis* group, and (E) other species of *Asthenodipsas* (Fig.

656 3). Monophyly of both *Pareas* sensu lato (clades A + B) and *Asthenodipsas* sensu lato (clades

657 D+E) is strongly supported, while *Asthenodipsas* does not seem to be monophyletic according to

658 mtDNA data alone. Should all five major lineages of Pareinae be recognized as distinct taxa?

659   As we argue below, we find there to be substantial evidence supporting the treatment of the

660 major clades within *Pareas* sensu lato and *Asthenodipsas* sensu lato as separate subgenera. The

661 taxonomic framework ideally should be optimized for utility, reflecting monophyly of taxa and

662 their differences in sets of biologically significant characters, as well as stability, reducing the

663 need for additional taxonomic changes in future (*Vences et al., 2013*; *Gorin et al., 2021*).

664 Although, the present evidence indicates that we can be confident in the respective monophyly of

665 *Pareas* sensu lato and of *Asthenodipsas* sensu lato, it should be noted that the basal radiations

666 within the both genera are very old: the two clades of *Pareas* diverged in early Oligocene (ca.

667 31.3 mya), while the basal radiation within *Asthenodipsas* happened soon afterwards (ca. 30.0

668 mya). These estimates are comparable with the split between *Pareas* sensu lato and *Aplopeltura*

669 (ca. 33.6 mya), and are of equal or greater age than many other Caenophidian genera (see *Zaher*

670 *et al., 2019*). While taxon age is usually not taken into account in higher taxonomy, it is however

671 desirable for taxa of equal rank to be of generally comparable age (*Hennig, 1966*; *Vences et al.,*

672 *2013*; *Gorin et al., 2021*). In addition to their substantial age, a number of important characters of

673 external morphology, scalation, and scale ultrastructure distinguish the major clades within

674 *Pareas* and *Asthenodipsas*, allowing their recognition both in collections and in the field

675 (summarized below in taxonomic accounts). Furthermore, there are pronounced differences in

676 the patterns of geographical distribution among the five clades of Pareinae: our hypothesis of the

677 biogeographic history of this subfamily demonstrated that while the whole group evolved in

678 Sundaland, *Pareas* clade A likely originated in Himalaya and Indo-Burma, and further dispersed

679 to East Asia and Indochina, while *Pareas* clade B likely originated in Western Indochina, from

680 where it colonized Sundaland and Eastern Indochina (Fig. 2). The cumulative evidence suggests

681 that the lack of taxonomic recognition for the major clades within the genera *Pareas* and

682 *Asthenodipsas* would conceal information on the ancient divergence between these lineages, as

683   well as the significant differences between them in a set of biologically relevant traits
684   (summarized in Supplementary Table S14).

685   We propose to recognize the clades A and B of *Pareas* and clades D and E of
686   *Asthenodipsas* as separate subgenera. This would enhance the diagnosability of the respective
687   taxa and make them more comparable units to other genera of Pareinae, and as a consequence
688   fully stabilize the taxonomy of the subfamily. This taxonomic action would therefore be in
689   accordance with all three primary Taxon Naming Criteria (TNCs): Monophyly, Clade Stability,
690   and Diagnosability, as well as the secondary TNCs: Time Banding and Biogeography (see
691   *Vences et al., 2013*). The use of subgenera seems has been successfully applied in several recent
692   revisions of taxonomically challenging groups of reptiles, e.g. cobras of the genus *Naja*
693   (*Wallach, Wuester & Broadley, 2009*), *Trimeresurus*, the Asian pit-vipers (*David et al., 2011*),
694   and *Gekko* (geckoes) (*Wood et al., 2020*). *Wood et al. (2020)* argued that the defining subgenera
695   may aide taxonomists in species descriptions by allowing them to only diagnose putatively new
696   species from the most relevant members of the same subgenus. By creating formally available
697   supraspecific taxa, accompanied by character-based diagnoses and properly assigned type
698   species, the practice of recognizing subgenera also has the potential to restrain taxonomic
699   vandalism, a malpractice forming a long-standing problem in systematics (*Kaiser et al., 2013*;
700   *Wood et al., 2020*; *Wüster et al., 2021*), and thus further enhance taxonomic stability.

701

702   **Species-level diversity in Pareinae**
703   Based on our updated phylogeny of Pareinae, we report on previously unrecognized
704   diversity within the subfamily, and also confirm several taxonomic conclusions made in earlier
705   studies. We document the high degree of uncorrected pairwise sequence divergence between the
706   two samples of *Aplopeltura boa* from Peninsular Malaysia and Sabah in Malaysian Borneo: with
707   *p*-distances of 13.0% in cyt *b* gene and 16.7% in *ND4* gene, the divergence between these
708   populations is estimated as 12.3 mya (Fig. 2; Supplementary Table S9). Further integrative
709   taxonomic studies are needed to clarify the taxonomic status of Malayan and Bornean
710   populations of *A. boa* that might lead to recognition of several species within the genus
711   *Aplopeltura*.

712   In the present study we re-define species groups within the genus *Pareas* recognizing two
713   species groups within the clade A (A1: *P. carinatus* group; and A2: *P. nuchalis* group), and four

714   species groups within the clade B (B1: *P. hamptoni* group; B2: *P. chinensis* group; B3: *P.*

715   *margaritophorus* group; and B4: *P. monticola* group) (Fig. 3). Within the clade B of *Pareas* our

716   results are largely concordant with a number of earlier studies. In *P. montiocola* group our

717   analysis further confirms the species status of the recently described *P. victorianus* (*Vogel et al.,*

718   *2021*); the divergence between this species and its sister taxon *P. monticola* is estimated as 14.1

719   mya (Fig. 2). In *P. margaritophorus* group our results fully agree with the data of *Vogel et al.*

720   *(2020)* in recognizing *P. andersonii*, *P. modestus*, and *P. macularius* as species distinct from *P.*

721   *margaritophorus*. Moreover we report on a deep divergence between the two samples of *P.*

722   *macularius* from Myanmar and Laos with *p*-distances of 11.5% in cyt *b* gene and 10.4% in *ND4*

723   gene (Supplementary Tables S7–S8); the divergence between these populations is estimated as

724   ca. 8.2 mya (Fig. 2), what might be an indicative of an incomplete taxonomy of the group. As the

725   type locality of *P. macularius* is located in Mon State, Myanmar, this raises the question of the

726   taxonomic status of the populations from Laos (this work is currently in progress and will be

727   presented elsewhere). Within *P. hamptoni* species group we confirm the results of *Ding et al.*

728   *(2020)* and *Yang et al. (2021)*, suggesting that *P. kaduri* and *P. nigriceps* are sister taxa, while the

729   phylogenetic position of *P. vindumi* remains unresolved. Genetic divergence among the three

730   members of the Taiwan – Ryukyus clade of this group (*P. atayal*, *P. komaii*, and *P. iwasakii*) is

731   comparatively low (6.9% < *p* < 9.0% in cyt *b* gene; see Supplementary Table S7), and the basal

732   radiation of this clade is estimated to happen only ca. 5.7 mya (Fig. 2). However a number of

733   recent integrative studies, combining molecular, morphological, behavioral, and ecological data

734   provide strong evidence that these taxa represent distinct species (*You, Poyarkov & Lin, 2015*;

735   *Chang et al., 2021*). Our data support the conclusions of *Liu & Rao (2021)* which state that *P.*

736   *mengziensis*, recently described by *Wang et al. (2020)* is conspecific to *P. niger*, a taxon which

737   has been for a long time placed into a synonymy of *P. hamptoni*. Genetic divergence between *P.*

738   *niger* and *P. mengziensis* is minimal (0.3% in cyt *b* gene; see Supplementary Table S7), and

739   given the morphological data reported by *Liu & Rao (2021)* there is little doubt that the latter

740   taxon represents a junior synonym of the former. We further confirm the earlier results of *Ding et*

741   *al. (2020)* in assigning the majority of populations of *P. hamptoni* complex from Vietnam,

742   including the specimen identified as "*P. tonkinensis*", to *P. formosensis* (Fig. 3). Our results also

743   agree with that of *Ding et al. (2020)* in recognizing *P. geminatus* as a species distinct from *P.*

744   *hamptoni*, but its relationships with the recently described *P. xuelinensis* (*Liu & Rao, 2021*; our

745 data) are less clear. In our analysis, *P. geminatus* consists of two major lineages (*P. geminatus* 1
746 from northern Thailand and *P. geminatus* 2 from southern Yunnan of China and northern Laos),
747 and is paraphyletic with respect to *P. xuelinensis*, which is grouped with *P. geminatus* 1 with
748 strong support (Fig. 3). Two taxonomic solutions are possible to keep the monophyly of the
749 recognized taxa: (1) to split *P. geminatus* sensu lato and assign the Thai population to *P.*
750 *xuelinensis*; or (2) to consider *P. xuelinensis* a junior synonym of *P. geminatus*. Genetic
751 divergence among *P. geminatus* 1 + *P. xuelinensis* and *P. geminatus* 2 is low (4.1% in cyt *b*
752 gene; see Supplementary Table S7), the divergence between these clades is estimated as only ca.
753 2.0 mya (Fig. 2), while the morphological characters distinguishing *P. xuelinensis* from *P.*
754 *geminatus* are vague (see Supplementary Table S13). For the time being, we refrain from a
755 taxonomic decision on *P. geminatus* – *P. xuelinensis* clade pending further integrative studies to
756 address this problem, which should include additional materials from China and northern
757 Indochina.

758   Our study reports on a previously unrecognized diversity within the clade A of the genus
759 *Pareas*: altogether, we reveal nine well-supported and highly-divergent clades within this group,
760 five of which were previously unknown. Phylogenetic relationships among these lineages are
761 generally well resolved (Fig. 3) and genetic divergence between them varies from *p* = 4.8% to
762 22.1% in cyt *b* gene, and from *p* = 5.2% to 20.1% in *ND4* gene (Supplementary Tables S7–S8).
763 Recently *Wang et al. (2020)* revised the *P. carinatus* complex and described a new species from
764 southern Yunnan of China. In their analyses *Wang et al. (2020)* only included samples from
765 Peninsular Malaysia (*P. carinatus* sensu stricto) and from Yunnan, and based on genetic
766 divergence and concordant morphological differences between these two populations, concluded
767 that the Yunnan population should be regarded as a new distinct species – *P. menglaensis*.
768 However, this taxonomic decision had several flaws:

769   1) *Wang et al. (2020)* only included in their analyses two populations of *P. carinatus*
770   complex (from Yunnan and Peninsular Malaysia), but omitted any samples or
771   sequences of *P. carinatus* complex from the major part of its range in Indochina and
772   Sundaland, including the sequences available in GenBank.
773   2) *Wang et al. (2020)* overlooked two available species-level names presently coined as
774   junior synonyms of *P. carinatus*: *Pareas berdmorei* Theobald, 1868, and
775   *Amblycephalus carinatus unicolor* Bourret, 1934 (see Table 1).

776   3) Finally, in their revision *Wang et al. (2020)* did not examine any type specimens of the

777   *P. carinatus* species complex.

778   Our updated tree indicates that *P. carinatus* sensu lato is paraphyletic with respect to both

779   *P. menglaensis* and *P. nuchalis* + *P. temporalis*, and that the taxonomy of the complex needs to

780   be reconsidered. The preponderance of data suggests that the pronounced phylogeographic

781   structure within *P. carinatus – P. nuchalis* groups that bear deep genetic divergences, generally

782   wide morphospatial separation among the sampled populations, and statistically different

783   character state means is indicative of a species complex and as such we consider each population

784   to be recognized as a distinct taxon, which we formally describe below:

785   1) The lineage of *P.* cf. *carinatus* from mountains of central Vietnam (lineage 7) and *P.*

786   *temporalis* from southern Vietnam (lineage 8) form a well-supported clade with sister

787   relationships to *P. nuchalis* (though with moderate node support) (Fig. 3). Genetic

788   distance between these lineages is high (12.7% in cyt *b* gene, 9.6% in *ND4* gene; see

789   Supplementary Tables S7–S8); the divergence between them is estimated as ca. 9.3 mya

790   (Fig. 2); they differ in a number of taxonomically significant characters from each other

791   and other congeners (see below; summarized in Table 2), and are widely separated in

792   PCA analysis (Fig. 4). We recognize lineage 7 as a separate new species and together

793   with *P. nuchalis* and *P. temporalis* assign them to the *P. nuchalis* species group

794   (subclade A2, Fig. 3), while all other members of clade A we assign to the *P. carinatus*

795   species group (subclade A1, Fig. 3).

796   2) The population from Peninsular Malaysia (lineage 5), which morphologically and

797   biogeographically corresponds to *P. carinatus* sensu stricto, forms a clade with lineage

798   6 from Tenasserim Mountains in western Thailand and adjacent Myanmar. Lineages 5

799   and 6 are separated by the Isthmus of Kra and likely diverged ca. 5.0 mya (Fig. 2); they

800   are characterized by a moderate level of divergence in mtDNA gene sequences (*p* =

801   7.7% in cyt *b* gene, 5.7% in *ND4* gene; see Supplementary Tables S7–S8), well

802   separated in PCA analysis (Fig. 4), and are diagnosed by stable differences in a number

803   of morphological characters (see below). We propose to recognize the Tenasserim

804   lineage 6 as a new subspecies within *P. carinatus*.

805   3) All samples of *P. carinatus* complex from the mainland Southeast Asia form a clade

806   sister to the clade inhabiting Thai-Malay Peninsula and Sundaland. Within the mainland

807   clade a single specimen from Phu Yen Province of Vietnam (lineage 4) is highly

808   divergent (p = 11.9%–12.7% cyt b gene, 13.8%–14.2% in *ND4* gene; see

809   Supplementary Tables S7–S8), forming a sister lineage with respect to all remaining

810   populations (Fig. 3). Though no geographic barrier is known to separate the Phu Yen

811   population from other mainland lineages of *P. carinatus* complex, the divergence

812   between them is estimated as ca. 11.3 mya (Fig. 2). Moreover, the Phu Yen specimen is

813   different from all other congeners in a number of diagnostic morphological features (see

814   below) and is widely separated from them in the PCA morphospace (Fig. 4). Below we

815   describe the Phu Yen lineage 4 as a new species.

816   4)   Finally, all mainland populations of *P. carinatus* complex except the Phu Yen lineage 4

817   form a clade with three well-supported subclades (see Fig. 3): (1) the basal subclade

818   (lineage 3) encompasses populations from northern Tenasserim to Thailand and

819   Yunnan, and includes the topotypic population of *P. berdmorei* from Mon State,

820   Myanmar (Fig. 1, loc. 16) and *P. menglaensis* (Fig. 1, loc. 22); (2) populations from

821   southern Vietnam (lineage 1), including the type of *Amblycephalus carinatus unicolor*

822   in Kampong Speu, Cambodia (Fig. 1, loc. 29); and (3) populations from Northern

823   Annamites in Vietnam and Laos (lineage 2). These three lineages are separated from

824   each other by moderate genetic distances (p = 4.8%–7.4% in cyt b gene, 5.2%–6.8% in

825   *ND4* gene; see Supplementary Tables S7–S8) with estimated divergence times of 5.9–

826   4.0 mya. They are only partially separated in PCA analysis, with a wide overlap in the

827   morphospace for lineages 1 and 3, and moderate separation of lineage 2 (Fig. 4), but are

828   readily distinguished from each other in a number of chromatic and certain

829   morphological differences (see below). We thus suggest that *P. menglaensis* Wang et

830   al., 2020 represents a subjective junior synonym of *P. berdmorei* Theobald, 1868, and

831   propose to recognize *P. berdmorei* as a full species with three subspecies: *berdmorei*

832   (for lineage 3), *unicolor* (for lineage 1), and a new subspecies for lineage 2 described

833   below.

834   In the updated taxonomy for *P. carinatus – P. nuchalis* complex we propose to recognize

835 two new species and two new subspecies (see above). Though there has been a certain skepticism

836 regarding the usage of subspecies in herpetological taxonomy in the past (e.g., *Wilson & Brown,*

837 *1953*; *Frost & Hillis, 1990*; *Frost, Kluge & Hillis, 1992*), recently the category of subspecies is

838 getting more popular in scope of wide application of phylogenomic data allowing to reveal new

839 cases of mito-nuclear discordance due to ongoing or ancient hybridization (e.g., *Kindler & Fritz,*

840 *2018*; *De Queiroz, 2020*; *Hillis, 2021*; *Marshall et al., 2021*). *Marshall et al. (2021)* define the

841 subspecies as a geographically circumscribed lineage that may has been temporarily isolated in

842 the past, but which has since merged over broad zones of intergradation that show no evidence of

843 reproductive isolation. We tend to tentatively recognize the lineages 1–3 within *P. berdmorei*,

844 and the lineages 5–6 within *P. carinatus* as subspecies but not as full species due to the following

845 reasons: (1) genetic distances among the lineages 1–3 within *P. berdmorei*, and the lineages 5–6

846 within *P. carinatus* are notably lower than between the 'good' species within the *P. carinatus*

847 group (see above); (2) though lineages 5–6 within *P. carinatus* are well separated in the PCA

848 analysis, lineages 1–3 within *P. berdmorei* are poorly separated in the PCA analysis (see Fig. 4)

849 and are differentiated from each other primarily by chromatic traits; (3) the estimated time of

850 divergence between the lineages 1–3 (ca. 5.9–4.0 mya), and the lineages 5–6 (ca. 5.0 mya) within

851 *P. carinatus* is notably younger than the age of divergence of 'good' species within the *P.*

852 *carinatus* group (ca. 17.2–9.3 mya) and is comparable with the age of basal divergence of other

853 wide-ranged species of *Pareas*, e.g. *P. margaritophorus* (ca. 5.2 mya), *P. formosensis* (ca. 3.6

854 mya), and *P. monticola* (ca. 3.4 mya) (see Fig. 2); (4) lineages 2 and 6 are represented in our

855 analyses by a limited sampling of two specimens for each lineage; this material may be not

856 sufficient to fully assess the variation of diagnostic morphological characters; (5) last but not

857 least, *Amblycephalus carinatus unicolor* was traditionally recognized as a subspecies of *P.*

858 *carinatus* (*Nguyen, Ho & Nguyen, 2009*), thus keeping this taxon along with its sister lineages 2

859 and 3 in the rank of subspecies would support the taxonomic stability. Further studies including

860 examination of additional materials and localities are needed to test whether the lineages within

861 *P. carinatus* and *P. berdmorei* have zones of intergradation or are reproductively isolated from

862 each other.

863

864 **Taxonomic accounts**

865

866 **Family Pareidae Romer, 1956**

867 **Subfamily Pareinae Romer, 1956**

868 **Type genus:** *Pareas* Wagler, 1830, by original designation.

869

Revised key to the genera and subgenera of the subfamily Pareinae

870

871   1a. Dorsal scales in 13 rows; subcaudals undivided……genus *Aplopeltura*

872   1b. Dorsal scales in 15 rows; all subcaudals divided……2

873   2a. Anterior single inframaxillary shield absent; vertebrals scales weakly or not enlarged;

874   preocular and subocular scales present; supralabials usually not in contact with the

875   eye……genus *Pareas*

876   *2aa*. Frontal hexagonal with its lateral sides parallel to the body axis; anterior pair of

877   chin shields generally broader than long or slightly longer; two or three distinct narrow

878   suboculars……subgenus *Pareas*

879   *2ab*. Frontal subhexagonal with the lateral sides converging posteriorly; anterior pair of

880   chin shields much longer than broad; one thin elongated subocular……subgenus

881   *Eberhardtia* **stat. nov.**

882   2b. Anterior single inframaxillary shield present; vertebral scales strongly enlarged;

883   preocular and subocular scales absent; supralabials in contact with the eye……genus

884   *Asthenodipsas*

885   *2ba.* Two pairs of chin shields; the third pair of infralabials in contact with each

886   other……subgenus *Asthenodipsas*

887   *2bb*. Three pairs of chin shields; the first pair of infralabials in contact with each

888   other……subgenus *Spondylodipsas* **subgen. nov.**

889

890   **Phylogenetic definition:** Pareinae is a maximum crown-clade name referring to the clade

891 originating with the most recent common ancestor of *Asthenodipsas malaccana* and *Pareas*

892 *carinatus*, and includes all extant species that share a more recent common ancestor with these

893 taxa than with *Xylophis captaini*.

894   **Updated diagnosis:** Body strongly laterally compressed with long tail; a short skull, head

895 strongly distinct from neck; large eyes with vertical pupil; vertebrals sharp, weakly enlarged or

896 not enlarged; 13–15 rows dorsal scale rows (DSR) throughout the body; no mental groove;

897 ventrals preceded by a strongly enlarged preventral larger than the first ventral scale.

898   **Natural history notes:** Pareinae are nocturnal, generally arboreal, oviparous snakes,

899 mainly inhabiting of moist tropical and subtropical forests, all members are specialized feeders

900   on snails and slugs.

901   **Distribution:** Widely distributed through the Oriental zoogeographic region from Eastern

902   Himalaya and Northeastern India, central, southern and eastern China including the islands of

903   Hainan and Taiwan, the Yaeyama group of the Ryukyus across the Indochina and the Thai-

904   Malay Peninsula to the Greater Sunda Islands.

905   **Content:** includes all members of the three genera: *Pareas* Wagler, 1830, *Aplopeltura*

906   Duméril, 1853, and *Asthenodipsas* Peters, 1864 (see below).

907   **English name:** Slug-eating snakes or Snail-eating snakes.

908   **Remark:** Diagnostic morphological features for the genera and subgenera of the subfamily

909   Pareinae recognized herein are summarized in Supplementary Table S14.

910

911   **Genus *Asthenodipsas* Peters, 1864**

912   **Type species:** *Asthenodipsas malaccana* Peters, 1864: 273–274, pl., figs. 3, 3a–3d, by

913   monotypy.

914   **Synonyms:** *Internatus* Yang & Rao in *Rao & Yang, 1992* (type species – *Amblycephalus*

915   *laevis* Boie, 1827).

916   **Phylogenetic definition:** *Asthenodipsas* sensu lato is a maximum crown-clade name

917   referring to the clade originating with the most recent common ancestor of *Asthenodipsas*

918   *malaccana* and *Asthenodipsas vertebralis*, and includes all extant species that share a more

919   recent common ancestor with these taxa than with any of the type species of other Pareinae

920   genera recognized herein.

921   **Updated diagnosis:** Dorsal scales smooth, in 15 rows throughout the body; vertebrals

922   enlarged, hexagonal; sharp vertebral keel developed; head distinct from neck, snout blunt; one or

923   two loreals; preocular and subocular scales absent; supraoculars may be fused to the postoculars;

924   nasal undivided; prefrontal, loreal and at least one supralabial in contact with the eye;

925   supraoculars may be fused to the postocular; frontal subhexagonal with the lateral sides

926   converging posteriorly; two anterior temporals; the anterior single inframaxillary shield present

927   (Fig. 5C–F); inframaxillaries wider than long in two or three pairs; the first or third pair of

928   inframaxillaries in contact with each other (Fig. 5C–F); cloacal plate entire; subcaudals divided

929   (*Peters, 1864*; *Grossmann & Tillack, 2003*; *Quah et al., 2019, 2020*; our data; see Supplementary

930   Table S14).

931   **Distribution:** Sundaic region, including the southern Peninsular Thailand, West Malaysia,
932 and the Greater Sunda Islands (Sumatra, Java and Borneo).

933   **Content:** Nine species, including *A. borneensis* Quah, Grismer, Lim, Anuar & Chan; *A.*
934 *ingeri* Quah, Lim & Grismer, 2021; *A. jamilinaisi* Quah, Grismer, Lim, Anuar & Imbun; *A.*
935 *laevis* (Boie); *A. malaccana* Peters; *A. lasgalenensis* Loredo, Wood, Quah, Anuar, Greer, Ahmad
936 & Grismer; *A. tropidonota* (Lidth de Jeude); *A. stuebingi* Quah, Grismer, Lim, Anuar & Imbun;
937 and *A. vertebralis* (Boulenger).

938   **Etymology:** The genus name is derived from the Greek word "*asthenos*" (*ασθενώς*) for
939 "weak", "lacking strength", and the generic name "*Dipsas*", which is believed to come from the
940 name of a snake in Greek mythology "*Dipsas*" (*Διψας*), the bite of which was believed to cause
941 intense thirst (or "*dipsa*" [*διψά*] in Ancient Greek meaning "thirst"). The word "*Dipsas*" is
942 feminine in gender, therefore *Asthenodipsas* must be treated as feminine, and the names of the
943 included species have to be adjusted to feminine gender (e.g., *malaccana*). The species name
944 "*tropidonotus*" (meaning "keel-backed" in Greek) represents a latinized adjective and therefore
945 its gender has to be adjusted to the feminine gender of *Asthenodipsas* as "*tropidonota*".

946   **Recommended English name:** Sundaic slug-eating snakes.

947   **Material examined (n= 38):** For the detailed information (specimen IDs, locality, sex, and
948 the main morphological characteristics) of *Asthenodipsas borneensis* (n=1), *A. laevis* (n=15), *A.*
949 *lasgalensis (n=5)*, *A. malaccana* (n=10), *A. stuebingi* (n=1), *A. tropidonota* (n=5), and *A.*
950 *vertebralis* (n=1); see Supplementary Table S15 and Appendix II.

951   **Remark:** We recognize the following two subgenera within the genus *Asthenodipsas* for
952 the *A. laevis* and *A. vertebralis* species groups based on stable morphological differences
953 between their members concordant with the ancient phylogenetic divergence between these
954 groups (see above). We propose the subgenus level for the taxa recognized below based on (1)
955 strong support for the monophyly of the genus *Asthenodipsas* sensu lato (see above); (2)
956 biogeographic similarity between these two groups, which are both distributed in the Sundaland
957 region.

958

959   **Subgenus *Asthenodipsas* Peters, 1864**

960   **Type species:** *Asthenodipsas malaccana* Peters, 1864: 273–274, pl., figs. 3, 3a–3d, by
961 monotypy.

962   **Synonyms:** *Internatus* Yang & Rao in *Rao & Yang, 1992* (type species – *Amblycephalus*
963 *laevis* Boie, 1827).

964   **Phylogenetic definition:** *Asthenodipsas* sensu stricto is a maximum crown-clade name
965 referring to the clade originating with the most recent common ancestor of *Asthenodipsas*
966 *malaccana* and *A. laevis,* and includes all extant species that share a more recent common
967 ancestor with these taxa than with *A. vertebralis*.

968   **Diagnosis:** The subgenus *Asthenodipsas* differs from the subgenus *Spondylodipsas*
969 **subgen. nov.** (described below) by the following morphological characters: two pairs of chin
970 shields (vs. three pairs); 5–7 supralabials; 4–7 infralabials; the third pair of infralabials in contact
971 with each other behind the single anterior inframaxillary shield (vs. the first pair) (Fig. 5C–D; see
972 Supplementary Table S14 for details).

973   **Distribution:** Southern Peninsular Thailand, West Malaysia, Borneo, Sumatra, Java, and
974 Bangka islands, Mentawai, and Natuna Archipelagos.

975   **Content:** Six species, including *A. borneensis* Quah, Grismer, Lim, Anuar & Chan; *A.*
976 *ingeri* Quah, Lim & Grismer; *A. jamilinaisi* Quah, Grismer, Lim, Anuar & Imbun; *A. laevis*
977 (Boie); *A. malaccana* Peters; and *A. stuebingi* Quah, Grismer, Lim, Anuar & Imbun.

978   **Recommended English name and Etymology:** as for the genus *Asthenodipsas*.

979

980   **Subgenus *Spondylodipsas* Poyarkov, Nguyen TV & Vogel subgen. nov.**
981   [urn:lsid:zoobank.org:act:3FE7563C-2BFE-4BA4-A084-1A66E3D9B706]

982   **Type species:** *Amblycephalus vertebralis* Boulenger, 1900: 307–308, by original
983 designation.

984   **Phylogenetic definition:** *Spondylodipsas* **subgen. nov.** is a maximum crown-clade name
985 referring to the clade originating with the most recent common ancestor of *Asthenodipsas*
986 *vertebralis* and *A. lasgalenensis*, and includes all extant species that share a more recent common
987 ancestor with these taxa than with *A. malaccana*.

988   **Diagnosis:** The subgenus *Spondylodipsas* **subgen. nov.** differs from *Asthenodipsas* sensu
989 stricto by the following characteristics: three pairs of chin shields (vs. two pairs); 6–8
990 supralabials; 6–8 infralabials; the first pair of infralabials in contact with each other behind the
991 mental (vs. the third pair) (Fig. 5E–F; see Supplementary Table S14 for details).

992   **Distribution:** Mountain areas of Sumatra and Peninsular Malaysia, and Pulau Tioman.

993   **Content:** Three species, including *A. lasgalenensis* Loredo, Wood, Quah, Anuar, Greer,

994   Ahmad & Grismer, *A. tropidonota* (Lidth de Jeude), and *A. vertebralis* (Boulenger).

995   **Etymology:** The genus name is a Latinized noun in feminine gender and is derived from

996   the Greek word "*spondylon*" (σπονδύλων) for "vertebra", and the generic name "*Dipsas*" (for

997   etymology of this name see above). The name is given in reference to the well-developed

998   vertebral keel in the members of the subgenus.

999   **Recommended English name:** Ridged slug-eating snakes.

1000

1001   **Genus *Aplopeltura* Duméril, 1853**

1002   **Type species:** *Amblycephalus boa* Boie, 1828: 1035, by monotypy.

1003   **Phylogenetic definition:** *Aplopeltura* is a maximum crown-clade name referring to

1004   *Aplopeltura boa* originating as the sister lineage to *Pareas* sensu lato.

1005   **Updated diagnosis:** Dorsal scales smooth, in 13 rows throughout the body; vertebral keel

1006   weakly developed; two or three loreals; preocular and subocular scales present; supralabials not

1007   in contact with the eye; three anterior temporals; the anterior single inframaxillary shield absent

1008   (Fig. 5G); generally four (rarely three) pairs of chin shields, anterior pair of chin shields broader

1009   than long; at least the first and second pairs of chin shields in contact; subcaudals undivided

1010   (*Duméril, 1853*; *Taylor, 1965*; our data; see Supplementary Table S14 for details).

1011   **Distribution:** Sundaic region, including: southern Peninsular Thailand, Peninsular

1012   Malaysia, Borneo, Sumatra, Java, Nias, Bangka, and Natuna Islands, and the Philippines (reliably

1013   recorded from the Balabac, Basilan, Mindanao, Palawan, and Luzon islands). The published

1014   record from southern Peninsular Myanmar by *Dowling & Jenner (1998)* requires further

1015   verification.

1016   **Content:** A monotypic genus including the single species, *A. boa* Boie.

1017   **Etymology:** The genus name is likely derived from the Greek words "*aplos*" (απλώς) for

1018   "simple", and "*pelte*" (πέλτη), for "scale", originally a name of a type of a small shield used in

1019   Ancient Greece.

1020   **Recommended English name:** Blunt-headed slug-eating snakes.

1021   **Material examined (n= 2):** For detailed information (specimen IDs, locality, sex, and

1022   main morphological characteristics) of *Aplopeltura boa* (n=2) see Supplementary Table S15 and

1023   Appendix II.

1024   **Remark:** Our study reports on the significant genetic divergence between the samples of

1025   *A. boa* from Borneo (Sabah) and Peninsular Malaysia, corresponding to the species level in

1026   Pareinae (see above). Further integrative taxonomic studies are required to clarify the status of

1027   the lineages within this species.

1028

1029   **Genus *Pareas* Wagler, 1830**

1030   **Type species:** *Dipsas carinata* Wagler, 1830, by monotypy (see account for *Pareas*

1031   *carinatus* for details).

1032   **Phylogenetic definition:** *Pareas* sensu lato is a maximum crown-clade name referring to

1033   the clade originating with the most recent common ancestor of *Pareas carinatus* and *P.*

1034   *formosensis*, and includes all extant species that share a more recent common ancestor with these

1035   taxa than with any of the type species of other Pareinae genera recognized herein.

1036   **Updated diagnosis:** Dorsal scales smooth or keeled, in 15 rows throughout the body;

1037   vertebrals slightly larger than other dorsal scales or not enlarged; one (rarely two) loreals;

1038   preocular and subocular scales present; supralabials generally not contacting the eye (except for

1039   *P. monticola* and *P. stanleyi*); three anterior temporals; the anterior single inframaxillary shield

1040   absent (Fig. 5H–G); three pairs of inframaxillaries, all in contact with each other; subcaudals

1041   divided (*Wagler, 1830*; *Smith, 1943*; *Taylor, 1965*; *Vogel et al., 2020*; our data; see

1042   Supplementary Table S14 for details).

1043   **Distribution**: Widely distributed throughout the Oriental zoogeographic region from

1044   Northeastern India and Himalaya to Eastern China and the Greater Sunda Islands.

1045   **Content:** 26 species, including *P. andersonii* Boulenger; *P. atayal* You, Poyarkov & Lin;

1046   *P. berdmorei* Theobald; *P. boulengeri* (Angel); *P. carinatus* Wagler; *P. chinensis* (Barbour); *P.*

1047   *formosensis* (van Denburgh); *P. geminatus* Ding, Chen, Suwannapoom, Nguyen, Poyarkov &

1048   Vogel; *P. hamptoni* (Boulenger); *P. iwasakii* (Maki); *P. kaduri* Bhosale, Phansalkar, Sawant,

1049   Gowande, Patel & Mirza; *P. komaii* (Maki); *P. macularius* Theobald; *P. margaritophorus* (Jan);

1050   *P. modestus* Theobald; *P. monticola* (Cantor); *P. niger* (Pope); *P. nigriceps* Guo & Deng; *P.*

1051   *nuchalis* (Boulenger); *P. stanleyi* (Boulenger); *P. temporalis* Le, Tran, Hoang & Stuart; *P.*

1052   *victorianus* Vogel, Nguyen & Poyarkov; *P. vindumi* Vogel; *P. xuelinensis* Liu & Rao; and the

1053   two new species described herein below: *P. abros* Poyarkov, Nguyen & Vogel **sp. nov.**; and *P.*

1054   *kuznetsovorum* Poyarkov, Yushchenko & Nguyen **sp. nov.**

1055   **Etymology:** The genus name is a latinized noun in masculine gender derived from the

1056 Greek noun "*pareias*" (*παρείας*), a name of a mythological snake dedicated to Asclepius, and

1057 which was believed to be non-venomous and create a furrow anytime it moves.

1058   **Recommended English name:** Oriental slug-eating snakes.

1059   **Material examined (n= 265):** Detailed information (specimen IDs, locality, sex, and main

1060 morphological characteristics) for *P. abros* (n=3), *P. berdmorei* (n=21), *P. carinatus* (n=26), *P.*

1061 *kuznetsovorum* (n=1), *P. nuchalis* (n=9), and *P. temporalis* (n=6) is presented in Table 2 and

1062 Appendix II; for *P. vindumi* (n=1) see *Vogel (2015)*; for *P. andersonii* (n=13), *P. macularius*

1063 (n=15), *P. margaritophorus* (n=51), and *P. modestus* (n=8) see *Vogel et al. (2020)*; for *P.*

1064 *geminatus* (n=9) and *P. hamptoni* (n=5) see *Ding et al. (2020)*; for *P. formosensis* (n=29), *P.*

1065 *kaduri* (n=1), *P. monticola* (n=24), and *P. victorianus* (n=1) see *Vogel et al. (2021)*; for the

1066 abovementioned species and *P. atayal* (n=6), *P. boulengeri* (n=10), *P. chinensis* (n=7), *P. komaii*

1067 (n=9),*P. stanleyi* (n=4), *P. xuelinensis* (n=3) and *P.* cf. *yunnanensis* (n=3) the information is

1068 summarized in Supplementary Table S16 and Appendix II.

1069   **Remark**: The taxonomic status of *Amblycephalus yunnanensis* Vogt (1922), currently

1070 considered a junior synonym of *Pareas chinensis*, is unclear due to the high morphological

1071 similarity within the group and the geographic proximity of the type localities of two taxa (both

1072 described from Yunnan Province in China). *Ding et al. (2020)* discussed this issue and suggested

1073 that the integrative taxonomic analysis including detailed comparisons of the type specimens is

1074 required to clarify the relations of these taxa (see Supplementary Table S13). Several recent

1075 studies on phylogenetic relationships within *Pareas* have revealed a deep divergence within the

1076 group, suggesting that its taxonomy still may be incomplete (*Guo et al., 2011*; *You, Poyarkov &*

1077 *Lin, 2015*; *Wang et al., 2020*; *Bhosale et al., 2020*; *Ding et al., 2020*; *Vogel et al., 2020, 2021*).

1078

1079 **Subgenus *Pareas* Wagler, 1830**

1080   **Type species:** *Dipsas carinata* Wagler, 1830, by monotypy (see the account for *Pareas*

1081 *carinatus* for details).

1082   **Phylogenetic definition:** *Pareas* sensu stricto is a maximum crown-clade name referring

1083 to the clade originating with the most recent common ancestor of *Pareas carinatus* and *Pareas*

1084 *nuchalis*, and includes all extant species that share a more recent common ancestor with these

1085 taxa than with *Pareas formosensis*.

1086   **Diagnosis:** The members of the subgenus *Pareas* differ from the members of the subgenus
1087 *Eberhardtia* (designated below) by the following morphological characteristics: frontal
1088 hexagonal with the lateral sides parallel to each other (Fig. 5B); anterior pair of chin shields
1089 broader than long (Fig. 5H); two or three distinct narrow suboculars; and the ravine-like
1090 ultrastructure of dorsal scales (*Wagler, 1830*; *Smith, 1943*; *Taylor, 1965*; *Vogel et al., 2020*; *He,*
1091 *2009*; *Guo et al., 2020*; our data; see Supplementary Table S14 for details).

1092   **Distribution**: Distributed in the south-eastern part of the Oriental zoogeographic region
1093 from the southernmost China throughout the Indochina Peninsula to Peninsular Malaysia,
1094 Sumatra, Java, and Borneo (see Fig. 1).

1095   **Content:** Six species, including *P. berdmorei* Theobald (with three subspecies: *P. b.*
1096 *berdmorei* **stat. nov.**, *P. b. unicolor* **comb. nov.**, and *P. b. truongsonicus* **ssp. nov.**); *P. carinatus*
1097 Wagler (with two subspecies: *P. c. carinatus*, and *P. c. tenasserimicus* **ssp. nov.**); *P. nuchalis*
1098 (Boulenger); *P. temporalis* Le, Tran, Hoang & Stuart, 2021; and the two new species described
1099 herein below: *P. abros* Poyarkov, Nguyen & Vogel **sp. nov.**; and *P. kuznetsovorum* Poyarkov,
1100 Yushchenko & Nguyen **sp. nov.**

1101   **Recommended English name and Etymology:** as for the genus *Pareas*.

1102

1103 **Key to the species of the subgenus *Pareas***

1104   1a. Prefrontal contacting the eye……*P. nuchalis*

1105   1b. Prefrontal not contacting the eye……2

1106   2a. Ratio TaL/TL≥0.25; large black blotch or a ring-shaped pattern on the nuchal
1107   area……3

1108   2b. Ratio TaL/TL<0.25; large black blotch or a ring-shaped figure on the nuchal area
1109   absent……5

1110   3a. All dorsal scales smooth, VEN<170; black blotch on the nuchal area not forming a
1111   ring-shaped pattern……*P. kuznetsovorum* **sp. nov.**

1112   3b. At least some dorsal scales strongly or slightly keeled, VEN>170; black blotch on the
1113   nuchal area forming a ring-shaped pattern……4

1114   4a. All dorsal scale rows strongly keeled; VEN>185; no transverse dark bands on the
1115   body……*P. temporalis*

1116   4b. 9–11 rows of dorsal scales keeled at midbody; VEN<185; faint transverse dark bands

1117   on the body……*P. abros* **sp. nov.**

1118   5a. Total length medium (up to 702 mm); dorsal scales generally keeled in 3–11 upper

1119   rows at midbody; upper postorbital stripes thick, contacting each other on the nape

1120   generally forming a X- or)(-shaped pattern; territories southwards from the Tenasserim

1121   Range in Thailand……*P. carinatus*

1122   *5aa*. VEN≤190; SC≤90; body with transverse dark bands; territories south of the

1123   Isthmus of Kra……*P. c. carinatus*

1124   *5ab*. VEN>190; SC>90; uniform light brown coloration of dorsum lacking transverse

1125   dark bands; Tenassenrim Range northwards from the Isthmus of Kra……*P. c.*

1126   *tenasserimicus* **ssp. nov.**

1127   5b. Total length large (up to 770 mm); dorsal scales keeled in 3–13 upper rows at midbody;

1128   upper postorbital stripes thin, generally forming a Y-shaped pattern on the nape or absent;

1129   mainland Indochina north from the Isthmus of Kra……*P. berdmorei*

1130   *5ba*. VEN 166–186; SC 57–89; dorsal scales keeled in 5–13 rows at midbody; body

1131   with transverse dark bars; ventral surfaces immaculate; iris golden-bronze to orange;

1132   restricted to northern Vietnam, northern Laos, northern Thailand, eastern Myanmar

1133   (northern Tennasserin), and southern Yunnan……*P. b. berdmorei* **stat. nov.**

1134   *5bb*. VEN 162–180; SC 57–75; dorsal scales keeled in 3–9 rows at midbody; body

1135   uniform orange to beige coloration lacking dark markings; ventral surfaces generally

1136   immaculate; iris bright orange-red; restricted to southern Vietnam and eastern

1137   Cambodia……*P. b. unicolor* **comb. nov.**

1138   *5bc*. VEN 187; SC 66–73; dorsal scales keeled in 13 rows at midbody; dense brownish

1139   mottling and spots on dorsal, lateral, and ventral surfaces of the head and body; iris

1140   uniform off-white to golden; restricted to the northern Annanmites (Truong Son)

1141   Mountains in central Vietnam and Laos……*P. b. truongsonicus* **ssp. nov.**

1142

1143   ***Pareas carinatus* species group**

1144   The monophyly of the *carinatus* group is well supported in both analyses (A1, Fig. 3); the

1145 members of this species group are widely distributed across the Indochina from southern Yunnan

1146 Province of China to the Thai-Malay Peninsula southwards to Sumatra, Java, Borneo and smaller

1147   adjacent islands (Fig. 1). Our phylogeny indicated that the group is composed of three species-

1148   level lineages, which were further supported by morphological analysis. The first lineage inhabits

1149   Sundaland and the Thai-Malay Peninsula and corresponds to *P. carinatus* sensu stricto. It

1150   includes two subgroups divided by the Isthmus of Kra, an important biogeographic boundary (*De*

1151   *Bruyn et al., 2005*). The populations from Sundaland and the Thai-Malay Peninsula south of Kra

1152   correspond to *P. c. carinatus* (lineage 5, Fig. 3), while the populations northwards of Kra

1153   inhabiting the southern part of Tenasserim Range in western Thailand and adjacent Myanmar, we

1154   assign to a new subspecies *P. c. tenasserimcus* **ssp. nov.** described below (lineage 6, Fig. 3). The

1155   second lineage which we identify as *P. berdmorei* inhabits the mainland Indochina and includes

1156   three subgroups which we treat as subspecies. The first subgroup (lineage 3, Fig. 3) is widely

1157   distributed from southern Myanmar, western and northern Thailand, to Yunnan Province, China,

1158   and corresponds to *P. b. berdmorei* **stat. nov.**). The second subgroup (lineage 1, Fig. 3) is

1159   restricted to southern Vietnam and southeastern Cambodia and represents the subspecies *P. b.*

1160   *unicolor* **comb. nov.** The third subgroup recorded from the northern part of the Annamite Range

1161   we assign to a new subspecies *P. b. truongsonicus* **ssp. nov.** described below (lineage 2, Fig. 3).

1162   Finally, the third species-level lineage of this group was recorded from the north-western

1163   foothills of the Langbian (Da Lat) Plateau in southern Vietnam (lineage 4, Fig. 3); we below

1164   describe it as a new species *P. kuznetsovorum* **sp. nov.** Morphological data on the *P. carinatus*

1165   group members is summarized in Table 2 and Supplementary Tables S11–13. All members of the

1166   *carinatus* group lack the characteristic large black ring-shaped blotch on the nape and lateral

1167   sides of the neck; in *P. kuznetsovorum* **sp. nov.** the black blotch on the nape is present, but it is

1168   not ring-shaped.

1169

1170   *Pareas carinatus* **Wagler, 1830**

1171   Figures 6A–B, 7–9; Table 2; Supplementary Tables S11–S13.

1172   *Dipsas carinata* Wagler, 1830: 181. – Type locality. Java (Indonesia), by inference and

1173   indication on the basis of the NHM and RMNH catalogues. None given in the original

1174   description. – Status. Species name, as published in the binomen *Dipsas carinata* Wagler, 1830,

1175   placed on the 'Official List of Specific Names in Zoology', as Name Nr 2452, after Opinion 963

1176   of I.C.Z.N. (1971: 44).

1177   **Chresonymy:**

1178   *Amblycephalus carinatus* H. Boie in *Schlegel, 1826*: 1035 (*nomen nudum*).

1179   *Amblycephalus carinatus Boie, 1828*: 251 (*nomen nudum*).

1180   *Pareas carinata Wagler, 1830*: 181; *Duméril, Bibron & Duméril, 1854*: 439.

1181   *Dipsas carinata — Schlegel, 1837*: 285; *Nguyen & Ho, 1996*: 61.

1182   *Leptognathus carinatus — Jan, 1863*.

1183   *Amblycephalus carinatus — De Rooij, 1917*: 277; *Smedley, 1931*: 53; *Kopstein, 1936*;
1184 *Deuve, 1961*: 30.

1185   *Pareas carinatus — Cochran, 1930*; *Smith, 1943*: 121; *Manthey & Grossmann, 1997*: 376;
1186 *Cox et al., 1998*: 78; *Schmidt & Kunz, 2005*: 41; *Wallach, Williams & Boundi, 2014*: 535.

1187   **Lectotype** (designated herein) (Fig. 6A; Fig. 7): RMNH 954C, adult male, collected by C.
1188 G. C. Reinwardt from Java Island, Indonesia. We designate the RMNH 954C as the lectotype,
1189 since it is the best preserved specimen of the type series fully agreeing with the original
1190 description, thus fulfilling the requirements of the Art. 74.7 of the Code (*ICZN, 1999*).

1191   **Paralectotypes** (designated herein): Two specimens, RMNH 954A and RMNH 954B, both
1192 adult males, with the same collection data as the lectotype.

1193   **Updated diagnosis:** *Pareas carinatus* differs from all other members of the genus *Pareas*
1194 by the following combination of morphological characters: body slender, maximal total length of
1195 702 mm; frontal scale hexagonal with lateral sides parallel to the body axis; anterior pair of chin
1196 shields longer than broad; loreal and prefrontal not contacting the eye; 1–3 suboculars; usually
1197 one postocular; temporals 3+4 or 3+3; three median vertebral rows slightly enlarged; 7–9
1198 infralabials; 15 dorsal scale rows, at midbody the five upper rows might be slightly keeled; 158–
1199 194 ventrals; 54–96 subcaudals, all divided; dorsum yellow-brown with dark vertebral blotches
1200 and dark mottling, transverse dark bands on the body present or absent; upper postorbital stripes
1201 continue to nape forming one or two longitudinal black spots; iris bronze laterally, beige dorsally
1202 (*Wagler, 1830*; our data).

1203   **Material examined:** We directly examined 26 specimens of *P. carinatus* sensu stricto
1204 from Malaysia, Indonesia and Thailand (Supplementary Table 11Table 1).

1205   **Description of the lectotype** (RMNH 954C) (Fig. 6A, Fig. 7): Adult male, body slender
1206 and notably flattened laterally; head comparatively large, narrowly elongated, clearly distinct
1207 from thin neck, snout blunt; eyes large, pupil vertical.

1208   ***Body size.*** SVL 373 mm; TaL 101 mm; TL 474 mm; TaL/TL: 0.213

1209   ***Body scalation.*** Dorsal scales in 15–15–15 rows, slightly keeled at midbody, and without

1210   apical pits; three vertebral scale rows slightly enlarged; outermost dorsal scale row not enlarged;

1211   ventrals 170 (+ 1 preventral), without lateral keels; subcaudals 67; cloacal plate single.

1212   ***Head scalation.*** Rostral not visible from above; one nasal; two internasals, much wider

1213   than long, narrowing and slightly curving back laterally (in dorsal view), anteriorly in contact

1214   with rostral, laterally in contact with nasal and loreal, posteriorly in contact with prefrontal, not

1215   contacting preocular; two large irregular pentagonal prefrontals, much larger than internasals and

1216   with a slightly diagonal suture between them, not contacting the eye; frontal scale hexagonal with

1217   the lateral sides parallel to the body axis, longer than wide, smaller than parietals; one preocular;

1218   two suboculars; one postocular, not fused with subocular; one loreal in contact with prefrontal,

1219   not touching the eye; 7/7 supralabials, 3rd and 5th SL touching the subocular, none of them

1220   reaching the eye, 7th by far the largest, elongated; temporals 3+4; 9/9 infralabials, the anterior

1221   most in contact with the opposite along the midline, bordering mental, anterior 5 pairs of

1222   infralabials bordering anterior chin shields; 3 pairs of chin shields interlaced, no mental groove

1223   under chin and throat; anterior chin shields relatively large, generally wider than long, followed

1224   by two pairs of chin shields much wider than long.

1225   ***Coloration.*** After over 200 years in preservative, the dorsal and ventral surfaces of the

1226   head, brownish with some dark-brown dusted spots (Fig. 7). Head with two lateral dark-brown

1227   postorbital stripes: the lower one is an interrupted dark line starting from the posterior edge of the

1228   eye, going diagonally down onto the anterior part of the last supralabial; the upper postorbital

1229   stripe is a dark-brown line running from the postocular backwards to the dorsal scales on the

1230   neck, where it meets the similar line on the opposite side of the body forming a narrow X-shaped

1231   dark-brown marking on the nuchal area (Fig. 7A). Upper labials marked with some fine irregular

1232   brown speckling (Fig. 7C–D). Dorsal surface is nearly uniformly light brown with slightly visible

1233   dark cross bands; ventral surfaces yellowish with sparse brownish mottling forming the

1234   interrupted line along the midline, descending backwards. Coloration in life unknown.

1235   **Comparisons:** *Pareas carinatus* differs from *Pareas berdmorei* (revalidated below) by the

1236   generally smaller body size (494.3±73.3 mm vs. 554.9±73.3 mm); by slightly lower number

1237   keeled dorsal scale rows (6.5±2.9 vs. 8.9±2.8); and by generally thicker upper postorbital stripe

1238   and more pronounced dark markings on the nape (vs. thinner postorbital stripe and less

1239   pronounced dark markings on the nape); *P. carinatus* differs from *P. nuchalis* by prefrontal not

1240 contacting the eye (vs. in contact); by the absence of the large ring-shaped black blotch on the

1241 nape (vs. present); by lower number of ventrals (171.35±9.3 vs. 209.89±5.3); lower number of

1242 subcaudals (73.3±7.6 vs. 111.1±6.1); and by having keeled dorsal scales (vs. dorsal scales totally

1243 smooth). Morphological comparisons between all species of the subgenus *Pareas* are detailed in

1244 Table 2. *Pareas carinatus* can be distinguished from other species of *Pareas* belonging to

1245 subgenus *Eberhardtia* **stat. nov.** by having two or three distinct narrow suboculars (vs. one thin

1246 and elongated) and by having a hexagonal frontal with its lateral sides parallel to the body axis

1247 (vs. subhexagonal) (see Supplementary Tables S13–S14).

1248   **Distribution**: Based on molecular and morphological data, we suggest that this species is

1249 restricted to the Greater Sunda Islands (Java, Borneo and Sumatra), Peninsular Malaysia and

1250 Thailand, including the Tenasserim Mountains in western Thailand and south-eastern Myanmar,

1251 the northernmost known locality is Yaephyu, Tanintharyi Region, Myanmar (Fig. 1).

1252   **Etymology:** The species name "*carinatus*" is a Latin adjective in nominative singular,

1253 masculine gender, derived from "*carina*" for a "keel of a ship", and is given in reference to the

1254 keeled dorsal scales in this species.

1255   **Recommended English name:** Keeled slug-eating snake.

1256   **Remark:** Based on the concordant results of morphological and molecular analyses, we

1257 recognize two subspecies within *P. carinatus*: the populations south of the Isthmus of Kra

1258 correspond to the nominative subspecies *P. c. carinatus*, while the populations from the

1259 Tenasserim Mountains northwards from Kra we describe below as *P. c. tenasserimcus* **ssp. nov.**

1260 Although the morphological variation among the sampled specimens of *P. c. carinatus* is

1261 significant (Fig. 4; Supplementary Tables S11–S12), in molecular analyses this subspecies is

1262 only represented by specimens from Peninsular Malaysia. Further phylogenetic analyses of *P.*

1263 *carinatus* populations from Java, Sumatra and Borneo are required and might reveal new

1264 presently unknown lineages within this species.

1265

1266   ***Pareas carinatus carinatus* Wagler, 1830**

1267   Figures 6A, 7, 9A–C; Supplementary Tables S11–S12.

1268   *Dipsas carinata* Wagler, 1830: 181.

1269 **Chresonymy:**

1270   *Amblycephalus carinatus carinatus* — (in part) *Mertens, 1930.*

1271   *Pareas carinatus carinatus* — (in part) *Haas, 1950*; *Chan-ard et al., 1999*: 177; *Nguyen,*

1272   *Ho & Nguyen, 2009*: 374.

1273   **Diagnosis:** *Pareas carinatus carinatus* differs from *Pareas carinatus tenasserimicus* **ssp.**

1274   **nov.** described below by the following combination of morphological characters: maximal total

1275   length of 608 mm; anterior pair of chin shields wider than long; one postocular; temporals

1276   generally 3+4 (rarely 3+3, 2+3); 15 dorsal scale rows slightly keeled in 3–11 scale rows at

1277   midbody; 158–190 ventrals; 54–84 subcaudals; dorsum light brown with distinct dark vertebral

1278   spots and generally 44–73 transverse dark brownish or blackish bands (Fig. 9A–C); upper

1279   postorbital stripes generally contacting each other on the nuchal area forming a narrow X-shaped

1280   dark marking with curved branches; ventral scales yellowish with sparse brownish mottling

1281   forming the interrupted line along the midline.

1282   **Variation:** Measurements and scalation features of the subspecies *P. c. carinatus* (n=25)

1283   are presented in Supplementary Tables S11. There is a certain variation among the sexes

1284   observed in the body size and the number of ventral scales. Males are generally smaller (TL

1285   337.0–571.0 mm, average 471.5±59.5 mm, n=15) than females (TL 446.0–608.0 mm, average

1286   511.0±56.8 mm, n=8); males also have a generally lower number of ventrals than females (158–

1287   183, average 167.3±6.2, n=15 in males vs. 162–190 average 175.2±8.8, n=10 in females). In five

1288   specimens from from Java (ZMH R11546 and R11542), Sumatra (SMF 37825–37826) and

1289   Borneo (NMW 28131:1) keels on dorsal scales are hardly visible; it is unclear if this feature

1290   reflects the geographic variation, or it might arise from the poor preservation of the specimens.

1291   Other morphological features showed no significant variation among the specimens of the series

1292   examined. In our phylogenetic analysis, *P. c. carinatus* was represented only by specimens from

1293   Peninsular Malaysia; further integrative molecular and morphological studies are needed to

1294   assess the geographic variation among the populations of *P. c. carinatus* from Java, Sumatra,

1295   Borneo, and Peninsular Malaysia.

1296   **Distribution:** Peninsular Thailand south of the Isthmus of Kra, Malaysia (Peninsular

1297   Malaysia, Sarawak and Sabah within Borneo), Brunei, and Indonesia (Kalimantan Province,

1298   Sumatra, Java, Lombok, and Bali Islands) (Fig. 1).

1299   **Recommended English name and Etymology:** as for *Pareas carinatus*.

1300

1301   ***Pareas carinatus tenasserimicus* Poyarkov, Nguyen TV, Vogel**, **Pawangkhanant,**

1302   **Yushchenko & Suwannapoom ssp. nov.**

1303   [urn:lsid:zoobank.org:act:11F7F6BA-4733-41FB-8E2D-405DCA5743E5]

1304   Figures 6B, 8, 9D–E; Supplementary Tables S11–S12.

1305 **Chresonymy:**

1306   *Pareas carinatus* — (in part) *Mulcahy et al., 2018*: 98.

1307   **Holotype** (Fig. 6B, Fig. 8): ZMMU R-16800 (field number NAP-10160), adult male,

1308 collected by P. V. Yushchenko from mountain forest in Joot Chomwil area, Suan Phueng

1309 District, Ratchaburi Province, western Thailand (N 13.56346, E 99.19465, elevation 800 m asl.)

1310 on 16 July 2019.

1311   **Diagnosis:** *Pareas carinatus tenasserimicus* **ssp. nov.** differs from the nominative

1312 subspecies by the following combination of morphological characteristics: total length 702 mm;

1313 anterior pair of chin shields as long as broad; two postoculars; temporals 3+3; 15 dorsal scale

1314 rows slightly keeled in 7 scale rows at midbody; 194 ventrals; 96 subcaudals; dorsum light brown

1315 to beige, 73 weak dark vertebral spots; transverse dark bands on the body absent (Fig. 9D–E);

1316 upper postorbital stripes not contacting each other on the nuchal area forming a weak X-shaped

1317 dark marking with curved branches; ventral scales beige with dense brownish mottling not

1318 forming the interrupted midventral line.

1319   **Description of the holotype:** Adult male, specimen in a good state of preservation (Fig. 8),

1320 body slender and notably flattened laterally; head comparatively large, narrowly elongated,

1321 clearly distinct from the thin neck, snout blunt; eye rather large, pupil vertical and slightly

1322 elliptical.

1323   *Body size.* SVL 524 mm; TaL 178 mm; TL 702 mm; TaL/TL: 0.254.

1324   *Body scalation.* Dorsal scales in 15–15–15 rows, slightly keeled in 7 upper scale rows at

1325 midbody, without apical pits; vertebral scales (three median rows) slightly enlarged; outermost

1326 dorsal scale row not enlarged; ventrals 194 (+ 1 preventral), lacking lateral keels; subcaudals 96,

1327 paired; cloacal plate single.

1328   *Head scalation.* Rostral not visible from above; nasal single; two internasals, much wider

1329 than long, narrowing and slightly curving back laterally (in dorsal view), anteriorly in contact

1330 with rostral, laterally in contact with nasal and loreal, posteriorly in contact with prefrontal, not

1331 contacting preocular; two large irregular pentagonal prefrontals, much larger than internasals and

1332 with a slightly diagonal suture between them, not contacting the eye; frontal scale hexagonal with

1333   the lateral sides parallel to the body axis, longer than wide, of the same size as the parietals; two

1334   preoculars; two suboculars; two postoculars, not fused with suboculars; one loreal in contact with

1335   prefrontal, not touching the eye; 7/7 supralabials, 3rd and 5th SL touching suboculars, none of

1336   them reaching the eye, 7th subocular the largest, elongate; temporals 3+3; 9/9 infralabials, the

1337   anterior most in contact with the opposite along the midline, bordering mental, anterior five pairs

1338   of infralabials bordering anterior chin shields, 3rd pair of infralabials in contact with each other

1339   (Fig. 8F); unpaired inframaxillary shield absent; two pairs of chin interlaced shields contacting

1340   each other, no mental groove under chin and throat; anterior chin shields relatively large, as long

1341   as broad, the second pair of chin shields much broader than long.

1342   *Coloration.* In life, the dorsal and ventral surfaces of the head are uniform light brown

1343   dorsally, yellowish-beige ventrally (Fig. 9E). Head with two lateral postorbital stripes: the lower

1344   one is a thin dark-brown line starting from the lower posterior edge of the eye onto the anterior

1345   part of the last supralabial; the upper one is a strong dark-brown line running from postocular

1346   backwards to the medial dorsal scale rows on the neck; upper postorbital stripes not contacting

1347   each other on the nuchal area forming a weak X-shaped dark marking with curved branches.

1348   Upper labials marked with numerous irregular dark-brown speckling continuing and getting

1349   denser on lateral and dorsal surfaces of the head; 5th supralabial with a larger black spot. Dorsal

1350   surfaces with ca. 73 faint dark blotches along the vertebral keel; transverse dark bands on the

1351   body absent; ventral surfaces of body and tail yellowish cream with very sparse small black spots

1352   concentrating laterally, dark spots and speckles getting denser on the posterior portion of the

1353   belly. Iris yellowish-orange laterally and ventrally, light beige dorsally; pupil black. **In**

1354   **preservative:** After two years of storage in ethanol (Fig. 8) the general coloration pattern has not

1355   changed; light brown of the coloration of dorsum, head and eye has faded becoming grayish-

1356   brown; other features of coloration remain unchanged.

1357   **Variation:** A single male specimen observed in Kaeng Krachan N.P., Phetchaburi

1358   Province, Thailand (specimen not collected) is overall similar to the holotype of the new

1359   subspecies, but demonstrates certain differences in color pattern, including more pronounced

1360   dark vertebral spots and a series of dark spots along the lower raw of dorsal scales (Fig. 9D),

1361   while the holotype has a more uniform coloration lacking dark markings on dorsum and body

1362   sides (Fig. 9E). Given the geographic proximity of the Kaeng Krachan N.P. (Fig. 1, a) to the type

1363   locality of the new subspecies, and morphological similarity, we tentatively identify the Kaeng

1364   Krachan population as *P. c.* cf. *tenasserimicus* **ssp. nov.**; its taxonomic status requires further

1365   verification using morphological examination and molecular data.

1366   **Comparisons:** *Pareas carinatus tenasserimicus* **ssp. nov.** differs from *P. c. carinatus* by

1367   its generally larger size (702 mm vs. 337–608 [485.2±59.7] mm); a slightly higher number of

1368   ventrals (194 vs. 158–190 [170.4±8.2]); a higher number of subcaudals (96 vs. 54–84

1369   [68.1±7.2]); by two postoculars (vs. single postocular); by the 3rd pair of infralabials in contact

1370   with each other (vs. not in contact); by a uniform light brown coloration of dorsum lacking

1371   transverse dark bands (vs. transverse dark bands present); and by upper postorbital stripes not

1372   contacting each other on the nuchal area forming a weak dark marking with curved branches (vs.

1373   usually contacting each other forming a dark X-shaped marking). For the detailed comparison of

1374   the two subspecies of *P. carinatus* see Supplementary Table S12.

1375   **Distribution:** To date the new subspecies is reliably known from only three localities in

1376   the southern portion of Tenasserim Range: the type locality in Suan Phueng District, Ratchaburi

1377   Province and Kaeng Krachan N.P., Phetchaburi Province of Thailand (locality 14, Fig. 1), and

1378   from Yaephyu area in Tanintharyi Region of Myanmar (locality 15, Fig. 1).

1379   **Etymology:** The new subspecies name "*tenasserimicus*" is a Latin toponymic adjective in

1380   nominative singular, adopting the masculine gender of the genus name *Pareas*, and is given in

1381   reference to the Tenasserim Mountain Range in western Thailand and southeastern Myanmar,

1382   where the new subspecies occurs.

1383   **Recommended English name:** Tenasserim slug-eating snake.

1384   **Ecology notes:** The new subspecies inhabits montane evergreen forests of the Tenasserim

1385   Range on elevations above 800 asl. This is a nocturnal snake, all three specimens were recorded

1386   at night while perching or crawling on the tree branches and bushes ca. 1–2 m above the ground.

1387   The diet of the new subspecies is not known in detail, though it likely consists of land snails or

1388   slugs. In Suan Phueng area (locality 14, Fig. 1), the new subspecies occurs in sympatry with *P. b.*

1389   *berdmorei*, but was not recorded in the same habitats: the new subspecies inhabits montane

1390   forests at ca. 800–1000 m asl., while the specimens of *P. b. berdmorei* were recorded in lowland

1391   bamboo forest at 300 m asl. Other co-occurring species of *Pareas* include *P. margaritophorus*.

1392

1393   *Pareas berdmorei* **Theobald, 1868**

1394   Figures 6C–F, 10–13; Supplementary Tables S11–S13.

1395   *Pareas berdmorei Theobald, 1868b*: 63.

1396   **Chresonymy and synonymy:**

1397   *Amblycephalus carinatus unicolor Bourret, 1934.*

1398   *Pareas carinatus* — (in part) *Smith, 1943*; *Taylor, 1965*; *Yang & Rao, 2008*; *Nguyen, Ho &*

1399   *Nguyen, 2009*; *Teynié & David, 2010*; *Le et al., 2014*; *Wallach, Williams & Boundi, 2014*; *Chan-*

1400   *ard et al., 2015*; *Pham & Nguyen, 2019.*

1401   *Pareas berdmorei* — *Das et al., 1998.*

1402   *Pareas carinatus unicolor* — (in part) *Nguyen, Ho & Nguyen, 2009.*

1403   *Pareas menglaensis Wang, Che, Liu, Ki, Jin, Jiang, Shi & Guo, 2020.*

1404   **Lectotype** (designated herein) (Fig. 6C; Fig. 10): ZSI 8022, adult male collected by T. M.

1405   Berdmore from "Tenasserim", corresponding to Mon Region in southeastern Myanmar according

1406   to *Das et al. (1998)* (locality 16, Fig. 1). The specimen ZSI 8022 is designated herein as the

1407   lectotype as it is the best preserved specimen of the type series, and clearly corresponds to the

1408   morphological characteristics mentioned in the original description of *Pareas berdmorei*

1409   *Theobald, 1868b*, thus fulfilling the requirements of the Art. 74.7 of the Code (*ICZN, 1999*),

1410   modified by *Anonymous (2003; Declaration 44).*

1411   **Paralectotype** (designated herein): one specimen, ZSI 8021, adult male, with the same

1412   collection information as the lectotype.

1413   **Referred specimen:** ZSI 8023, juvenile, with the same collection information as the

1414   lectotype.

1415   **Remark:** *Theobald (1868b)* described *Pareas berdmorei* based on a series of five

1416   specimens collected from "Tenasserim" by Major T. M. Berdmore. The description of *Pareas*

1417   *berdmorei* is based on a series of two adults; the three smaller specimens, which *Theobald*

1418   *(1868b)* were considered to be juveniles, were almost simultaneously described as *P. macularius*

1419   (*Theobald, 1868a*: 54). Therefore *Theobald (1868b)* proposed the new name for the two larger

1420   specimens "to prevent confusion of synonyms" (*Theobald, 1868b*: 63). According to *Das et al.*

1421   *(1998)*, the type series of *P. macularius* includes three specimens ZSI 8024–26, while the

1422   specimens catalogued under the name *P. berdmorei* bear the museum numbers ZSI 8021–23.

1423   *Bhosale et al. (2020)* noted that only the specimens ZSI 8021 and ZSI 8022 are adults, therefore

1424   they correspond to the syntypes of *P. berdmorei* (Z. Mirza, pers. comm.).

1425   We have obtained morphological data and a photograph of ZSI 8022, which we designate

1426 as the lectotype of *P. berdmorei*, as it is the best preserved specimen of the type series which
1427 fully agrees with the original description of *P. berdmorei* (*Theobald, 1868b*: 63). We designate
1428 ZSI 8021 as the paralectotype, while ZSI 8023, without nomenclatural status, is listed in the
1429 referred specimens. The designation of lectotype for *P. berdmorei* is necessary due to the
1430 historical confusion between the descriptions of *P. macularius* and *P. berdmorei*; thus fulfilling
1431 the requirements of the Art. 74.7 of the Code (*ICZN, 1999*).

1432   **Updated diagnosis:** *Pareas berdmorei* differs from other members of the genus *Pareas* by
1433 the following combination of morphological characters: maximal total length of 770 mm; frontal
1434 scale hexagonal with its lateral sides parallel to the body axis; the anterior pair of chin shields
1435 broader than long; loreal and prefrontal not contacting the eye; generally 1 or 2 preoculars;
1436 regularly 2 (rarely 1 or 3) suboculars; generally single postocular (rarely 0 or 2); temporals 3+4
1437 or 3+3; one to three median vertebral dorsal scale rows slightly enlarged; generally 8 (7–9)
1438 infralabials; 15 dorsal scale rows, of them 3–13 scale rows at midbody feebly keeled; 162–187
1439 ventrals; 57–89 subcaudals, all divided; dorsum yellow-brown to orange, dark markings on
1440 dorsum variable; thin upper postorbital stripes continue to nape often forming elongated dark
1441 markings; iris uniform, color varies from beige to bright reddish-orange (*Theobald, 1868b*;
1442 *Bourret, 1934*; *Taylor, 1965*; *Ziegler et al., 2006*; *Yang & Rao, 2008*; *Le et al., 2014*;*Pham &*
1443 *Nguyen, 2019*; *Wang et al., 2020*; our data).

1444   **Material examined:** In this study we used morphological data from 38 specimens of *P.*
1445 *berdmorei*, including the 21specimens examined directly (among them the lectotype of *Pareas*
1446 *berdmorei* Theobald and the holotype of *Amblycephalus carinatus unicolor* Bourret) and the
1447 published data for 17 specimens formerly listed as "*P. carinatus*" (*Taylor, 1965*; *Ziegler et al.,*
1448 *2006; Yang & Rao, 2008*; *Le et al., 2014*; and *Pham & Nguyen, 2019*), and "*P. menglaensis*"
1449 (*Wang et al., 2020*) (Supplementary Table S11).

1450   **Description of the lectotype** (ZSI 8022): Adult male, a well-preserved specimen, with
1451 coloration significantly faded due to the long time of preservation in ethanol (Fig. 10), body
1452 slender and notably flattened laterally; head comparatively large, narrowly elongated, slightly
1453 distinct from neck, snout blunt; eyes large.

1454   ***Body size.*** SVL 490 mm; TaL 120 mm; TL 610 mm; TaL/TL: 0.197.

1455   ***Body scalation.*** Dorsal scales in 15–15–15 rows, slightly keeled in 9 scale rows at
1456 midbody, lacking apical pits; vertebral scales in three median rows slightly enlarged; the

1457   outermost dorsal scale row not enlarged; ventrals 174 (+ 1 preventral), lacking lateral keels;

1458   subcaudals 64; cloacal plate single.

1459   *Head scalation.* Rostral not visible from above; single nasal; two internasals, much wider

1460   than long, narrowing and slightly curving back laterally (in dorsal view), anteriorly in contact

1461   with rostral, laterally in contact with nasal and loreal, posteriorly in contact with prefrontal, not

1462   contacting preocular; two large irregular pentagonal prefrontals, much larger than internasals and

1463   with a slightly diagonal suture between them, not in contact with eye; the frontal scale hexagonal

1464   with the lateral sides parallel to the body axis, longer than wide, smaller than parietals; two

1465   preoculars; one subocular; one postocular, not fused with subocular; one loreal in contact with

1466   prefrontal, not touching the eye; 7/7 supralabials, 3rd and 5th SL touching the subocular, none of

1467   them reaching the eye, 7th SL the largest, elongate; temporals 3+4; 8/8 infralabials, 3 pairs of

1468   chin shields interlaced, all notably broader than long, no mental groove under chin and throat;

1469   anterior chin shields relatively large.

1470   *Coloration.* Due to preservation in ethanol for over 150 years, the colors of the holotype

1471   have significantly faded, the specimen is uniform light brownish-yellow (Fig. 10A); the present

1472   body pattern of the lectotype no longer retains the original characteristics, though the thin dark

1473   postorbital stripes are still discernable and faded to orange-brown (Fig. 10B). In the original

1474   description, *Theobald (1868*: 63*)* gives the following information on the type coloration: "color is

1475   uniform ochraceous, with obsolete traces of vertical bands down the body; two dark lines

1476   converge on the nape; <…> belly white", indicating that the specimen has already significantly

1477   faded at the moment of the original description.

1478   **Comparisons**: *Pareas berdmorei* is distinguishable from *P. carinatus* by the generally

1479   larger body size (554.2±76.5 mm vs. 494.3±73.3 mm); by slightly higher number of ventrals

1480   (177.3±5.8 vs. 171.4±9.3); slightly higher number of keeled dorsal rows (9.0±2.8 vs. 6.1±3.3); by

1481   generally less pronounced dark markings in the nuchal area, thinner postorbital stripes and a

1482   more uniform coloration of the iris; from *P. nuchalis* by prefrontal not contacting the eye (vs. in

1483   contact); by the absence of the ring-shaped black blotch on the nape (vs. present); by lower

1484   number of ventrals (177.3±5.8 vs. 209.9±5.3); lower number of subcaudals (71.2±7.5 vs.

1485   111.1±6.1); and by the presence of keeled dorsal scale rows (vs. dorsals totally smooth).

1486   Morphological comparisons between all species of the subgenus *Pareas* are detailed in Table 2

1487   and Supplementary Table S13. *Pareas berdmorei* can be distinguished from other species of

1488 *Pareas* belonging to subgenus *Eberhardtia* **stat. nov.** by having two or three distinct narrow

1489 suboculars (vs. one thin and elongated) and by having a hexagonal frontal with its lateral sides

1490 parallel to the body axis (vs. subhexagonal) (Supplementary Tables S13–S14).

1491 **Distribution**: *Pareas berdmorei* is widely distributed across the mainland Indochina north

1492 from the Kra Isthmus (Fig. 1). Its range consists of the three major groups of populations (Fig.

1493 1): (1) populations from southeastern Myanmar, western and northern Thailand, northern Laos

1494 and the southernmost parts of Yunnan Province of China; (2) populations from eastern Laos and

1495 central Vietnam located along the Truong Son Range; (3) populations from southern Vietnam

1496 and the adjacent parts of eastern Cambodia. As this species occurs in lowland to submontane

1497 tropical forests, it is seemingly absent from seasonally dry lowlands of central Indochina and the

1498 lower part of the Mekong Valley (Fig. 1). However, the occurence of *P. berdmorei* is expected in

1499 the Cardamom Mountains of Cambodia and the montane areas of eastern Thailand; therefore

1500 further field survey efforts are required to clarify the real extent of *P. berdmorei* distribution.

1501 **Etymology:** *Theobald (1868)* named his new species in honor of British naturalist Captain

1502 Thomas Matthew Berdmore (1811–1859), who was the collector of the type specimens.

1503 **Recommended English name:** Berdmore's slug-eating snake.

1504 **Remark:** The cumulative evidence from molecular and morphological data strongly

1505 suggests that the populations of "*P. carinatus*" from the mainland Indochina are divergent and

1506 morphologically different from *P. carinatus* sensu stricto from Malayan Peninsula and the

1507 Greater Sunda Islands. Our results thus agree with the data of *Wang et al. (2020)*, who compared

1508 the samples of *P. carinatus* group from southern Yunnan Province of China and Peninsular

1509 Malaysia and based on the revealed differences described the Yunnan population as a new

1510 species *P. menglaensis*. *Wang et al. (2020)* postulated that *P. menglaensis* is endemic to China,

1511 but suggested that this species also may occur in the surrounding low mountainous areas of

1512 neighboring Laos and Myanmar. However, our analyses have demonstrated that the distribution

1513 of this lineage is much wider and covers the entire territory of the mainland Indochina, including

1514 the type localities of *Pareas berdmorei Theobald, 1868* (Mon State, southern Myanmar), and of

1515 *Amblycephalus carinatus unicolor Bourret, 1934* (Kampong Speu Province, eastern Cambodia),

1516 while the Yunnan population of "*P. menglaensis*" is deeply nested within this radiation (Fig. 3).

1517 We thus conclude that the name *Pareas berdmorei Theobald, 1868*, being the eldest available

1518 synonym, has to be applied to the mainland populations of *P. carinatus* species group, while

1519 *Amblycephalus carinatus unicolor Bourret, 1934* and *Pareas menglaensis Wang, Che, Liu, Ki,*
1520 *Jin, Jiang, Shi & Guo, 2020* represent subjective junior synonyms of this taxon.

1521   Altogether, based on the concordant results of morphological and molecular analyses we
1522 report that three geographically restricted lineages exist within *P. berdmorei* (lineages 1–3, Fig.
1523 3). Despite the significant morphological variation within *P. berdmorei*, these lineages can be
1524 readily distinguished from each other by a number of chromatic and scalation characters. We
1525 propose to recognize three subspecies within *P. berdmorei*: *P. b. berdmorei* **stat. nov.** from
1526 Thailand, southern Myanmar and southern China (including *P. menglaensis* as a junior
1527 subjective synonym), *P. b. unicolor* **comb. nov.** from southern Vietnam and Cambodia, and a
1528 new subspecies *P. b. truongsonicus* **ssp. nov.** for populations from the Northern Annamite
1529 Mountains in Vietnam and Laos described below.

1530

1531   *Pareas berdmorei berdmorei* **Theobald 1868 stat. nov.**
1532   Figures 6C–D, 10, 13A–D; Supplementary Tables S11–S12.
1533   *Pareas berdmorei Theobald, 1868*: 63.
1534 **Chresonymy and synonymy:**
1535   *Pareas carinatus* — (in part) *Smith, 1943*; *Taylor, 1965*; *Yang & Rao, 2008*; *Wallach,*
1536   *Williams & Boundi, 2014*; *Chan-ard et al., 2015*.
1537   *Pareas menglaensis Wang, Che, Liu, Ki, Jin, Jiang, Shi & Guo, 2020*.

1538   **Updated diagnosis:** *Pareas berdmorei berdmorei* differs from other subspecies of *P.*
1539 *berdmorei* by the combination of the following morphological characters: body size large (TL
1540 451–770 mm); anterior pair of chin shields wider than long; loreal and prefrontal not contacting
1541 the eye; two suboculars; one postocular; temporals generally 3+4 (rarely 3+3, or 2+3); three
1542 median vertebral scale rows slightly enlarged; 9 infralabial scales; 15 dorsal scale rows slightly
1543 keeled in 5–13 scale rows at midbody; 166–186 ventrals; 57–89 subcaudals, all divided; dorsum
1544 light brown to yellowish with distinct dark vertebral spots and 64–72 transverse dark brownish or
1545 blackish bands (Fig. 13A–D); upper postorbital stripes weak generally not contacting each other
1546 on the nuchal area forming a narrow X-shaped dark marking with curved branches; ventral scales
1547 yellowish, generally immaculate, iris uniform from golden-bronze to orange (Fig. 13A–D).

1548   **Variation:** Measurements and scalation features of the subspecies *P. b. berdmorei* (n=23)
1549 are summarized in Supplementary Table S12. There is a certain variation among sexes observed

1550 in TaL/TL ratio and the number of subcadals scales: males have generally higher number of
1551 subcadals than females (73–89, average 78.33±6.67, n=6, in males vs. 57–82 average
1552 70.67±7.09, n=12 in females). In coloration, the specimens of *P. b. berdmorei* showed variation
1553 in iris color: golden-bronze iris in specimens from eastern Thailand (Fig. 13C); to orange iris in
1554 specimens from southern Yunnan and northern Thailand (Fig. 13A–B, D). Specimens also varied
1555 in the arrangement of dark markings in the nuchal area: thicker dark-brown to black markings in
1556 specimens from Thailand (Fig. 13A–C); less distinct dark markings in specimens from Laos and
1557 southern Yunnan (Fig. 13D). Other morphological features showed no significant variation
1558 among the specimens of the series examined.

1559   **Distribution:** Southeastern Myanmar, Northern peninsular Thailand north of the Isthmus
1560 of Kra, western, northern and eastern mainland Thailand, northern Laos, northern Vietnam,
1561 southernmost Yunnan Province of China; the southernmost known locality is in Suan Phueng
1562 District, Ratchaburi Province, Thailand (Fig. 1).

1563   **Recommended English name and Etymology:** as for *Pareas berdmorei*.

1564   **Ecology notes:** In Suan Phueng area (locality 14, Fig. 1), *P. b. berdmorei* occurs in
1565 sympatry with *P. c. tenasserimicus* **ssp. nov.**, though the two taxa are restricted to different
1566 habitats (see the account for *P. c. tenasserimicus* **ssp. nov.** for details). Across its range, *P. b.*
1567 *berdmorei* occurs in sympatry with various congeners, including *P. margaritophorus*, *P.*
1568 *macularius*, *P. geminatus*, and *P. xuelinensis*.

1569

1570   ***Pareas berdmorei unicolor*** **(Bourret, 1934) comb. nov.**
1571   Figures 6F, 11, 13E–F; Supplementary Tables S11–S12.
1572   *Amblycephalus carinatus unicolor Bourret, 1934*: 15.
1573 **Chresonymy:**
1574   *Pareas carinatus unicolor — Nguyen, Ho & Nguyen, 2009*.
1575   **Holotype**: MNHN 1938.0149, adult female collected by R. Bourret from "Kompong Speu"
1576 (indicated as "Kompong Pseu" on the original label, now Kampong Spoe), Kampong Spoe Prov.,
1577 eastern Cambodia.

1578   **Updated diagnosis:** *Pareas berdmorei unicolor* **comb. nov.** differs from other subspecies
1579 *P. berdmorei* by the following combination of morphological characteristics: body size medium
1580 to small (TL 459–576 mm); anterior pair of chin shields slightly longer than broad; loreal and

prefrontal not contacting the eye; two (rarely one) suboculars; two (rarely one) postoculars; temporals generally 3+3 (rarely 3+4); three median vertebral scale rows slightly enlarged; 9 infralabial scales; 15 dorsal scale rows slightly keeled in 3–9 scale rows at midbody; 162–180 ventrals; 57–75 subcaudals, all divided; dorsum uniform yellow-ochre to bright orange lacking distinct dark vertebral spots and transverse dark bands (Fig. 13E–F); upper postorbital stripes generally absent or weakly discernable not contacting each other on the nuchal area; ventral scales yellowish to orange, generally immaculate, iris uniform bright orange-red (Fig. 13E–F).

Description of the holotype (MNHN 1938.0149)**:** Adult female, specimen partially dehydrated due to preservation in ethanol for a long time (Fig. 11), body slender and notably flattened laterally; head comparatively large, narrowly elongated, clearly distinct from thin neck, snout blunt; eye rather large, pupil vertical and slightly elliptical.

Body size. SVL 390 mm; TaL 96 mm; TL 486 mm; TaL/TL: 0.198.

Body scalation. Dorsal scales in 15–15–15 rows, slightly keeled in seven scale rows at midbody, and without apical pits; three median vertebral scale rows slightly enlarged; the outermost dorsal scale row not enlarged; ventrals 164 (+ 2 preventrals), lacking lateral keels; subcaudals 64, all divided; cloacal plate single.

Head scalation. Rostral not visible from above; nasal entire; two internasals, much wider than long, narrowing and slightly curving back laterally (in dorsal view), anteriorly in contact with rostral, laterally in contact with nasal and loreal, posteriorly in contact with prefrontal, not contacting preocular; two large pentagonal prefrontals, much larger than internasals and with a slightly diagonal suture between them, not contacting the eye; single hexagonal frontal scale with its lateral sides parallel to the body axis, frontal longer than wide, smaller than parietals; two preoculars; one subocular; one postocular, not fused with subocular; one loreal in contact with prefrontal, not touching the eye; 7/7 supralabials, 3rd to 5th SL touching the subocular, none of them reaching the eye, 7th by SL the largest, elongate; temporals 3+3; 8/8 infralabials, the anterior most in contact with the opposite along midline, bordering mental, anterior 5 pairs of infralabials bordering anterior chin shields; 3 pairs of chin shields interlaced, no mental groove under chin and throat; anterior chin shields relatively large, slightly longer than broad, followed by the two pairs of chin shields that are much broader than long.

Coloration. Due to preservation in ethanol for almost a century, the color pattern has significantly faded; as the consequence the specimen no longer retains the original coloration

characteristics. Presently the specimen is uniform dark reddish-brown with no pattern discernable on the ground color (Fig. 11). The original description contains the following information on the type specimen coloration: "the color is light reddish brown, absolutely uniform, without any spots on the body or head, yellower and lighter below" (*Bourret, 1934*: 15).

Variation: Measurements and scalation features of the subspecies *Pareas berdmorei unicolor* **comb. nov.** (n=9) are presented in Supplementary Table S11. There is a certain sexual dimorphism observed in body size and the number of subcadal scales: males (TL 505.0–576.0 mm, average 552.2±40.9 mm, n=3) have slightly larger body size than females (TL 459.0–538.1 mm, average 498.4±32.6 mm, n=6); males also have a generally higher number of subcadals than females (73–75, average 73.7±1.2, n=3 in males vs. 58–75, average 66.3±5, n=6 in females). Coloration of the examined specimens varied in the ground color (from yellow-ochre to bright orange), and in the dark markings on the head and nuchal area (from upper postorbital stripes absent to weakly discernable). Other morphological features showed no significant variation among the examined specimens.

Comparisons: *Pareas berdmorei unicolor* **comb. nov.** differs from *P. b. berdmorei* by slightly lower number of ventrals (162–180 [average 173.6±5.1] vs. 166–186 [average 178.10±5.19]), by generally lower number of keeled dorsal scale rows (3–9 [average 6.8±1.9] vs. 5–13 [average 9.6±2.2]), and by uniform orange to beige coloration lacking dark markings and transverse bands (vs. present) and brighter orange-red coloration of iris (vs. golden-bronze to orange). *Pareas berdmorei unicolor* **comb. nov.** differs from *P. b. truongsonicus* **ssp. nov.** described below by slightly smaller total length (459–576 mm [average 516.3±42.5 mm] vs. 488–637 mm [average 587.0±67.6]), by a lower number of ventrals (162–180 [average 173.6±5.1] vs. 167–187 [average 179.5±9.6]), by lower number of keeled dorsal scale rows (3–9 [average 6.8±1.9] vs. 13), and by uniform orange to beige coloration lacking dark markings and transverse bands (vs. dark markings present) and brighter orange-red coloration of iris (vs. off-white to golden). For the detailed comparisons of the three subspecies of *Pareas berdmorei* see Supplementary Table S12.

Distribution: Based on our morphological and molecular data, *P. b. unicolor* **comb. nov.** inhabits the lowland and foothill tropical forests of southern Vietnam and eastern Cambodia (Fig. 1). The actual extend of the subspecies distribution in central Vietnam and central Cambodia is still unclear and requires further survey efforts.

1643   **Etymology:** The subspecies name "*unicolor*" is a Latin adjective in nominative singular

1644 meaning "monochrome" and was given in reference to the uniform coloration of this snake.

1645   **Recommended English name:** Cochinchinese slug-eating snake.

1646   **Ecology notes:** In Di Linh District, Lam Dong Province of southern Vietnam (locality 37,

1647 Fig. 1), *P. b. unicolor* **comb. nov.** occurs in sympatry with *P. temporalis* described below; these

1648 two taxa were recorded in the same habitat within the mid-elevation evergreen tropical forests of

1649 the Langbian Plateau (see the account for *P. temporalis* for details). Across its range, *P. b.*

1650 *unicolor* occurs in sympatry with other congeners, including *P. margaritophorus*, *P. macularius*,

1651 and *P. formosensis*.

1652

1653   *Pareas berdmorei truongsonicus* **Poyarkov, Nguyen TV, Vogel, Brakels &**

1654   **Pawangkhanant ssp. nov.**

1655   [urn:lsid:zoobank.org:act:3E45EE5B-8DD5-4FB1-814A-76DC2B821E29]

1656   Figures 6E, 12, 13G–H; Supplementary Tables S11–S12.

1657 **Chresonymy:**

1658   *Pareas carinatus* — (in part) *Ziegler et al., 2006, 2016*; *Nguyen, Ho & Nguyen, 2009*;

1659 *Teynié & David, 2010*; *Le et al., 2014*; *Pham & Nguyen, 2019*.

1660   **Holotype**: ZMMU R-16801 (field number NAP-09150), adult female collected by N. A.

1661 Poyarkov, P. Brakels, P. Pawangkhanant and T. V. Nguyen from limestone forest near the Tham

1662 Mangkon Cave, in Ban Nahin-Nai District, Khammouan Province, central Laos (N 18.22111, E

1663 104.81243; elevation 526 m asl.) on July 14, 2019.

1664   **Paratype**: ZMMU R-14796, adult male collected by N. A. Poyarkov and N. L. Orlov from

1665 limestone forest in environs of Kim Lich Village, Kim Hoa Commune, Tuyen Hoa District,

1666 Quang Binh Province, central Vietnam (N 18.01206, E 105.92215; elevation 41 m asl.) on

1667 September 7, 2015.

1668   **Referred specimens:** ZFMK 82890, adult male collected on July 5, 2014, and VNUH

1669 15.6.'05-1 collected on June 15, 2005 from Phong Nha - Ke Bang National Park, Quang Binh

1670 Province, Vietnam (see *Ziegler et al., 2006*).

1671   **Diagnosis:** *Pareas berdmorei truongsonicus* **ssp. nov.** differs from other subspecies of *P.*

1672 *berdmorei* by the combination of the following morphological characters: maximal total length

1673 of 637 mm; anterior pair of chin shields as long as broad; loreal and prefrontal not contacting the

1674 eye; one subocular; one postocular; temporals 3+4; three median vertebral scale rows slightly

1675 enlarged; 9 infralabial scales; 15 dorsal scale rows keeled in 13 scale rows at midbody; 167–187

1676 ventrals; 66–80 subcaudals, all divided; dorsum light brown with distinct dark-brown vertebral

1677 spots and 68–71 transverse dark bands, and with dense brownish-gray mottling covering dorsal,

1678 lateral and ventral surfaces of body and head (Fig. 13G–H); upper postorbital stripes discernable,

1679 contacting each other on the nuchal area forming a clear Y-shaped pattern; ventral scales

1680 yellowish-white with dense brownish mottling, iris uniform off-white to golden (Fig. 13G–H).

1681 **Description of the holotype** (ZMMU R-16801): Adult female, specimen in a good state of

1682 preservation (Fig. 12), body slender and notably flattened laterally; head large, narrowly

1683 elongated and flattened, clearly distinct from thin neck, snout blunt; eye large, pupil vertical and

1684 slightly elliptical.

1685 *Body size.* SVL 499 mm; TaL 123 mm; TL 622 mm; TaL/TL: 0.198.

1686 *Body scalation.* Dorsal scales in 15–15–15 rows, the medial 13 scale rows slightly keeled

1687 at midbody, all dorsal scales lacking apical pits; three median vertebral scale rows enlarged;

1688 outermost dorsal scale row not enlarged; ventrals 187 (+ 1 preventral), all lacking lateral keels;

1689 subcaudals 66; cloacal plate single.

1690 *Head scalation.* Rostral not visible from above; nasal single; internasals two, much wider

1691 than long, narrowing and slightly curving back laterally (in dorsal view), anteriorly in contact

1692 with rostral, laterally in contact with nasal and loreal, posteriorly in contact with prefrontal, not

1693 contacting preocular; two large irregular pentagonal prefrontals, much larger than internasals and

1694 with a slightly diagonal suture between them, not contacting the eye; the single frontal scale

1695 hexagonal with the lateral sides parallel to the body axis, longer than wide, smaller than parietals;

1696 one preocular; one subocular; one postocular, not fused with subocular; one loreal in contact with

1697 prefrontal, not touching the eye; 7/7 supralabials, 3rd to 5th SL touching the subocular, none of

1698 them reaching the eye, 7th SL the largest, elongate; temporals 3+4; 9/9 infralabials, the anterior

1699 most in contact with the opposite along the midline, bordering mental, anterior 5 pairs of

1700 infralabials bordering the anterior chin shields; 3 pairs of chin shields interlaced, no mental

1701 groove under chin and throat; anterior chin shields relatively large, as long as broad, followed by

1702 two pairs of chin shields that are much broader than long.

1703 *Coloration.* In life, dorsal surfaces of the head brownish with numerous marbled markings

1704 and dense brownish mottling (Fig. 13H). Head with two lateral postorbital stripes: the lower one

1705   is thick dark-brown line continuing from the middle of the eye onto the anterior part of the last
1706   supralabial; the upper one is a slightly thinner dark line running from postocular backwards to the
1707   dorsal scales on the neck (Fig. 12D). The upper postorbital stripes from the both sides of the
1708   body meet each other in the nape area forming a dark Y-shaped pattern (Fig. 13H). Lateral and
1709   ventral surfaces of the head marked with a dense brown dusting and larger dark spots (Fig. 12E–
1710   D). Dorsal surfaces light-brown with ca. 68 faint vertical dark brown bands. Ventral surfaces of
1711   the head, body and tail yellowish-cream with dense brown dusting. Iris uniform off-white, pupil
1712   black. **In preservative:** After two years of storage in ethanol the general coloration pattern has
1713   not changed (Fig. 12); yellowish tint in the coloration of dorsum, the head and eyes have faded
1714   becoming grayish-brown; other coloration features remain unchanged.

1715   **Variation:** Measurements and scalation features of the subspecies *Pareas berdmorei*
1716   *truongsonicus* **ssp. nov.** (n=4) are presented in Supplementary Table S11. The two specimens
1717   examined in our study have a very similar coloration with the two specimens from Phong Nha-
1718   Ke Bang N. P. (ZFMK 82890 and VNUH 15.6.'05-1) reported by *Ziegler et al. (2006)*; this
1719   population is geographically close (ca. 50 km direct distance; see Fig. 1, c) to the loaclity of the
1720   new subspecies in Kim Hoa Commune, Tuyen Hoa District, Quang Binh Province. However, the
1721   members of the type series of the new subspecies have slightly lower number of ventral and
1722   subcaudal scales as compared to the specimens reported in *Ziegler et al. (2006)*: VEN 187 vs
1723   167–177; SC 66–73 vs. 78–80. We also report on a population from Xe Pian N.P.A., Champasak
1724   Province, Laos (Fig. 1, b) which agrees well with the specimens examined in our study in
1725   coloration (Fig. 13, G); the morphological or genetic data on this population is lacking.
1726   Therefore, in this study we tentatively assign the specimens from Phong Nha-Ke Bang N.P. and
1727   from Xe Pian N.P.A. to *P.* cf. *b. truongsonicus* **ssp. nov.**; the taxonomic status of this population
1728   has to be clarified in the future.

1729   **Comparisons:** In our sample of four specimens *Pareas berdmorei truongsonicus* **ssp. nov.**
1730   differs from *P. b. berdmorei* by slightly higher of number of ventrals (187 vs. 166–186
1731   [178.10±5.19]), by slightly higher number of keeled dorsal scale rows (13 vs. 5–13 [9.60±2.20]);
1732   by the dense brownish mottling and bigger brown spots on dorsal, lateral, and ventral surfaces of
1733   the head and body (vs. ventral surfaces immaculate, lateral and dorsal surfaces with sparse
1734   dusting); and by uniform off-white to golden color of iris (vs. golden-bronze to orange). The new
1735   subspecies differs from *P. b. unicolor* **comb. nov.** by slightly larger maximal total length (622–

1736 637 mm vs. 459–576 mm [516.3±42.5 mm]), by a generally higher number of ventrals (187 vs.
1737 162–180 [173.6±5.1]), by a higher of number keeled dorsal scale rows (13 vs. 3–9 [6. 8±1.9]); by
1738 the presence of dark markings on dorsum and ventral surfaces, including the dark transverse
1739 bands and brownish mottling (vs. uniform orange to beige coloration lacking dark markings),
1740 and by off-white to golden coloration of iris (vs. bright orange-red color of iris). Detailed
1741 comparisons of the three subspecies of *Pareas berdmorei* are presented in Supplementary Table
1742 S12.

1743   **Distribution**: To date the new subspecies is known only from the northern portion of the
1744 Annamite (Truong Son) Mountain Range in central Vietnam and eastern Laos (localities 27–28,
1745 Fig. 1).

1746   **Etymology:** The new subspecies name "*truongsonicus*" is a Latin toponymic adjective in
1747 nominative singular, adopting the masculine gender of the genus name *Pareas*, and is given in
1748 reference to the Truong Son (Annamite) Mountain Range in Vietnam and Laos, where the new
1749 subspecies occurs.

1750   **Recommended English name:** Annanmite slug-eating snake.

1751   **Ecology notes:** In Tuyen Hoa District, Quang Binh Province of Vietnam, where the
1752 paratype of the new subspecies was collected, it was recorded in sympatry with *P.*
1753 *margaritophorus* and *P. formosensis*. This taxon seems to be associated with karst evergreen
1754 forests (*Ziegler et al., 2006*; this study). As other members of the genus *Pareas*, *Pareas*
1755 *berdmorei truongsonicus* **ssp. nov.** is a nocturnal semi-arboreal snake, all specimens were
1756 recorded while crawling on branches of bushes ca. 1 m above the ground or on limestone rocks;
1757 the diet is unknown but it likely includes terrestrial mollusks.

1758

1759   ***Pareas kuznetsovorum* Poyarkov, Yushchenko & Nguyen TV sp. nov.**
1760   [urn:lsid:zoobank.org:act:1CD26CB3-F3E9-4370-B501-6F678851C9FB]
1761   Figures 6G, 14–15; Table 2; Supplementary Tables S11, S13.

1762   **Holotype:** ZMMU R-16802 (field number NAP-10333), adult male collected by N. A.
1763 Poyarkov from the lowland semideciduous monsoon forest in Song Hinh Protected Forest, Song
1764 Hinh District, Phu Yen Province, southern Vietnam (N 12.77522, E 109.04606; elevation 583 m
1765 asl.) on January 16, 2021.

1766   **Diagnosis:** *Pareas kuznetsovorum* **sp. nov.** differs from other members of the genus

1767 *Pareas* by the combination of the following morphological characteristics: total length up to 639

1768 mm; anterior pair of chin shields longer than broad; loreal and prefrontal not contacting the eye;

1769 two suboculars; one postocular; temporals 3+4; the single median vertebral scale row slightly

1770 enlarged; 7 supralabial scales; 7–8 infralabial scales; 15 dorsal scale rows, all smooth; 167

1771 ventrals; 87 subcaudals, all divided; dorsum tan to light brown with distinct dark-brown vertebral

1772 line, blackish vertebral spots and 70 transverse dark-brown bands; upper postorbital stripes thick,

1773 black, contacting each other on the nuchal area forming a dark black Ψ-shaped chevron; lower

1774 postorbital stripes thin, black, reaching the anterior part of SL7, not continuing to the lower jaw

1775 and chin; belly yellow with sparce dark-gray dusting and brown elongated spots forming three

1776 longitudinal lines on ventrals; iris uniform off-white with beige lateral parts.

1777 **Description of the holotype** (ZMMU R-16802): Adult male, specimen in a good state of

1778 preservation (Fig. 14); body slender and notably flattened laterally; head large, narrowly

1779 elongated, clearly distinct from thin neck (head more than two times wider than neck width near

1780 the head basis); snout blunt; eye rather large, pupil vertical and elliptical.

1781 *Body size.* SVL 478 mm; TaL 161 mm; TL 639 mm; TaL/TL: 0.252.

1782 *Body scalation.* Dorsal scales in 15–15–15 rows, all scales smooth and lacking apical pits;

1783 vertebral scales slightly enlarged; the outermost dorsal scale row not enlarged; ventrals 167 (+ 1

1784 preventral), lacking lateral keels; subcaudals 87, all divided; cloacal plate single.

1785 *Head scalation.* Rostral not visible from above; nasal single; two internasals, much wider

1786 than long, narrowing and slightly curving back laterally (in dorsal view), anteriorly in contact

1787 with rostral, laterally in contact with nasal and loreal, posteriorly in contact with prefrontal, not

1788 contacting preocular; two large pentagonal prefrontals, much larger than internasals and with a

1789 straight suture between them, not in contact with eye; one hexagonal frontal, longer than wide,

1790 with the lateral sides parallel to the body axis, roughly the same size as the parietals; single

1791 preocular; single postocular, semicrescentic in shape, not fused with subocular; two suboculars;

1792 single loreal, in contact with preocular, prefrontal, internasal and nasal, not touching the eye; 7/7

1793 supralabials, 3rd to 5th SL touching the subocular, none of them reaching the eye, 7th by far the

1794 largest, elongated; 1/1 supraoculars; 3/3 anterior temporals and 3/4 posterior temporals; 8/7

1795 infralabials, the anteriormost in contact with opposite along midline forming a straight suture,

1796 bordering mental, the anterior 5 pairs of infralabials bordering the anterior chin shields; 3 pairs of

1797 chin shields interlaced, no mental groove under chin and throat; anterior chin shields relatively

1798 large, notably longer than broad, followed by the two pairs of chin shields that are much broader

1799 than long.

1800 ***Hemipenial morphology.*** Fully everted hemipenis symmetrical, bilobed, forked (Fig. 15B–

1801 C); the surface from base to crotch smooth, with several (5–6) weakly discernable dermal ridges

1802 on the asulcal surface (Fig. 15C) and few (3–4) shallow folds on the sulcal surface (Fig. 15B).

1803 Sulcus spermaticus deep, with fleshy swollen edges, bifurcate into two separate canals towards or

1804 on the apical lobes. Apical lobes curved with well-developed ornamentation, covered with large

1805 fleshy transverse occasionally interwining folds, separated with deep slits and forming a complex

1806 pattern resembling the bellows of an accordion (Fig. 15B–C).

1807 ***Coloration.*** In life, the dorsal surfaces of the head brownish with dense darker marbling

1808 (Fig. 15A). Head laterally off-white with dark-brown spots and blotches, ventrally yellowish-

1809 white with few small black spots. Head with two lateral postorbital stripes: the lower one is a thin

1810 black line starting from the posterior portion of subocular and running ventrally and posteriorly

1811 towards lower temporals to the posterior part of the 6th supralabial and further to the anterior part

1812 of 7th supralabial; the upper one is a well-defined thick black line starting from the upper part of

1813 postocular backwards to the dorsal scales of neck (Fig. 14C–D), where it joins a large rectangular

1814 black spot covering the nape, overall forming a dark black Ψ-shaped chevron pattern (Fig. 14E).

1815 Upper labials marked with a dense brown dusting. Dorsal surfaces of the body tan to light brown

1816 with a distinct dark-brown line running along the vertebral scale row, and with about 70 black

1817 vertebral spots and transverse dark-brown bands (Fig. 14A–B); ventral surfaces of the head, body

1818 and tail yellowish with sparce dark-gray dusting and brown elongated spots forming three

1819 longitudinal lines on ventrals (Fig. 14A–B). Iris uniform off-white with beige lateral parts; pupil

1820 black (Fig. 14C–D). **In preservative**: After six months of storage in ethanol the general

1821 coloration pattern has not changed; the tan coloration of dorsum slightly faded becoming light

1822 grayish-brown, light coloration on head and iris faded becoming brownish; other features of

1823 coloration remain unchanged.

1824 **Comparisons:** *Pareas kuznetsovorum* **sp. nov.** differs from *P. berdmorei* by all dorsal

1825 scales smooth (vs. 3–13 dorsal scale rows keeled), higher number of subcaudals (87 vs. 63–78

1826 [average 71.13±7.23]), by the presence of black chevron on the nuchal area (vs. absent); the new

1827 species further differs from *P. carinatus* by the presence of two postoculars (vs. single or

1828 absent); by a generally higher number of subcaudals (87 vs. 54–96 [average 69.24±8.98]), by all

1829   dorsal scale rows smooth (vs. 3–11 dorsal scale rows keeled [average 6.52±2.94]), by the

1830   presence of black nuchal chevron (vs. absent); and by a lower number of enlarged vertebral scale

1831   rows (1 vs. 3 [average 2.83±0.56]); it further differs from *P. nuchalis* (Boulenger) by prefrontal

1832   not contacting the eye (vs. in contact); by lower number of ventrals (167 vs. 201–220 [average

1833   209.89±5.25]); and by a lower number of subcaudals (87 vs. 102–120 [average 111.11±6.05]).

1834   Morphological comparisons between all species of the subgenus *Pareas* are detailed in

1835   Supplementary Table S13.

1836   **Distribution:** To date *Pareas kuznetsovorum* **sp. nov.** is known only from the type locality

1837   in the north-eastern foothills of the Langbian Plateau in Phu Yen Province of Vietnam (locality

1838   41, Fig. 1). Though only single specimen of the new species is known up to date, its occurrence

1839   is expected in the remaining fragments of lowland to mid-elevation evergereen forests of the

1840   north-western slopes of the plateau, particularly in the adjacent parts of Dak Lak and Khanh Hoa

1841   provinces of southern Vietnam.

1842   **Etymology:** The new species name "*kuznetsovorum*" is the plural possessive form of the

1843   family name Kuznetsov. This species is named in honor of two biologists, Andrei N. Kuznetsov

1844   and Svetlana P. Kuznetsova. They have greatly contributed to organization of biological

1845   expedtions of the Joint Russian-Vietnamese Tropical Center in various parts of Vietnam from

1846   1996 to 2021; without their enthusiasm and support our fieldwork in Vietnam, including the

1847   expedition during which the holotype of the new species was collected, would have not been

1848   possible.

1849   **Recommended English name:** Kuznetsovs' slug-eating snake.

1850   **Ecology notes:** The single specimen of the new species was collected in middle January

1851   during the period where most of reptile species were not active; the specimen was recorded at

1852   00:00 h while perching on a *Calamus* sp. palm leaf near a forest trail ca. 1.5 m above the ground,

1853   when the air temperature was around 12°C under a drizzling rain. The specimen was not moving.

1854   No other members of Pareidae were recorded in the area of survey. The diet of the new species is

1855   unknown but, as in other congeners, it presumably consists of terrestrial mollusks.

1856

1857   ***Pareas nuchalis* species group**

1858   The monophyly of the *nuchalis* group is strongly supported in BI-analysis, and got only

1859   poor support in ML-analysis (0.99/80); this group includes *P. nuchalis* from Borneo and Sumatra

1860 (lineage 9, Fig. 3) and two lineages from the montane areas in central and southern Vietnam, one

1861 of which we describe below as a new species, forming a strongly-supported group (1.0/100)

1862 (lineages 7–8, Fig. 3). The lineage inhabiting the Kon Tum – Gia Lai Plateau in central Vietnam

1863 represents *Pareas abros* **sp. nov.** (lineage 7, Fig. 3), and the second lineage from Langbiang

1864 Plateau in southern Vietnam corresponds to the recently described *P. temporalis* (lineage 8, Fig.

1865 3). All members of the *nuchalis* group are characterized by the presence of a large black ring-

1866 shaped blotch on the nape, connected to the upper and lower postorbital stripes anteriorly.

1867

1868 ***Pareas nuchalis* (Boulenger, 1900)**

1869 Figures 6H, 16–17; Table 2; Supplementary Tables S11, S13.

1870 *Amblycephalus nuchalis Boulenger, 1900*: 185.

1871 **Chresonymy:**

1872 *Amblycephalus nuchalis — De Rooij, 1917*: 277.

1873 *Pareas nuchalis — Malkmus & Sauer, 1996*; *Malkmus et al., 2002*; *Wallach, Williams & Boundi,*

1874 *2014*: 537.

1875 *Pareas carinatus —* (in part) *David & Vogel, 1996*.

1876 **Holotype:** NHMUK 1912247 (formely BMNH 1901.5.14.2), adult male from Saribas,

1877 Betong Division, State of Sarawak, Borneo, Malaysia (approximately N 1.410, E 111.527;

1878 elevation 15 m asl.), collected by A. H. Everett.

1879 **Updated diagnosis:** *Pareas nuchalis* differs from other members of the genus *Pareas* by

1880 the following combination of morphological characters: maximal total length up to 678 mm;

1881 anterior pair of chin shields longer than broad; loreal not contacting the eye; prefrontal in contact

1882 with the eye; 1–3 suboculars; 1–2 postoculars; temporals generally 3+4 or 3+3; one to three

1883 median vertebral scale rows slightly enlarged; 7–8 supralabial scales; generally 7 (rarely 6 or 8)

1884 infralabials; 15 dorsal scale rows at midbody, all totally smooth; 201–220 ventrals; 102–120

1885 subcaudals, all divided; dorsum tan to light brown with weak dark-brown vertebral spots and 61–

1886 78 distinct transverse dark-brown bands (Figs. 16–17); upper postorbital stripes thick, black,

1887 bifurcating posterior to the secondary temporals, forming a vertical black bar to the mouth angle;

1888 upper postorbital stripes contacting each other on the nuchal area forming a large black ring-

1889 shaped blotch (Fig. 17); lower postorbital stripes thick, black, reaching the anterior part of SL6,

1890 often continuing to the lower jaw and chin; belly yellowish immaculate or with sparce brown

1891   dusting (Figs. 16–17); iris in life whitish with brownish speckles and veins getting denser around

1892   the pupil (Fig. 17) (*Boulenger, 1900*; *Stuebing et al., 2014*; our data).

1893   **Material examined:** In this study we directly examined nine specimens of *Pareas nuchalis*

1894   from Borneo (Malaysia, Indonesia) and Sumatra, including the holotype of *Amblycephalus*

1895   *nuchalis* (see Supplementary Table S11, Appendix II).

1896   ***Coloration.*** Due to preservation in ethanol for more than a century, the coloration and the

1897   pattern of the holotype has been changed, as the consequences the type specimen no longer

1898   retains the original coloration characteristics (Fig. 16). Dorsal surface of the head uniform dark

1899   brown, head with two postorbital stripes, the upper running laterally backwards to the dorsal

1900   scales on the neck, bifurcating posterior to the secondary temporal scales, forming a dark vertical

1901   bar reaching the mouth angle, upper postorbital stripes contacting each other on the nuchal area

1902   forming a large black ring-shaped blotch (Fig. 16); lower postorbital stripes partially faded,

1903   reaching the anterior part of SL6. Dorsal surface of the body light brown with 78 vertical faint

1904   dark-brown bands; ventral surface of the body and tail yellowish-cream with sparse brown

1905   dusting.

1906   **Variation:** Measurements and scalation features of *Pareas nuchalis* specimens examined

1907   (n=9) are presented in Supplementary Table S11. There is a certain sexual variation observed in

1908   the body size, numbers of ventral and subcadal scales: males have slightly lager total length (TL

1909   345.0–678.0 mm, average 529.0±110.2 mm, n=6) than females (TL 352.0–503.0 mm, average

1910   422.3±76.0 mm, n=3); males also have generally slightly higher number of ventral and subcaudal

1911   scales than females (VEN 207–220, average 212.2±4.5, n=6; SC 108–120, average 114.2±4.7,

1912   n=6 in males vs. VEN 201–208, average 205.3±3.8, n=3; SC 102–107, average 105.0±2.7, n=3

1913   in females). Other morphological and coloration features showed no significant variation among

1914   the specimens of the examined series.

1915   **Distribution:** Until recently, this species was considered to be endemic to the island of

1916   Borneo (*Stuebing et al., 2014*), and was recorded both from the State of Sarawak and Sabah in

1917   Malaysia, Brunei and from the Indonesian part of the island (Kalimantan). In this study we for

1918   the first time recorded *P. nuchalis* from central Sumatra, where it was previously confused with

1919   *P. carinatus* (see *David & Vogel, 1996*).

1920   **Etymology:** The species name "*nuchalis*" is a Latin adjective in nominative singular
1921   meaning "nuchal" and was given in reference to the characteristic black ring-shaped spot in the
1922   nuchal area in this species.

1923   **Recommended English name:** Barred slug-eating snake.

1924

1925   ***Pareas abros* Poyarkov, Nguyen TV, Vogel & Orlov sp. nov.**
1926   [urn:lsid:zoobank.org:act:85CA3212-E8D4-48D1-8ED2-DC8CB183E7E9]
1927   Figures 6I, 18–19; Table 2; Supplementary Tables S11, S13.

1928   **Holotype:** ZMMU R-16393 (field number NAP-08867), adult male collected by N. A.
1929   Poyarkov from the montane evergreen tropical forest near the offsprings of the Paete River,
1930   within the Song Thanh N.P., La Dee Commune, Nam Giang District, Quang Nam Province,
1931   central Vietnam (N 15.53353, E 107.38434; elevation 1083 m asl.) on May 05, 2019.

1932   **Paratypes:** ZMMU R-16392 (field number NAP-06251), adult male, and ZMMU R-14788
1933   (field number NAP-06252), adult female, both collected by N. A. Poyarkov and N. L. Orlov from
1934   the montane evergreen tropical forest within the Sao La Nature Reserve, A Roang area, A Luoi
1935   Distict, Thua Thien – Hue Province, central Vietnam (N 16.10334, E 107.444453; elevation 796
1936   m asl.) on September 11–17, 2015.

1937   **Diagnosis:** *Pareas abros* **sp. nov.** differs from all other members of the genus *Pareas* by
1938   the combination of the following morphological characters: body size medium (TL 434–565
1939   mm); head notably flattened dorsoventrally; anterior pair of chin shields longer than broad; loreal
1940   and prefrontal not contacting the eye; three suboculars; two postoculars; temporals 3+3; the
1941   single median vertebral scale row slightly enlarged; 9 supralabial scales; generally 8 (rarely 9)
1942   infralabials scales; 15 dorsal scale rows at midbody, of them 9–11 median scale rows slightly
1943   keeled; 180–184 ventrals; 83–95 subcaudals, all divided; dorsum yellowish-brown with distinct
1944   dark-brown vertebral line, barely distinct blackish vertebral spots and 44–56 faint interrupted
1945   transverse dark-brown bands (Fig. 19A–C); upper postorbital stripes thick, slate-black,
1946   bifurcating posterior to the secondary temporals, forming a thick black line, continuing to the 7th
1947   SL and further on the neck; upper postorbital stripes contacting each other on the nuchal area
1948   forming a large ring-shaped blotch (Fig. 19A–C); two thick, black lower postorbital stripes
1949   reaching the 6th and 8th SL, and continuing to the lower jaw; belly beige with dense brownish-
1950   gray dusting and dark brown elongated spots forming two longitudinal lines on the lateral sides

1951 of ventrals (Fig. 18D); iris in life beige with ochraceous to orange speckles and veins getting
1952 denser around the pupil (Fig. 19).

1953   **Description of the holotype** (ZMMU R-16393): Adult male, specimen in a good state of
1954 preservation (Fig. 18); body slender and notably flattened laterally; head very large, notably
1955 flattened dorsoventrally, clearly distinct from thin neck (head more than two times wider than
1956 neck near the head basis), snout obtusely rounded in profile and in dorsal view; eye very large,
1957 pupil vertical and elliptical. Hemipenis not everted.

1958   *Body size.* SVL 314 mm; TaL 120 mm; TL 434 mm; TaL/TL: 0.276.

1959   *Body scalation.* Dorsal scales in 15–15–15 rows, slightly keeled on 11 upper scale rows at
1960 midbody (Fig. 18F), all lacking apical pits; the single median vertebral scale row slightly
1961 enlarged; the outermost dorsal scale row not enlarged; ventrals 184 (+ 1 preventral), lacking
1962 lateral keels; subcaudals 92; cloacal plate single.

1963   *Head scalation.* Rostral not visible from above; single nasal; two internasals, much wider
1964 than long, narrowing and slightly curving back laterally (in dorsal view), anteriorly in contact
1965 with rostral, laterally in contact with nasal and loreal, posteriorly in contact with prefrontal, not
1966 contacting preocular; two large irregularly pentagonal prefrontals, much larger than internasals
1967 and with a straight suture between them, not in contact with eye; the single frontal scale
1968 hexagonal with the lateral sides slightly concave, parallel to the body axis, longer than wide,
1969 smaller than parietals; single preocular; two postoculars, semicrescentic in shape, not fused with
1970 subocular; single presubocular; three suboculars; two loreals, upper larger then lower, irregularly
1971 pentagonal, in contact with presubocular, prefrontal, internasal and nasal, not touching the eye;
1972 9/9 supralabials, 4th to 6th SL touching the subocular, none of them reaching the eye, 9th by far the
1973 largest, elongated; 1/1 supraoculars; 3/3 anterior temporals and 3/3 posterior temporals; 8/8
1974 infralabials, the anteriormost in contact with the opposite along midline forming a diagonal
1975 suture between them, bordering mental, the anterior five pairs of infralabials bordering the
1976 anterior chin shields; 3 pairs of chin shields interlaced, no mental groove under chin and throat;
1977 the anterior chin shields relatively large, much longer than broad, followed by two pairs of chin
1978 shields that are much broader than long.

1979   *Coloration.* In life, dorsal and ventral surfaces of the head brownish with dense dark-brown
1980 mottling. Head with three lateral postorbital stripes: the upper postorbital stripes thick, slate-
1981 black lines running from postocular backwards towards the dorsal scales of neck, bifurcating

1982   posterior to the secondary temporals, forming a ventral branch – a thick black line, continuing to

1983   the 9th SL and further to the posterior corner of the jaw and on the neck; the dorsal branch

1984   extending to the top of the nape contacting each other on the nuchal area; both of the branches of

1985   the upper postorbital stripe join at the front of the neck to form a large black ring-shaped blotch

1986   that covers the entire nape area (Fig. 18C). Two lower postorbital stripes: the posterior one is a

1987   thick, black line starting from the lower portion of postorbital, running ventrally and posteriorly

1988   towards lower temporals to 8th and 9th supralabials, and further and continuing to the lower jaw;

1989   the anterior lower postorbital stripe is a short thick black vertical stripe starting from the middle

1990   subocular, reaching the 6th SL and continuing further to the 4th IL as a line of black spots (Fig.

1991   18C). Upper labials beige with dense brown dusting. Dorsal surfaces of body yellowish-brown

1992   with distinct dark-brown line running along the vertebral dorsal scale row, barely distinct

1993   blackish vertebral spots and ca. 56 faint interrupted transverse dark-brown bands (Fig. 18A–B).

1994   Ventral surfaces of the head, body and tail cream-beige with dense brownish-gray dusting and

1995   dark brown elongated spots forming two longitudinal lines on the lateral sides of ventrals (Fig.

1996   18D). Iris in life beige with orange speckles and veins getting denser around the pupil; pupil

1997   black (Fig. 18C). **In preservative**: After two years of storage in ethanol the general coloration

1998   pattern did not change; the tan tint of the dorsal coloration, and orange tints on the head and eye

1999   have faded becoming grayish-brown; other features of coloration remain unchanged.

2000   **Variation:** Measurements and scalation features of the type series (n=3) is presented in

2001   Supplementary Table S11. The holotype has two loreals while there is only one in the two

2002   paratypes. There is a certain variation observed in the number of ventral and dorsal scales: males

2003   have higher number of subcaudals (92–95, n=2) than the single female (83, n=1); dorsal scales

2004   are keeled in 11 scale rows at midbody in males vs. in 9 scale rows are keeled in the single

2005   female. Coloration features among the members of the type series were very similar.

2006   ***Hemipenial morphology.*** The hemipenis is partially everted in the adult male paratype

2007   ZMMU R-16392 (Fig. 19D). The partially everted organ symmetrical, bilobed, forked, the

2008   surface from base to crotch smooth, with numerous (7–11) shallow folds and on the sulcal

2009   surface and fewer 3–6 larger dermal ridges on the asulcal surface. Sulcus spermaticus deep, with

2010   fleshy swollen edges, bifurcating into two separate canals towards the apical lobes. Apical lobes

2011   with well-developed ornamentation, covered with large fleshy irregularly curved folds in 4–5

2012 rows and fleshy protuberances, separated with deep slits, forming a complex pattern resembling
2013 brain cortex.

2014 **Comparisons:** *Pareas abros* **sp. nov.** differs from *P. berdmorei* by the anterior pair of chin
2015 shields longer than broad (vs. broader than long), by slightly longer tail (TaL/TL 0.26–0.29
2016 [average 0.28±0.01] vs. 0.17–0.27 [average 0.21±0.02]), by slight higher number of ventrals (83–
2017 95 [average 90.00±6.24] vs. 57–89 [average 71.13±7.25]), by the presence of a large ring-shaped
2018 black blotch in the nuchal area (vs. absent); and by the presence of the dark vertebral line (vs.
2019 absent). The new species differs from *P. carinatus* by longer tail (TaL/TL 0.26–0.29 [average
2020 0.28±0.01] vs. 0.18–0.25 [average 0.22±0.02]), by a slightly higher number of subcaudals (83–95
2021 [average 90.0±6.2] vs. 54–96 [average 69.2±9.0]), by the presence of a large ring-shaped black
2022 blotch in the nuchal area (vs. absent); by the presence of the dark vertebral line (vs. absent); and
2023 by weakly-discernable faint transverse dark bands on body (vs. well-discernable dark bands).
2024 *Pareas abros* **sp. nov.** differs from *P. nuchalis* by prefrontal not in contact with the eye (vs. in
2025 contact); by 9–11 dorsal scale rows keeled (vs. all dorsal scales totally smooth); and by the black
2026 nuchal blotch forming a complete ring (vs. incomplete ring-shaped blotch). The new species
2027 differs from *P. kuznetsovorum* **sp. nov.** (described above) by a higher number of ventrals (180–
2028 184 [average 182.7±2.3] vs. 167); by keeled 9–11 dorsal scale rows (vs. all dorsal scales totally
2029 smooth); by smaller body size (TL 434–565 mm [average 506.7±66.7 mm] vs. 639 mm). *Pareas*
2030 *abros* **sp. nov.** differs from *Pareas temporalis* by a slightly lower number of ventrals (180–184
2031 vs. 185–198), by weak keels present only on 9–11 dorsal scale rows (vs. all dorsal scale rows
2032 strongly keeled), by a lower number of enlarged vertebral scales rows (1 vs. 3), and by having
2033 44–56 faint dark transverse bands (vs. absence of dark cross-bands on the body). Morphological
2034 comparisons between all species of the subgenus *Pareas* are detailed in Table 2 and
2035 Supplementary Table S13.

2036 **Distribution:** The new species is to date known only from two localities in Quang Nam
2037 (locality 42, Fig. 1) and Thua Thien – Hue (locality 43, Fig. 1) provinces of central Vietnam,
2038 both of them are located within the Kon Tum – Gia Lai Plateau, the northern portion of the
2039 Central Highlands (Tay Nguyen) Region of Vietnam. The Kon Tum – Gia Lai Plateau is isolated
2040 from the adjacent mountain massifs by lowland areas and is characterized by a high level of
2041 herpetofaunal endemism (*Bain & Hurley, 2011*; *Poyarkov et al., 2021*); the new species is also
2042 likely an endemic of this mountain region. The holotype of the new species was collected in just

2043   2 km from the national border of Vietnam and Lao PDR (locality 42, Fig. 1), hence the

2044   occurrence of *Pareas abros* **sp. nov.** in Laos is highly anticipated.

2045   **Etymology:** The new species name "*abros*" is a Latinized adjective in nominative singular

2046   derived from the classical Greek word "*abros*" (*αβρός*), meaning "cute", "handsome", and

2047   "delicate". The name is given in reference to the appealing and cute appearance of the new

2048   species, as well as other members of the genus *Pareas*.

2049   **Recommended English name:** Cute slug-eating snake.

2050   **Ecology notes:** *Pareas abros* **sp. nov.** inhabits montane evergreen tropical forests of Kon

2051   Tum – Gia Lai Plateau and was recorded on the elevations from 796 to 1,083 m asl. In both

2052   localities, the new species was recorded in fragments of primary polydominant forest along the

2053   banks of montane streams. The new species was active at 21:00 – 00:00 h, the specimens were

2054   usually located while crawling on the branches of bushes and trees ca. 1–1.5 m above the

2055   ground; the holotype was spotted while crossing a small forest trail. Other sympatric members of

2056   Pareidae in both localities include *Pareas formosensis*. The diet of *Pareas abros* **sp. nov.** is

2057   unknown; it likely consists of terrestrial mollusks as in other congeners.

2058

2059   ***Pareas temporalis*** **Le, Tran, Hoang & Stuart, 2021**

2060   Figures 6J, 20–21; Table 2; Supplementary Tables S11, S13.

2061   **Holotype:** UNS 09992 (field number LD25711), adult female, Doan Ket Commune, Da

2062   Huoai District, Lam Dong Province, Vietnam (11.340370°N, 107.620561°E, elevation of 496 m

2063   a.s.l.), coll. 25 July 2020 by Duong T.T. Le and Thinh G. Tran.

2064   **Reffered specimens** (n=6): ZMMU R-13656 (field number NAP-01610), adult male

2065   collected by N. A. Poyarkov from the low-elevation disturbed bamboo forest within the valley of

2066   the Sui Lan River in the environs of Ben Cau and Phuok Son ranger stations, Cat Loc sector of

2067   the Cat Tien National Park, Lam Dong Province, southern Vietnam (N 11.69444, E 107.30639;

2068   elevation 135 m asl.) on June 20, 2011; DTU 471, adult female, collected by L. H. Nguyen and

2069   H. M. Pham from the valley of Suoi Lanh Stream, Rung Ge Commune, Di Linh District, Lam

2070   Dong Province, southern Vietnam (N 11.46725, E 108.06915; elevation of ca. 1,320 m asl.) on

2071   March 1, 2019; SIEZC 20214, adult female, collected by L. H. Nguyen in Gia Bac District, Lam

2072   Dong Province, southern Vietnam (N 14.220392, E 108.317133; elevation of ca. 1,050 m asl.) on

2073   August 10, 2018; and SIEZC 20215, adult female, collected by V. B. Tran from Biduop – Nui Ba

2074   N.P., Lam Dong Province, southern Vietnam (N 12.23383, E 108.44866; elevation of ca. 790 m

2075   asl.) on May 30, 2017; DTU 486–487 (two adult females) collected by T. A. Pham and T. V.

2076   Nguyen in Rung Ge Commune, Di Linh District, Lam Dong Province, southern Vietnam (N

2077   11.46725, E 108.06915; elevation of ca. 1,320 m asl.), on May 10, 2020.

2078   **Remark:** Until our study this recently discovered species was known only from a single

2079   female specimen (*Le et al., 2021*). In the present work we provide morphological and genetic

2080   data for six additional specimens of this species of the both sexes from three previously unkown

2081   localities from southern Vietnam (see Fig. 1).

2082   **Updated diagnosis:** *Pareas temporalis* differs from other members of the genus *Pareas* by

2083   the following combination of morphological characters: body size large (TL 555–665 mm); head

2084   distinctly flattened dorsoventrally; the anterior pair of chin shields notably longer than broad;

2085   loreal and prefrontal not contacting the eye; two suboculars; generally two (rarely one or absent)

2086   postoculars; temporals generally 3+3 (rarely 3+4); three median vertebral scale rows slightly

2087   enlarged; generally 8 (rarely 7) supralabial scales; generally 8 (rarely 7) infralabials scales; 15

2088   dorsal scale rows, all of them notably keeled; 187–198 ventrals; 86–92 subcaudals, all divided;

2089   dorsum bright yellowish-brown to light-orange with distinct blackish vertebral line edged with

2090   two light yellowish paravertebral lines; vertebral spots and transverse dark bands absent (Fig.

2091   21); dorsal scales with few scattered small black spots; two very clear thin black postorbital

2092   stripes beginning from the lower and upper edges of each postorbital scale; the lower postorbital

2093   stripe as two thin parallel black lines reaching the anterior part of 8th SL, not continuing to the

2094   lower jaw and chin; the left and right upper postorbital stripes contacting each other at the nuchal

2095   area forming a black ring-shaped blotch (Fig. 21A–C); belly yellowish-cream with sparse

2096   brownish dusting and irregular small spots; iris in life amber-colored to bright-orange (Fig. 21A–

2097   C).

2098   **Description of a male specimen** (ZMMU R-13656): Adult male, specimen in a good state

2099   of preservation, body dissected longitudinally along the ventral scales (Fig. 20); body slender and

2100   notably flattened laterally; head very large, distinctly flattened dorsoventrally, clearly distinct

2101   from the thin neck (head more than three times wider than neck width near the head basis), snout

2102   blunt in dorsal and lateral views; eye very large, pupil vertical and elliptical. Hemipenis not

2103   everted.

2104   ***Body size.*** SVL 413 mm; TaL 142 mm; TL 555 mm; TaL/TL: 0.256.

2105   ***Body scalation.*** Dorsal scales in 15–15–15 rows, all scales notably keeled and lack apical

2106   pits; vertebral scale rows and the two adjacent rows of scales (3 medial dorsal scale rows)

2107   slightly enlarged; the outermost dorsal scale row not enlarged; ventrals 198 (+ 1 preventral),

2108   lacking lateral keels; subcaudals 98, all paired; cloacal plate single.

2109   ***Head scalation.*** Rostral not visible from above; single nasal; two internasals, much wider

2110   than long, narrowing and slightly curving back laterally (in dorsal view), anteriorly in contact

2111   with rostral, laterally in contact with nasal and loreal, posteriorly in contact with prefrontal, not

2112   contacting preocular; two large irregular pentagonal prefrontals, much larger than internasals and

2113   with a slightly diagonal suture between them, not in contact with the eye; one subhexagonal

2114   frontal, longer than wide, smaller than parietals, with the lateral sides almost parallel to each

2115   other, slightly converging posteriorly; single preocular; single postocular present on the left side,

2116   absent on the right side of the head, semicrescent in shape, not fused with subocular;

2117   presubocular absent; two suboculars; single loreal, in contact with presubocular, prefrontal,

2118   internasal and nasal, not touching the eye; 9/9 supralabials, 3rd to 5th or 3rd to 7th SL touching the

2119   subocular, none of them reaching the eye, 9th by far the largest, elongated; 1/1 supraocular; 3/3

2120   anterior temporals and 3/4 posterior temporals; 7/8 infralabials, the anterior most in contact with

2121   the opposite along the midline forming a diagonal suture between them, bordering mental, the

2122   anterior five pairs of infralabials bordering the anterior chin shields; three pairs of chin shields

2123   interlaced, no mental groove under chin and throat; the anterior chin shields relatively large,

2124   much longer than broad, followed by two pairs of chin shields that are much broader than long.

2125   ***Coloration.*** In life, dorsal surface of the head brownish with some blackish mottling and

2126   larger spots, getting denser on frontal and prefrontals. Head with two clear thin black lateral

2127   postorbital stripes: the upper one is a well-developed slate-black line starting from postocular and

2128   running backwards to dorsal scales of the neck, the left and right upper postorbital stripes

2129   contacting each other at the nuchal area forming a black X-shaped pattern in dorsal view (Fig.

2130   20E), and a large ring-shaped blotch in lateral view (Fig. 20C); the lower postorbital stripe is an

2131   interrupted black line starting from the lower portion of postorbital, and running ventrally and

2132   posteriorly towards lower temporals and to 8th and 7th supralabials and not continuing to the

2133   lower jaw and chin. Other markings on the lateral surfaces of the head include a large dark,

2134   elongated spot on the 6th supralabial, and a thick slate-black line running from the posterior edge

2135   of the 9th supralabial backwards to the and further on the lateral surfaces of the neck, where it

2136 joins the ring-shaped nuchal blotch ventrally (Fig. 20C; Fig. 21A). Supralabials yellowish-white

2137 with rare tiny brown spots. Dorsal surfaces of the body bright yellowish-brown to light-orange

2138 with distinct blackish vertebral line edged with two light yellowish paravertebral lines; vertebral

2139 spots and transverse dark bands absent (Fig. 21); dorsal scales on the sides of the body with few

2140 irregularly scattered small dark spots; the ventral surfaces of the head, body and tail is yellowish-

2141 cream with sparse brownish dusting and irregular small spots; iris in life amber-colored to bright-

2142 orange; pupil black (Fig. 21A–C). **In preservative**: After ten years of storage in ethanol, the

2143 general coloration pattern has not changed; light brownish and yellowish tints in the coloration of

2144 dorsum, head and eyes faded becoming grayish-brown; other features of the coloration remain

2145 unchanged (Fig. 20).

2146   **Variation:** Measurements and scalation features of additional specimens of *P. temporalis*

2147 (n=7) is presented in Supplementary Table S11. All coloration features of the additional

2148 specimens are very similar to those described for the holotype (*Le et al., 2021*). The holotype

2149 UNS 09992 generally agrees with the series of specimens examined by us, it has slightly higher

2150 number of supralabials (9/8 vs. 7–8) and infralabials (8/9 vs. 7–8), higher number of anterior

2151 temporals (4/5 vs. 3/3), and generally slightly lower number of posterior temporals (3/3 vs. 3–4),

2152 it also has 2/3 postoculars, while in the specimens we examined generally had 2/2 postoculars

2153 and 1/0 postoculars in the single male specimen ZMMU R-13656. We observed a certain sexual

2154 dimorphism in *P. temporalis*: male ZMMU R-13656 has a higher number of ventrals (198 in a

2155 single male vs. 185–188 in five females), and subcaudals (92 in male vs. 86–89 in five females).

2156 Other morphological and chromatic features showed no significant variation among the

2157 examined specimens.

2158   **Updated comparisons:** *Pareas temporalis* differs from its sister species *Pareas abros* **sp.**

2159 **nov.** by a higher number of ventrals (185–198 vs. 180–184), by all dorsal scale rows strongly

2160 keeled (vs. weak keels present only on 9–11 dorsal scale rows), by a higher number of enlarged

2161 vertebral scales rows (3 vs. 1), and by the absence of dark cross-bands on the body (vs. 44–56

2162 faint dark transverse bands present). *Pareas temporalis* differs from *P. berdmorei* by a higher

2163 number of ventrals (185–198 vs. 164–186), by a higher number of subcaudals (86–92 vs. 63–78),

2164 by the presence of a black ring-shaped blotch on the collar (vs. absent), and by having all dorsal

2165 scale rows strongly keeled (vs. weak keels present only on 3–13 dorsal scale rows). *Pareas*

2166 *temporalis* differs from *P. carinatus* by having two postoculars (vs. single or absent); by

2167   generally slightly higher number of subcaudals (86–92 vs. 54–96), by having all dorsal scale

2168   rows strongly keeled (vs. weak keels present on 3–11 dorsal scale rows), and by the presence of

2169   a black ring-shaped blotch on the collar (vs. absent). *Pareas temporalis* differs from *P. nuchalis*

2170   by prefrontal not contacting the eye (vs. in contact), by a slightly lower number of ventrals (187–

2171   198 vs. 201–220), by a lower number of subcaudals (86–92 vs. 102–120), and by having all

2172   dorsal scale rows strongly keeled (vs. all dorsal scales smooth). Finally, *P. temporalis* differs

2173   from *Pareas kuznetsovorum* **sp. nov.** in having all dorsal scale rows strongly keeled (vs. all

2174   dorsal scales smooth), by a higher number of enlarged vertebral scales rows (3 vs. 1), and by a

2175   higher number of vetrals (185–198 vs. 167). Morphological comparisons between all species of

2176   the subgenus *Pareas* are detailed in Supplementary Table S13.

2177   **Updated distribution:** In addition to the type locality of this species, *P. temporalis* is also

2178   known from four localities, all in the Lam Dong Province of southern Vietnam (localities 37–40,

2179   Fig. 1). All these localities belong to the Langbian (Da Lat) Plateau – the southernmost part of

2180   the Annamite Range, well-known by its high level of endemism in herpetofauna (*Bain & Hurley,*

2181   *2011*; *Poyarkov et al., 2021*). We assume that *Pareas temporalis* is endemic to the Langbian

2182   Plateau; it is expected to occur on middle elevations in the adjacent provinces of southern

2183   Vietnam: Binh Phuoc, Dak Nong, Dak Lak, Ninh Thuan and Binh Thuan, and also likely might

2184   inhabit the southeasternmost part of the Mondulkiri Province of Cambodia.

2185   **Etymology:** The species name "*temporalis*" is a Latin adjective in nominative singular,

2186   meaning "temporal" and was given in reference tothe high number of temporal scales in this

2187   species (*Le et al., 2021*).

2188   **Recommended English name:** Di Linh slug-eating snake.

2189   **Ecology notes:** *Pareas temporalis* is a nocturnal, elusive forest-dwelling snake inhabiting

2190   mid-elevation montane evergreen tropical forests of the Langbian Plateau and its foothills; it was

2191   recorded from elevations from 135 to 1,320 m asl. All specimens were spotted after rain at night

2192   between 21:00 and 01:00 h while crawling or perching on branches of bushes, bamboo and

2193   *Calamus* sp. palm leafs. The holotype was found at 21:00 h on a tree branch 1.5 m above the

2194   ground in disturbed mixed broadleaf and bamboo forest, where it occurred in sympatry with P.

2195   *margaritophorus* (*Le et al., 2021*). Diet of *P. temporalis* is unknown, but as in other congeners, it

2196   likely consists of terrestrial mollusks. It is sympatric with a number of other *Pareas* species

2197   across its range, and is commonly recorded in the same habitats with *P. b. unicolor* **comb. nov.**

2198 In Di Linh District of Lam Dong Province, *P. temporalis* was recorded in sympatry with four
2199 species of the genus *Pareas*, including *P. b. unicolor* **comb. nov.**, *P. margaritophorus*, *P.*
2200 *macularius* and *P. formosensis*. With five species of *Pareas* co-occurring in the same habitat, the
2201 area of Di Linh represents the center of the genus diversity in Vietnam.

2202
2203 **Subgenus *Eberhardtia* Angel, 1920 stat. nov.**
2204 *Eberhardtia Angel, 1920*: 291, by monotypy.
2205 **Synonymy:**
2206 *Northpareas Wang et al., 2020*: Appendix S3 (*nomen nudum*).
2207 **Type species:** *Eberhardtia tonkinensis* Angel, 1920; this taxon is currently considered a
2208 junior synonym of *Pareas formosensis* (Van Denburgh, 1909); see *Ding et al. (2020)* for
2209 discussion.
2210 **Phylogenetic definition:** *Eberhardtia* is a maximum crown-clade name referring to the
2211 clade originating with the most recent common ancestor of *Pareas formosensis* and *Pareas*
2212 *monticola*, and includes all extant species that share a more recent common ancestor with these
2213 taxa than with *Pareas carinatus*.
2214 **Diagnosis:** The members of the subgenus *Eberhardtia* differ from the members of the
2215 subgenus *Pareas* by the following combination of morphological characters: frontal
2216 subhexagonal to diamond-shaped with its lateral sides converging posteriorly (Fig. 5A); anterior
2217 pair of chin shields longer than broad (Fig. 5I–J); a single thin elongated subocular; and the
2218 ultrastructure of dorsal scales not ravine-like, having pore and arc structures, with arcs
2219 connecting to each other forming characteristic lines (*Wagler, 1830*; *Smith, 1943*; *Taylor, 1965*;
2220 *Vogel et al., 2020*; *He, 2009*; *Guo et al., 2020*; our data; see Supplementary Table S14 for
2221 details).
2222 **Etymology:** *Angel (1920)* dedicated his new genus to the collector of the single specimen
2223 of its type species, the French botanist Philippe Albert Eberhardt (1874–1942).
2224 **Distribution**: Distributed in the north-eastern part of the Oriental zoogeographic region
2225 from the Eastern Himalaya to central and eastern China, islands of Hainan, Taiwan and the
2226 southern Ryukyus, southwards throughout the Indochina to the Peninsular Malaysia and
2227 Sumatra.
2228 **Content:** 20 species, including *P. andersonii* Boulenger; *P. atayal* You, Poyarkov & Lin;

2229   *P. boulengeri* (Angel); *P. chinensis* (Barbour); *P. formosensis* (van Denburgh); *P. geminatus*

2230   Ding, Chen, Suwannapoom, Nguyen, Poyarkov & Vogel; *P. hamptoni* (Boulenger); *P. iwasakii*

2231   (Maki); *P. kaduri* Bhosale, Phansalkar, Sawant, Gowande, Patel & Mirza; *P. komaii* (Maki); *P.*

2232   *macularius* Theobald; *P. margaritophorus* (Jan); *P. modestus* Theobald; *P. monticola* (Cantor);

2233   *P. niger* (Pope); *P. nigriceps* Guo & Deng; *P. stanleyi* (Boulenger); *P. victorianus* Vogel,

2234   Nguyen & Poyarkov; *P. vindumi* Vogel; and *P. xuelinensis* Liu & Rao.

2235   **Recommended English name:** Northern slug-eating snakes.

2236

2237   **DISCUSSION**

2238   ***Phylogeny and classification of Pareinae***

2239   In this study, we present an updated multilocus phylogeny for the ancient Asian subfamily

2240   of slug-eating snakes, the Pareinae. We estimate the basal divergence within the Pareinae as the

2241   late Eocene (ca. 39.3 mya) making this group one of the oldest radiations of Colubroidea snakes

2242   (*Zaher et al., 2019*; *Li et al., 2020*). Our study includes representatives of all currently recognized

2243   taxa within of the subfamily and is, to the best of our knowledge, the most comprehensive among

2244   the published works both in terms of taxon and gene sampling. Our integrative analysis of the

2245   molecular and morphological data resolves several long-standing systematic controversies

2246   regarding the subfamily Pareinae. In particular, we confidently resolve the phylogenetic

2247   relationships among the three genera of the Pareinae: *Aplopeltura* is strongly suggested as the

2248   sister genus of *Pareas* sensu lato, while the genus *Asthenodipsas* is reconstructed as the most

2249   basal taxon within the subfamily with sister relationships to the clade *Aplopeltura + Pareas*. This

2250   topology contradicts several earlier studies on the taxonomy of the group (e. g., *Guo et al., 2011*;

2251   *Wang et al., 2020*), but generally agrees with the recent multilocus phylogenetic study by *Deepak*

2252   *et al. (2019)*, though in our phylogeny we got higher values of node support.

2253   We also provide strong evidence for the monophyly of all Pareinae genera. While

2254   monophyly of the presently monotypic genus *Aplopeltura* was never questioned, a number of

2255   studies suggested that the genera *Pareas* and *Asthenodipsas* might represent paraphyletic taxa

2256   (*Guo et al., 2011*; *Pyron et al., 2011*; *Wang et al., 2020*), or were recovered as monophyletic

2257   groups but without a significant support (e.g., *Deepak et al., 2019*). At the same time, we

2258   demonstrate the deep differentiation within both *Pareas* and *Asthenodipsas*, each of these genera

2259   comprises two reciprocally monophyletic groups, which diverged almost simultaneously during

2260 the early to middle Oligocene (ca. 30–31.3 mya). We also show that, though the monophyly of

2261 *Pareas* and *Asthenodipsas* is not questioned anymore, the major clades within these genera

2262 demonstrate significant differences among each other in external morphology, scale

2263 microornamentation, and biogeographic affinities; similar results were also obtained by a number

2264 of earlier studies (*Grossmann & Tillack, 2003*; *He, 2009*; *Guo et al., 2011*; *Guo, Wang &*

2265 *Rao2020*; *Wang et al., 2020*). We argued that the groups within *Pareas* and *Asthenodipsas*

2266 should be taxonomically recognized, what would enhance the diagnosability and clade stability

2267 of these taxa, make them more comparable units to other snake genera, restrain taxonomic

2268 vandalism, and eventually fully stabilize the taxonomy of Pareinae. Therefore, we recognize two

2269 subgenera within the genus *Pareas* sensu lato (*Pareas* sensu stricto and *Eberhardtia* **stat. nov.**),

2270 and two subgenera within the genus *Asthenodipsas* sensu lato (*Asthenodipsas* sensu stricto and

2271 *Spondylodipsas* **subgen. nov.**). Earlier studies which addressed the genus-level taxonomy of

2272 *Pareas* have either wrongly identified the type species of the genus (*Guo et al., 2011*), or have

2273 overlooked the existence of an available genus-level name for one of the clades (*Eberhardtia*

2274 Angel, 1920), what resulted in the creation of a nomen nudum ('*Northpareas*', see *Wang et al.,*

2275 *2020*). We would like to emphasize the importance of a thorough analysis of the available

2276 literature and possible synonyms prior to making a taxonomic decision in order to prevent

2277 publication of unavailable names or junior synonyms. Within the genus *Pareas*, our phylogenetic

2278 results support the recognition of two species groups within the subgenus *Pareas* sensu stricto (*P.*

2279 *carinatus* and *P. nuchalis* groups), and four species groups within the subgenus *Eberhardtia* **stat.**

2280 **nov.** (*P. hamptoni*, *P. chinensis*, *P. margaritophorus*, and *P. monticola* groups) (see Fig. 3); this

2281 taxonomy is largely concordant with the results of the previous studies (*Guo et al., 2011*; *You,*

2282 *Poyarkov & Lin, 2015*; *Bhosale et al., 2020*; *Vogel et al., 2020, 2021*; *Wang et al., 2020*; *Ding et*

2283 *al., 2020*).

2284   Although our understanding of the phylogenetic relationships within the Pareinae is now

2285 improved, it is still far from complete. For example, our phylogeny included only five of nine

2286 currently recognized species of *Asthenodipsas*; five species of the genus were described within

2287 the last decade, of which four were described based solely on morphological evidence (*Quah et*

2288 *al., 2019, 2020, 2021*). We would like to further stress herein that in this age of molecular

2289 genetics and biodiversity crises, the application of molecular methods became crucial for

2290 taxonomic practice in studies of herpetofaunal diversity in Southeast Asia (*Smith et al., 2008*;

2291 *Murphy et al., 2013*). Not only the phylogenetic hypothesis is crucial for any comparative or
2292 biogeographic analyses, it now also became a keystone of biodiversity conservation (*Shaffer et*
2293 *al., 2015*; *Chomdej et al., 2020*). Phylogenetic studies on the remaining species of *Asthenodipsas*
2294 are required to fully resolve the taxonomy of the genus; furthermore, additional taxon and gene
2295 sampling will likely enhance the phylogenetic resolution on the level of the subfamily Pareinae
2296 and might lead to discovery of additional new lineages and species.

2297

2298 ### *Underestimated species diversity of Pareas in Indochina*

2299   Though not being the most species-rich group of Asian snakes, the slug-eating snakes are
2300 widely distributed across the Southeast Asia and have a number of specialized morphological
2301 and ecological characteristics that are hypothesized to facilitate speciation. Being dietary
2302 specialists on terrestrial slugs and snails, the Pareinae occupy ecological niches inaccessible to
2303 other groups of Asian snakes, at the same time several species of the slug-eating snakes can
2304 successfully coexist with their congeners, likely due to niche partitioning and further
2305 specialization in preferred prey, dentition asymmetry, and feeding behavior (*Chang et al., 2021*).
2306 For example, up to three closely-related species of *Pareas* share same habitats in the areas of
2307 sympatry in Taiwan (*You, Poyarkov & Lin, 2015*; *Chang et al., 2021*); we report for the first time
2308 the sympatric co-occurrence of six *Pareas* species in the montane forests of Lam Dong Province
2309 of southern Vietnam (*P. temporalis*, *P. kuznetsovorum* **sp. nov.**, *P. b. unicolor*, *P. macularius*, *P.*
2310 *margaritophorus*, and *P. formosensis*), of which five species were recorded sharing the same
2311 habitat in Di Linh District. On the other hand, the sympatric co-occurrence of several often
2312 closely related species of *Pareas*, often makes correct species identification difficult, and may
2313 also lead to some cryptic species being overlooked.

2314   Several recent taxonomic studies on *Pareas* have demonstrated that this genus has a high
2315 level of hidden and yet undescribed diversity (e.g. *You, Poyarkov & Lin, 2015*; *Bhosale et al.,*
2316 *2020*; *Vogel et al., 2020, 2021*; *Ding et al., 2020*; *Liu & Rao, 2021*; *Yang et al., 2021*). Out of 26
2317 currently recognized species of *Pareas* (including those described in this work), twelve species
2318 were discovered within the last twelve years (*Uetz, Freed & Hošek, 2021*), of which eleven
2319 species were described based on an integrative evidence from morphological and molecular data.
2320 At the same time, hasty taxonomic revisions may often lead to creation of unnecessary synonyms
2321 and taxonomic inflation (*Isaac, Mallet & Mace, 2004*). For example, recently *Wang et al. (2020)*

2322   revised the taxonomy of the genus *Pareas* and described two new species from China: *P.*
2323   *mengziensis* (member of the *P. hamptoni* group) and *P. menglaensis* (member of the *P. carinatus*
2324   group). Subsequent work by *Liu & Rao (2021)* noted that *Wang et al. (2020)* described their
2325   species without first resolving the historical taxonomic confusions of *P. yunnanensis* (Vogt) and
2326   *P. niger* (Pope), at that time considered junior synonyms of *P. chinensis* (*Wallach, Williams &*
2327   *Boundi, 2014*). *Liu & Rao (2021)* further showed that *P. mengziensis* represents a subjective
2328   junior synonym of *P. niger*, and clarified distribution and the phylogenetic placement of this
2329   species, which was also confirmed by our analyses. Furthermore, as demonstrated in our study,
2330   in their description of *P. menglaensis*, *Wang et al. (2020)* did not provide any comments on the
2331   distribution and existing junior synonyms of *P. carinatus*, including *P. berdmorei*, originally
2332   described from Myanmar. Herein we also analyze the distribution of phylogenetic relationships
2333   within the *P. carinatus* species group and further demonstrate that *P. menglaensis* actually
2334   represents a subjective junior synonym of *P. berdmorei* (see Results). Therefore we would like to
2335   further emphasize herein the importance of careful treatment of the available synonyms and
2336   especially of the examination of the respective type specimens in taxonomic practice. It is thus
2337   recommended that scientists, before describing a new taxon would thoroughly evaluate the
2338   available old names, the existing type specimens and / or new materials from the respective type
2339   localities. This would prevent the taxonomy from becoming confusing and the available taxa
2340   from being overlooked. We would also like to further stress herein the importance of
2341   international collaboration in resolving taxonomically confusing species complexes distributed
2342   across the international borders.

2343   The combination of molecular and morphological data allowed this study to assess the
2344   diversity, clarify the actual geographical distribution as well as to evaluate the validity of the taxa
2345   included in the *P. carinatus-nuchalis* complex. As a result, our study revealed an unprecedented
2346   diversity within this complex, with six major lineages representing distinct species, each with
2347   significant genetic and morphological differences from the others (see Results). In our study, we
2348   consider *P. carinatus* sensu stricto distributed from the Tenasserim Range in the Peninsular
2349   Thailand and Myanmar southwards to Malayan Peninsula, Sumatra, Java, and Borneo Islands.
2350   We also revise the populations from the mainland Indochina and southern China previously
2351   referred to as *P. carinatus* or *P. menglanensis* (*Wang et al., 2020*), and revalidate *P. berdmorei*
2352   as a distinct species; this taxon is widely distributed across Indochina and the adjacent parts of

2353   Yunnan and eastern Myanmar, while *P. menglaensis* is considered a subjective junior synonyms
2354   of this species. We also describe two new previously completely unknown species of *Pareas*
2355   from Vietnam, namely: *Pareas kuznetsovorum* **sp. nov.** (it belongs to *P. carinatus* species group
2356   and represents a sister species of *P. berdmorei*) and *Pareas abros* **sp. nov.**, respectively. We
2357   provide additional information on morphological variation and distribution of the recently
2358   described *P. temporalis*. The recent discovery of the latter two species is quite unexpected since
2359   they are morphologically profoundly different from all other mainland members of the subgenus
2360   *Pareas* and according to our phylogeny and morphological similarities belong to *P. nuchalis*
2361   species group, what is also indicated by an earlier study of *Le et al. (2021)*. It also should be
2362   noted, that our study represents the first record of *P. nuchalis* on Sumatra Island; this species has
2363   been previously considered to be restricted to Borneo. Overall, the revalidation of *P. berdmorei*
2364   along with description of *Pareas abros* **sp. nov. and** *Pareas kuznetsovorum* **sp. nov.** brings the
2365   total number of species in *Pareas* to 26 and the number of Pareinae species to 36.

2366   In our study we also analyze geographic variation of morphological, chromatic and
2367   molecular characters within the wide-ranged species of the subgenus *Pareas*, namely *P.*
2368   *carinatus* and *P. berdmorei*. We report on a significant diversity within these species with two
2369   divergent, allopatric (to the best of our knowledge), and morphologically diagnosable groups
2370   revealed within *P. carinatus*, and three such groups within *P. berdmorei*. Should they be
2371   taxonomically recognized? The phylogenetic species concept (PSC, see *Cracraft, 1983*;
2372   reviewed by *De Queiroz, 2007*) suggests that the minimal monophyletic group on a tree should
2373   be considered a species. However, the recent progress in evolutionary phylogenomics allows
2374   revealing population genetic structure and estimate the geneflow among populations and even
2375   species in unparalleled detail (e.g., *Benestan et al., 2015*). This, however, often makes an
2376   accurate characterization of species boundaries within an evolutionary framework quite
2377   challenging: distinguishing between population-level genetic structure and species divergence is
2378   often problematic (*Chan et al., 2020*). A number of recent phylogenomic studies have
2379   demonstrated that a number of what was considered complexes of cryptic species actually
2380   represent highly admixed and structured metapopulation lineages, rather than true cryptic species
2381   (e.g., *Chan et al., 2020, 2021*). One of the adverse consequences of ignoring gene flow in species
2382   delimitation is the overestimation of species numbers by interpreting population structure as
2383   species divergence, thus enhancing taxonomic inflation (*Chan et al., 2020*). Therefore, in the

2384   present paper, in order to assess the revealed diversity within *P. carinatus* and *P. berdmorei* we

2385   apply the subspecies concept sensu *Hillis (2020)* and *Marshall et al. (2021)*, where subspecies

2386   are defined as geographically circumscribed lineages that may have been temporarily isolated in

2387   the past, but which may have since merged over broad zones of intergradation that not

2388   necessarily show the evidence of reproductive isolation between them. We recognize two

2389   subspecies within *P. carinatus*: *P. c. carinatus* (Sundaland and Malayan Peninsula south of Kra)

2390   and *P. c. tenasserimicus* **ssp. nov.** (Tenasserim Range north of Kra), and three subspecies within

2391   *P. berdmorei*: *P. b. berdmorei* (from eastern Mayanmar across Thailand to northern Laos,

2392   northern Vietnam and southern China), *P. b. unicolor* (southern Vietnam and Cambodia), and *P.*

2393   *b. truongsonicus* **ssp. nov.** (Northern Annamites in central Vietnam and Laos). Though with the

2394   data in hand we do not have any evidence of genetic admixture between these groups, it cannot

2395   be excluded that the future studies with a finer sampling might reveal a certain degree of

2396   geneflow among them. We herein prefer recognizing them as subspecies due to the overall

2397   morphological similarity of these lineages, which are mostly distinguished by coloration rather

2398   than scalation features, their presumably allopatric distribution pattern, their comparatively

2399   young evolutionary age (5.9–4.0 mya), and the historical precedent of use of the subspecies for

2400   describing diversity within these snakes (*P. b. unicolor* was originally described as a subspecies

2401   of *P. carinatus*) (see Results).

2402   Despite the recent significant progress (*Ding et al., 2020*; *Vogel et al., 2020, 2021*;*Le et al.,*

2403   *2021*), our understanding of *Pareas* diversity is still incomplete. Our study revealed a high

2404   morphological variation among the examined specimens of *P. berdmorei* and *P. carinatus*;

2405   however our genetic sampling is not fully comparable to the morphological sampling. For

2406   example, our phylogenetic analysis lacked specimens of *P. carinatus* from the Greater Sunda

2407   Islands and the adjacent smaller offshore islands; many areas in the central Indochina also

2408   remained unassessed. Further field survey and taxonomic efforts both in Indochina and

2409   Sundaland will likely reveal additional lineages within the widely-distributed and insufficiently

2410   sampled species of *Pareas*.

2411

2412   ***Historical biogeography of Pareinae***

2413   The results of our biogeographic reconstruction suggest that the common ancestor of the

2414   Pareinae likely inhabited Sundaland (Fig. 2), while its sister group the Xylophiinae is restricted

2415   to peninsular India (*Deepak et al., 2019*). The split between Pareinae and Xylophiinae is dated to

2416   happen during the middle Eocene (ca. 42.2 mya in our analysis, estimated as ca. 44.9 mya in

2417   *Deepak et al., 2019*), and likely reflects the ancient faunal exchange between the Indian

2418   Subcontinent and the Sundaland via a land bridge which existed during the early and middle

2419   Eocene (*Ali & Aitchison, 2008*; *Morley, 2018*). Similar patterns were reported, for example, in

2420   Draconinae agamid lizards (*Grismer et al., 2016*), and Microhylinae narrow-mouth frogs (*Garg

2421   & Biju, 2019*; *Gorin et al., 2020*). In particular, the assumptive vicariance between Pareinae and

2422   Xylophiinae and the distribution patterns of the two subfamilies remarkably resembles the

2423   divergence pattern between microhylid genera *Micryletta* (widely distributed across the

2424   Southeast Asia) and *Mysticellus* (restricted to southern peninsular India), which was dated as

2425   39.7 – 40.6 mya (*Garg & Biju, 2019*). Our study thus provides further evidence for faunal

2426   exchange between the Indian Subcontinent and Sundaland during the middle Eocene.

2427   Our results accord with the "upstream" colonization hypothesis in Pareinae. The general

2428   pattern of colonization in Pareinae is from Sundaland to the mainland Asia, this dispersal and

2429   subsequent vicariance likely happened during the early Oligocene (ca. 33.6 mya; Fig. 2). It

2430   should be noted, that though now the Sundaland is mostly represented by a number of

2431   archipelagos, in Oligocene it was connected to the mainland Southeast Asia via the Sunda shelf,

2432   which remained subaerial during the most part of Cenozoic (*Cao et al., 2017*; *Morley, 2018*).

2433   Therefore, the general direction of diversification in Pareinae was likely from the tropical

2434   continental margins of Sundaland to a nontropical Asian landmass. Starting with at least middle

2435   Eocene, Sundaland was covered with perhumid rainforests and became a major source of

2436   mainland Asian lineages for a vast number of taxa of plants and animals (see *De Bruyn et al.,*

2437   *2014*; *Grismer et al., 2016*, *Grismer et al., in press*; *Morley, 2018*, and references therein).

2438   Examples include the stream toad genus *Ansonia* (*Grismer et al., 2017*), the litter toads

2439   *Leptobrachella* (*Chen et al., 2018*), and the breadfruit genus *Artocarpus* (*Williams et al., 2017*).

2440   Our study is probably the first example of "upstream" colonization in Asian snakes. Further

2441   studies on the diversification patterns of other endemic Asian genera on a broad geographic scale

2442   might yield key insights into the drivers of speciation in Asia and result in a comprehensive

2443   picture of the regional source-sink dynamics between islands and continents.

2444   Our analyses suggest that the common ancestor of the genus *Pareas* likely inhabited parts

2445   of the Indochinese Peninsula, Indo-Burma, and the areas which now became the Himalayas (Fig.

2446 2). The basal split within *Pareas* is dated as early Oligocene (ca. 31.3 mya; Fig. 2), and

2447 temporally coincides with climatic shifts during this time. The period of late Eocene-early

2448 Oligocene transition was characterized by dramatically cool and dry climate in Southeast Asia

2449 (*Zachos et al., 2001*); during this time the perhumid forests contracted and fragmented (*Milne &*

2450 *Abbott, 2002*; *Bain & Hurley, 2011*; *Buerki et al., 2013*; *Morley, 2018*). These processes could

2451 potentially drive the initial diversification of *Pareas* through vicariance (Fig. 2). Moreover, the

2452 two major clades of *Pareas* (Fig. 2) are estimated to have begun diversification during the

2453 Miocene along with the significant growth of average temperature and humidity (ca. 23–12 mya;

2454 see *Bain & Hurley, 2011*). These climatic changes lead to expansion of perhumid tropical forests

2455 and likely promoted the expansion and further diversification of *Pareas*. A similar pattern was

2456 recently reported by *Chen et al. (2018)* for *Leptobrachella* toads.

2457   The large region of the Himalayas and Indo-Burma is suggested as the possible ancestral

2458 area for the subgenus *Eberhardtia* **stat. nov.**, the most species-rich group of *Pareas*. The further

2459 diversification of this clade into species groups took place during the early to middle Miocene

2460 and likely took place in Himalaya and the adjacent parts of western and southern China, with

2461 subsequent dispersals to Indochina and the East Asian islands (Fig. 2). The Himalaya are now

2462 recognized as an area of exceptional diversity and endemism largely due to the uplift-driven

2463 speciation, suggesting that orogeny created conditions favoring rapid in situ diversification of

2464 resident lineages, which accelerated during the Miocene (reviewed in *Xu et al., 2020*). Our data

2465 suggest that geomorphological factors are also likely responsible for shaping the diversification

2466 within the subgenus *Eberhardtia* **stat. nov.** The origin and diversification of the four species

2467 groups within *Eberhardtia* **stat. nov.** temporally coincide with the rapid increase of uplifting of

2468 the Qinghai–Tibet Plateau during the Miocene (15–7 mya, *An et al., 2001*; *Che et al., 2010*),

2469 which finally gave rise to the intensification of the modern South Asian monsoon climate. This

2470 process is concidered to have accelerated the diversification of numerous Asian animal groups

2471 that share similar distributions with *Eberhardtia* **stat. nov.** (e.g., *Che et al., 2010*; *Blair et al.,*

2472 *2013*; *Gao et al., 2013*; *Chen et al., 2017, 2018*; *Xu et al., 2020*). It is noteworthy that following

2473 the dispersal of *Eberhardtia* **stat. nov.** across the mainland East Asia, its members at least twice

2474 have independently colonized the East Asian islands of Taiwan and the southern Ryukyus during

2475 the late Miocene to early Pliocene, giving rise to an in situ diversification of a number of

2476 endemic island species (*You, Poyarkov & Lin, 2015*; *Chang et al., 2021*). Similar patterns were

2477 reported in other groups of Asian herpetofauna (e.g., *Yuan et al., 2016*; *Nguyen et al., 2020a*;

2478 *Yang & Poyarkov, 2021*; *Gorin et al., 2020*).

2479   The origin of the subgenus *Pareas* likely took place in what is now Western Indochina,

2480 from where, during the early to middle Miocene, it colonized Eastern Indochina leading to

2481 formation of several endemic lineages and species (Fig. 2). The Annamite or Truong Son Range,

2482 including the mountains areas of the Kon Tum–Gia Lai and Langbian plateaus, are reknown as

2483 the center of floral and faunal endemism (e.g. *Averyanov et al., 2003*; *Bain & Hurley, 2011*;

2484 *Monastyrskii & Holloway, 2013*; *Poyarkov et al., 2014, 2021*). According to our analyses,

2485 Eastern Indochina appears as an evolutionary hotspot for *Pareas*, having the high species

2486 diversity and degree of endemism, with up to six species of the genus sympatrically distributed

2487 in the montane forests of the Langbian Plateau. Among the surprising results of our study is the

2488 independent "downstream" colonization of Sundaland from Indochina during the late Miocene,

2489 which happened twice by the members of the *P. carinatus* and *P. nuchalis* species groups (Fig.

2490 2). The recent discovery of two new species of the *P. nuchalis* group in mountain areas of

2491 Eastern Indochina (*Pareas abros* **sp. nov.**, and *P. temporalis* by *Le et al., 2021*) is quite

2492 unexpected, and provides further evidence for faunal interchange between Eastern Indochina and

2493 Borneo (e.g., see *Teynié et al., 2004*). Throughout the late Cenozoic these territories were

2494 directly connected by a landbridge along the eastern edge of Sunda Shelf formed by the ancient

2495 delta joining the modern river systems of Mekong and Chao Phraya, and covered by lowland

2496 evergreen rain-forests (*De Bruyn et al., 2014*). However, similar biogeographic patterns are

2497 rarely reported for the herpetofauna (but see *Wood et al., 2012*; *Geissler et al., 2015*; *Chen et al.,*

2498 *2017*; *Suwannapoom et al., 2018*; *Poyarkov et al., 2018a; Gorin et al., 2020*; *Grismer et al., in*

2499 *press*), therefore additional sampling from other regions, including the different parts of the

2500 Sundaland, is needed to test this hypothesis. Overall, our study reinforces the idea that Indochina

2501 represents an indispensable hotspot for the evolution and maintenance of Southeast Asian

2502 biodiversity (*De Bruyn et al., 2014*).

2503

2504 **CONCLUSIONS**

2505

2506   In this work, we provide an updated phylogenetic hypothesis for the slug-eating snakes of

2507 the subfamily Pareinae based on mtDNA and nuDNA markers for 29 of 33 currently recognized

2508 Pareinae species (88%). We also included data for six lineages that have not been examined
2509 phylogenetically before our work, including the previously unknown two new species and two
2510 new subspecies of *Pareas*. Therefore, our study provides the most comprehensive taxon
2511 sampling for Pareinae published to date. This, along with morphological examination of 269
2512 preserved specimens of Pareinae, including the available type specimens for the genus *Pareas*,
2513 allowed us to revise the phylogenetic relationships and taxonomy of the subfamily. Our work
2514 further highlights the importance of broad phylogenetic sampling, ground-level field surveys,
2515 and careful examination of type materials to achieve an accurate picture of phylogenetic
2516 relationships, global biodiversity, and evolutionary patterns in cryptic groups such as the
2517 Pareinae slug-eating snakes.

2518   The present work clearly indicates a vast underestimation of diversity in the subgenus
2519 *Pareas*, and that the present taxonomy of the group is incomplete. Further integrative studies
2520 combining morphological and genetic analyses are essential for a better understanding of
2521 evolutionary relationships within this cryptic and taxonomically challenging radiation of Asian
2522 snakes. Overall, our study further highlights the importance of comprehensive and accurate
2523 taxonomic revisions not only for the better understanding of biodiversity and its evolution, but
2524 also for the elaboration of adequate conservation actions.

2525   While *P. c. carinatus* and *P. b. berdmorei* are quite widely distributed taxa and their
2526 conservation status is of the least concern, the distribution of *P. c. tenasserimicus* **ssp. nov.**, *P. b.*
2527 *unicolor*, and *P. b. truongsonicus* **ssp. nov.** is most likely restricted to comparatively narrow
2528 areas within the Indochina. At the same time, among the two newly described species *Pareas*
2529 *kuznetsovorum* **sp. nov.** is to date known only from a single specimen, while the ranges of
2530 *Pareas abros* **sp. nov.** and *P. temporalis* are restricted to isolated montane areas of Kon Tum –
2531 Gia Lai and Lam Dong plateaus, respectively. The estimated ranges of the two new *Pareas*
2532 species are likely relatively small, however the actual extent of their distribution and population
2533 trends remain unknown; urgent actions are needed for careful assessment of their conservation
2534 status. We herein tentatively suggest that at present *Pareas kuznetsovorum* **sp. nov.**, *Pareas*
2535 *abros* **sp. nov.**, and *P. temporalis* should be categorized as Data Deficient (DD) according to the
2536 *IUCN Red List criteria (2019)*. Further research is required to clarify the extent of their

2537   distribution population trends, and natural history, thereby facilitating elaboration of adequate
2538   conservation actions.

2539   Our work further highlights the importance of the Indochinese region, including the
2540   territories of Vietnam, Laos, Cambodia, and Thailand, as one of the key biodiversity hotspots
2541   with high levels of herpetofaunal diversity and endemism (*Bain & Hurley, 2011*; *Geissler et al.,*
2542   *2015*; *Duong et al., 2018*; *Nguyen et al., 2018, 2019, 2020b*; *Poyarkov et al., 2018b, 2019, 2021*;
2543   *Grismer et al., 2019, 2021a, 2021b*; *Chomdej et al., 2021*; *Uetz, Freed & Hošek, 2021*). This
2544   area is facing many pressures with major habitat loss by deforestation due to logging, the
2545   growing human population density and infrastructure development, agricultural extension, forest
2546   fires, and tourism development (*Lang, 2001*; *Meyfroidt & Lambin, 2009*). Therefore, further
2547   studies are urgently needed to assess and manage the biodiversity and elaborate the adequate
2548   conservation efforts before more undescribed species are lost.

2549   Overall, our study reinforces the idea of the global importance of Indochina as the
2550   principal evolutionary hotspot for the autochthonous herpetofaunal diversity, as well as a key
2551   area facilitating dispersals between East Asia, Indo-Burma and Sundaland. Further studies on
2552   phylogeny and the diversification patterns of different animal groups endemic to Asia on a broad
2553   geographic scale might provide key insights into the role of complex paleogeography and
2554   paleoclimate history as the drivers of speciation forming the extant Asian biodiversity.

2555

2556   **ACKNOWLEDGEMENTS**

2557

2558   The authors are grateful to Andrey N. Kuznetsov (JRVTTC) and Thai Van Nguyen (SVW)
2559   for supporting our study. We thank Vladislav A. Gorin, Evgeniya N. Solovyeva, Roman A.
2560   Nazarov, Sabira S. Idiatullina, The Anh Nguyen, Hieu Minh Pham, Huy Xuan Ngoc Nguyen,
2561   Bang Van Tran, Eduard A. Galoyan, and Anna B. Vassilieva for their support during the
2562   fieldwork and assistance in the lab or with data analysis. We are also grateful to Liudmila B.
2563   Salamakha for preparation of drawings for this paper. We are deeply bgrateful to Leonid A.
2564   Neimark, Indraneil Das, Guek Hock Ping aka Kurt Orion, Huy X. N. Nguyen, and Mali
2565   Naiduangchan for providing photos used in the present paper. We are grateful to Tasos Limnios
2566   for his advices on Ancient and Modern Greek grammar and lexicon. Furthermore, we thank the
2567   following collection curators, who gave access to specimens under their care and helped us while

we visited their respective institutions: Jens Vindum and Alan Leviton (CAS); Yuezhao Wang, Xiaomao Zeng, Jiatang Li and Ermi Zhao (CIB); Ding Li (DL); Alan Resetar (FMNH); Nicolas Vidal and Annemarie Ohler (MNHN); Giuliano Doria (MNSG); Hmar Tlawmte Lalremsanga (MNZU); Colin McCarthy and Patrick Campbell (NHMUK); Silke Schweiger and Georg Gassner (NMW); Esther Dondorp, Pim Arntzen and Ronald de Ruiter (RMNH); Gunther Köhler and Linda Acker (SMF); George Zug, Kenneth Tighe and Ronald Heyer (USNM); Dennis Rödder and Wolfgang Böhme (ZFMK); Oliver Rödel and Frank Tillack (ZMB); Jakob Hallermann (ZMH); Frank Glaw and Michael Franzen (ZSM); and Valentina F. Orlova and Roman A. Nazarov (ZMMU). Alan Leviton (CAS) is thanked for inviting GV to CAS. Ding Liee, Jiatang Li and Zening Chen are thanked for their support of the work of GV in China. We want to thank Anastasio Zographos (Montmorency, France) for his expertise in classical Greek grammar. The authors thank the academic editor of this paper, Patrick David (MNHN) and an anonymous reviewer for their useful comments which improved the earlier draft of the manuscript.

REFERENCES

Ali JR, Aitchison JC. 2008. Gondwana to Asia: plate tectonics, paleogeography and the biological connectivity of the Indian subcontinent from the Middle Jurassic through latest Eocene (166-35 Ma). *Earth-Science Reviews* **88(3–4)**:145–166. DOI 10.1016/j.earscirev.2008.01.007.

An Z, Kutzbach JE, Prell WL, Porter SC. 2001. Evolution of Asian monsoons and phased uplift of the Himalaya-Tibetan Plateau since late Miocene times. *Nature* **411(6833)**:62–66. DOI 10.1038/35075035.

Angel F. 1920. Sur deux Ophidiens nouveaux de la collection du Muséum. *Bulletin du Muséum National d'Histoire Naturelle*, 26(4):291–294 (in French).

Anonymous 2003. Declaration 44. Amendment of Article 74.7.3. *Bulletin of Zoological Nomenclature* **60(4)**:263.

Averyanov LV, Loc PK, Hiep NT, Harder DK. 2003. Phytogeographic review of Vietnam and adjacent areas of Eastern Indochina. *Komarovia* **3**:1–83.

Bain RH, Hurley MM. 2011. A biogeographic synthesis of the amphibians and reptiles of Indochina. *Bulletin of the American Museum of Natural History* **360**:1–138.

2599   **Barraclough TG, Birky CW, Burt A**. 2003. Diversification in sexual and asexual
2600   organisms. *Evolution* **57**:2166–2172.

2601   **Benestan L, Gosselin T, Perrier C, Sainte-Marie B, Rochette R, Bernatchez L.** 2015.
2602   RAD genotyping reveals fine-scale genetic structuring and provides powerful population
2603   assignment in a widely distributed marine species, the American lobster (*Homarus americanus*).
2604   *Molecular Ecology* **24**(13):3299–3315. DOI 10.1111/mec.13245.

2605   **Bhosale H, Phansalkar P, Sawant M, Gowande G, Patel H, Mirza ZA.** 2020. A new
2606   species of snail-eating snakes of the genus *Pareas* Wagler, 1830 (Reptilia: Serpentes) from
2607   eastern   Himalayas,   India.   *European   Journal   of   Taxonomy*   **729**:54–73.   DOI
2608   10.5852/ejt.2020.729.1191.

2609   **Blair C, Davy CM, Ngo A, Orlov NL, Shi HT, Lu, SQ, Gao L, Rao DQ, Murphy RW.**
2610   2013. Genealogy and demographic history of a widespread amphibian throughout Indochina.
2611   *Journal of Heredity* **104(1)**:72–85 DOI 10.1093/jhered/ess079.

2612   **Boie F**. 1828. Auszüge aus Briefen von Heinr. Boie zu Java an Hn. Schlegel, Conservator
2613   anim. vertebr. am Königl. niederl. Museum. lsis von Oken, Jena, **21**(10): col. 1025–1035 (in
2614   German).

2615   **Boulenger GA.** 1900. Description of new reptiles and batrachians from Bomeo.
2616   *Proceedings of the Zoological Society of London*:182–187.

2617   **Bourret R**. 1934. Notes herpétologiques sur l'Indochine française. IV. Sur une collection
2618   d'ophidiens de Cochinchine et du Cambodge. *Bulletin Général de l'Instruction Publique*
2619   **14(1)**:5–17 (in French).

2620   **Buerki S, Forest F, Stadler T, Alvarez N**. 2013. The abrupt climate change at the
2621   Eocene-Oligocene boundary and the emergence of South-East Asia triggered the spread of
2622   sapindaceous lineages. *Annals of Botany* **112**:151–160. DOI 10.1093/aob/mct106.

2623   **Cao W, Zahirovic S, Flament N, Williams S, Golonka J, Müller RD.** 2017. Improving
2624   global paleogeography since the late Paleozoic using paleobiology. *Biogeosciences* **14**(23):5425–
2625   5439.

2626   **Chan KO, Hutter CR, Wood Jr PL, Grismer LL, Das I, Brown RM.** 2020. Gene flow
2627   creates a mirage of cryptic species in a Southeast Asian spotted stream frog complex. *Molecular*
2628   *Ecology* **29(20):**3970–3987. DOI 10.1111/mec.15603.

Chan KO, Hutter CR, Wood PL, Su YC, Brown RM (2021). Gene flow increases phylogenetic structure and inflates cryptic species estimations: a case study on widespread Philippine puddle frogs (*Occidozyga laevis*). *Systematic Biology*, syab034. DOI 10.1093/sysbio/syab034.

Chan-ard T, Grossmann W, Gumprecht A, Schulz KD. 1999. Amphibians and reptiles of peninsular Malaysia and Thailand - an illustrated checklist [bilingual English and German]. Bushmaster Publications, Würselen, Gemany, 240 pp.

Chan–ard T, Parr JWK, Nabhitabhata J. 2015. *A field guide to the Reptiles of Thailand*. Oxford University Press, New York.

Chang KX, Huang BH, Luo MX, Huang CW, Wu SP, Nguyen HN, Lin SM. 2021. Niche partitioning among three snail-eating snakes revealed by dentition asymmetry and prey specialisation. *Journal of Animal Ecology* **90**(4):967–977. DOI: 10.1111/1365-2656.13426.

Che J, Zhou W-W, Hu J-S, Yan F, Papenfuss TJ, Wake DB, Zhang Y-P. 2010. Spiny frogs (*Paini*) illuminate the history of the Himalayan region and southeast Asia. *Proceedings of the National Academy of Sciences* **107**:13765–13770. DOI 10.1073/pnas.1008415107.

Chen J-M, Poyarkov NA, Suwannapoom C, Lathrop A, Wu Y-H, Zhou W-W, Yuan Z-Y, Jin J-Q, Chen H-M, Liu H-Q, Nguyen TQ, Nguyen SN, Duong TV, Eto K, Nishikawa K, Matsui M, Orlov NL, Stuart BL, Brown RM, Rowley JJL, Murphy RW, Wang Y-Y, Che J. 2018. Large-scale phylogenetic analyses provide insights into unrecognized diversity and historical biogeography of Asian leaf-litter frogs, genus *Leptolalax* (Anura: Megophryidae). *Molecular Phylogenetics and Evolution* **124**:162–171. DOI 10.1016/j.ympev.2018.02.020.

Chen J-M, Zhou W-W, Poyarkov NA, Stuart BL, Brown RM, Lathrop A, Wang Y-Y, Yuan Z-Y, Jiang K, Hou M, Chen H-M, Suwannapoom C, Nguyen SN, Duong TV, Papenfuss TJ, Murphy RW, Zhang Y-P, Che J. 2017. A novel multilocus phylogenetic estimation reveals unrecognized diversity in Asian horned toads, genus *Megophrys* sensu lato (Anura:Megophryidae). *Molecular Phylogenetics and Evolution* **106**:28–43. DOI 10.1016/j.ympev.2016.09.004.

Chiari Y, Vences M, Vieites DR, Rabemananjara F, Bora P, Ramilijaona Ravoahangimalala O, Meyer A. 2004. New evidence for parallel evolution of colour patterns in Malagasy poison frogs (*Mantella*). *Molecular Ecology* **13**:3763–3774.

2659   **Chomdej S, Pradit W, Suwannapoom C, Pawangkhanant P, Nganvongpanit K,**
2660   **Poyarkov NA, Che J, Gao Y-C, Gong S-P.** 2021. Phylogenetic analyses of distantly related
2661   clades of bent-toed geckos (genus *Cyrtodactylus*) reveal an unprecedented amount of cryptic
2662   diversity in northern and western Thailand. *Scientific Reports* **11**:2328. DOI 10.1038/s41598-
2663   020-70640-8.

2664   **Chomdej S, Suwannapoom C, Pawangkhanant P, Pradit W, Nazarov RA, Grismer**
2665   **LL, Poyarkov NA**. 2020. A new species of *Cyrtodactylus* Gray (Squamata:Gekkonidae) from
2666   western Thailand and the phylogenetic placement of *C. inthanon* and *C. suthep*. *Zootaxa*
2667   **4838(2)**:179–209. DOI 10.11646/zootaxa.4838.2.2.

2668   **Cochran DM.** 1930. The herpetological collections made by Dr. Hugh M. Smith in Siam
2669   from 1923 to 1929. *Proceedings of the United States National Museum* **77(2834)**:1–39.

2670   **Cox MJ, Van Dijk PP, Nabhitabhata J, Kumthorn T.** 1998. *A photographic guide to*
2671   *snakes and other reptiles of Peninsular Malaysia, Singapore and Thailand*. Ralph Curtis
2672   Publishing, 144 pp.

2673   **Coyne JA, Allen OH.** 1998. The evolutionary genetics of speciation. *Philosophical*
2674   *Transactions of the Royal Society B* **353(1366)**:287–305. DOI 10.1098/rstb.1998.0210.

2675   **Cracraft J.** 1983. Species concepts and speciation analysis. In: Johnston R.F. (eds).
2676   *Current Ornithology,* vol 1. Springer, New York, NY. DOI 10.1007/978-1-4615-6781-3_6.

2677   **Cundall D, Greene H.W.** 2000. Feeding in snakes. In: Feeding: Form, Function and
2678   Evolution in Tetrapod Vertebrates (K. Schwenk, ed), pp. 293–333. Academic Press, San Diego.

2679   **Danaisawadi P, Asami T, Ota H, Sutcharit C, Pahan S.** 2016. A snail-eating snake
2680   recognizes prey handedness. *Scientific Reports* **6**:23832. DOI 10.1038/srep23832.

2681   **Danaisawadi P, Asami T, Ota H, Sutcharit C, Panha S**. 2015. Subtle asymmetries in the
2682   snail-eating snake *Pareas carinatus* (Reptilia: Pareatidae). *Journal of Ethology* **33**:243–246. DOI
2683   10.1007/s10164-015-0432-x.

2684   **Das I, Dattagupta B, Gayen NC.** 1998. History and catalogue of reptile types in the
2685   collection of the Zoological Survey of India. *Journal of South Asian Natural History* **3**:121–172.

2686   **Das I.** 2012. *A naturalist's guide to the snakes of South-East Asia: Malaysia, Singapore,*
2687   *Thailand, Myanmar, Borneo, Sumatra, Java and Bali*. John Beaufoy Publishing, Oxford, 176 pp.

2688   **Das I.** 2018. *A naturalist's guide to the snakes of Thailand and South-east Asia. 2nd*
2689   *edition.* John Beaufoy Publishing, Oxford, 176 pp.

David P, Vogel G, Dubois A. 2011. On the need to follow rigorously the Rules of the Code for the subsequent designation of a nucleospecies (type species) for a nominal genus which lacked one:the case of the nominal genus *Trimeresurus* Lacépède, 1804 (Reptilia: Squamata: Viperidae). *Zootaxa* **2992**:1–51. DOI 10.11646/zootaxa.2992.1.1.

David P, Vogel G. 1996. *The snakes of Sumatra, an annotated checklist and key with natural history notes*. Ed. Chimaira, Frankfurt-am-Main, 260 pp.

De Bruyn M, Nugroho E, Hossain MM, Wilson JC, Mather PB. 2005. Phylogeographic evidence for the existence of an ancient biogeographic barrier: the Isthmus of Kra Seaway. *Herdedity* **94**:370–378. DOI 10.1038/sj.hdy.6800613.

De Bruyn M, Stelbrink B, Morley RJ, Hall R, Carvalho GR, Cannon CH, Van den Bergh G, Meijaard E, Metcalfe I, Boitani L, Maiorano L, Shoup R, Von Rintelen T. 2014. Borneo and Indochina are major evolutionary hotspots for Southeast Asian biodiversity. *Systematic Biology* **63(6)**:879–901. DOI 10.1093/sysbio/syu047.

De Queiroz A, Lawson R, Lemos-Espinal JA. 2002. Phylogenetic relationships of North American garter snakes (*Thamnophis*) based on four mitochondrial genes: how much DNA is enough? *Molecular Phylogenetics & Evolution* **22**:315–329. DOI 10.1006/mpev.2001.1074.

De Queiroz K. 2007. Species concepts and species delimitation. *Systematic biology* **56**(6):879–86. DOI 10.1080/10635150701701083.

De Queiroz K. 2020. An updated concept of subspecies resolves a dispute about the taxonomy of incompletely separated lineages. *Herpetological Review* **51(3)**:459– 461.

De Rooij NDE. 1917. The Reptiles of the Indo-Australian Archipelago. Il. Ophidia. Leiden (E. J. Brill), 334 pp.

Deepak V, Narayanan S, Das S, Rajkumar KP, Easa PS, Sreejith KA, Gower DJ. 2020. Description of a new species of *Xylophis* Beddome, 1878 (Serpentes: Pareidae: Xylophiinae) from the western Ghats, India. *Zootaxa* **4755**:231–250. DOI 10.11646/zootaxa.4755.2.2.

Deepak V, Ruane S, Gower DJ. 2019. A new subfamily of fossorial colubroid snakes from the Western Ghats of peninsular India. *Journal of Natural History* **52**:2919–2934. DOI10.1080/00222933.2018.1557756.

Deuve J. 1961. Liste annotée des Serpents du Laos. *Bulletin du Muséum National d'Histoire Naturelle* 1:5–32.

2721   **Ding L, Chen Z, Suwannapoom C, Nguyen TV, Poyarkov NA, Vogel G.** 2020. A new
2722   species of the *Pareas hamptoni* complex (Squamata Serpentes:Pareidae) from the Golden
2723   Triangle. *Taprobanica* **9**:174–193.

2724   **Dowling HG, Jenner JV.** 1988. Snakes of Burma: checklist of reported species &
2725   bibliography. *Smithsonian Herpetological Information Service* **76**:1–19.

2726   **Dowling HG.** 1951. A proposed standard system of counting ventrals in snakes. *British*
2727   *Journal of Herpetology* **1**:97–99.

2728   **Drummond AJ, Suchard MA, Xie D, Rambaut A.** 2012. Bayesian phylogenetics with
2729   BEAUti and the BEAST 1.7. *Molecular Biology and Evolution* **29**:1969–1973. DOI
2730   10.1093/molbev/mss075.

2731   **Duméril AMC.** 1853. Prodrome de la classifcation des reptiles ophidiens. *Mémoires de*
2732   *l'Académie de Sciences de l'Institut de France,* Paris 23, 399–536 (in French).

2733   **Duméril AMC, Bibron G, and Duméril A. H. A.** 1854. *Erpétologie générale, ou histoire*
2734   *naturelle complète des reptiles. Tomé septième*, *Première partie. Comprenant l'histoire des*
2735   *serpents non venimeux*, Librairie Encyclopédique de Roret, Pari. (In French).

2736   **Duong TV, Do DT, Ngo CD, Nguyen TQ, Poyarkov NA.** 2018. A new species of the
2737   genus *Leptolalax* (Anura:Megophryidae) from southern Vietnam. *Zoological Research* **39**:185–
2738   201. DOI 10.24272/j.issn.2095-8137.2018.009.

2739   **Figueroa A, McKelvy AD, Grismer LL, Bell CD, Lailvaux SP.** 2016. A species-level
2740   phylogeny of extant snakes with description of a new colubrid subfamily and genus. *PLoS ONE*
2741   **11**:e0161070. DOI 10.1371/journal.pone.0161070.

2742   **Filardi C, Moyle R**. 2005. Single origin of a pan-Pacific bird group and upstream
2743   colonization of Australasia. *Nature* **438**:216–219 (2005). DOI 10.1038/nature04057.

2744   **Flot JF.** 2010. SeqPHASE: a web tool for interconverting PHASE input/output files and
2745   FASTA sequence alignments. *Molecular ecology resources* **10**(1):162–166.

2746   **Fontaneto D, Herniou EA, Boschetti C, Caprioli M, Melone G, Ricci C, Barraclough**
2747   **TG**. 2007. Independently evolving species in asexual bdelloid rotifers. *PLoS Biology* **5(4)**:e87.
2748   DOI 10.1371/journal.pbio.0050087.

2749   **Frost DR, Hillis DM.** 1990. Species in concept and practice: Herpetological applications.
2750   *Herpetologica* **46**:87–104.

Frost DR, Kluge AG, Hillis DM. 1992. Species in contemporary herpetology: comments on phylogenetic inference and taxonomy. *Herpetological Review*, **23**:46–54.

Gao YD, Harris AJ, Zhou SD, He XJ. 2013. Evolutionary events in *Lilium* (including Nomocharis, Liliaceae) are temporally correlated with orogenies of the Q-T plateau and the Hengduan Mountains. *Molecular Phylogenetics and Evolution* **68(3)**:443–460. DOI 10.1016/j.ympev.2013.04.026.

Garg S, Biju SD. 2019. New microhylid frog genus from Peninsular India with Southeast Asian affinity suggests multiple Cenozoic biotic exchanges between India and Eurasia. *Scientific Reports* **9**:1906. DOI 10.1038/s41598-018-38133-x.

Geissler P, Hartmann T, Ihlow F, Rödder D, Poyarkov NA, Nguyen TQ, Ziegler T, Böhme W. 2015. The lower Mekong: an insurmountable barrier to amphibians in southern Indochina? *Biological journal of the Linnean Society* 114:905–914.

Gorin VA, Scherz MD, Korost DV, Poyarkov NA. 2021. Consequences of parallel miniaturisation in Microhylinae (Anura, Microhylidae), with the description of a new genus of diminutive South East Asian frogs. *Zoosystematics and Evolution* **97**:27–54. DOI: 10.3897/zse.97.57968.

Gorin VA, Solovyeva EN, Hasan M, Okamiya H, Karunarathna DMSS, Pawangkhanant P, de Silva A, Juthong W, Milto KD, Nguyen LT, Suwannapoom C, Haas A, Bickford DP, Das I, Poyarkov NA. 2020. A little frog leaps a long way: compounded colonizations of the Indian Subcontinent discovered in the tiny Oriental frog genus *Microhyla* (Amphibia: Microhylidae). *PeerJ* **8**:e9411. DOI 10.7717/peerj.9411.

Götz M. 2002. The feeding behavior of the snail-eating snake *Pareas carinatus* Wagler 1830 (Squamata: Colubridae). *Amphibia-Reptilia* **23(4)**:487–493. DOI 10.1163/15685380260462383.

Grismer JL, Schulte JA, Alexander A, Wagner P, Travers SL, Buehler MD, Welton LJ, Brown RM. 2016. The Eurasian invasion: phylogenomic data reveal multiple Southeast Asian origins for Indian Dragon Lizards. *BMC Evolutionary Biology* **16**(1):43. DOI 10.1186/s12862-016-0611-6.

Grismer L, Wood PL, Poyarkov NA, Le MD, Karunarathna S, Chomdej S, Suwannapoom C, Qi S, Liu S, Che J, Quah ESH, Kraus F, Oliver PM, Riyanto A, Pauwels OSG, Grismer JL. 2021a. Karstic landscapes are foci of species diversity in the World's third-

largest vertebrate genus *Cyrtodactylus* Gray, 1827 (Reptilia: Squamata: Gekkonidae). *Diversity* **13**:183. DOI 10.3390/d13050183.

Grismer LL, Wood PL, Aowphol A, Cota M, Grismer MS, Murdoch ML, Aguilar CA, Grismer JL. 2017 "2016". Out of Borneo, again and again: biogeography of the stream toad genus *Ansonia* Stoliczka (Anura:Bufonidae) and the discovery of the first limestone cave-dwelling species. *Biological Journal of the Linnean Society* **120**:371–395. DOI 10.1111/bij.12886.

Grismer LL, Wood PL, Poyarkov NA, Le MD, Kraus F, Agarwal I, Oliver PM, Nguyen N Sang Ngoc, Nguyen TQ, Welton LJ, Stuart BL, Luu VQ, Bauer AM, Quah ESH, Chan KO, Ziegler T, Ngo HT, Aowphol A, Chomdej S, Suwannapoom C, Siler D, Anuar S, Ngo TV, Grismer JL. 2021b. Phylogenetic partitioning of the third-largest vertebrate genus in the world, *Cyrtodactylus* Gray, 1827 (Reptilia; Squamata; Gekkonidae) and its relevance to taxonomy and conservation. *Vertebrate Zoology* **71**:101–154. DOI 10.3897/vz.71.e59307.

Grismer LL, Wood PL, Quah ESH, Anuar S, Poyarkov NA, Thy N, Orlov NL, Thammachoti P, Seiha H. 2019. Integrative taxonomy of the Asian skinks *Sphenomorphus stellatus* (Boulenger, 1900) and *S. praesignis* (Boulenger, 1900), with the resurrection of *S. annamiticus* (Boettger, 1901) and the description of a new species from Cambodia. *Zootaxa* **4683**(3):381–411. DOI 10.11646/zootaxa.4683.3.4.

Grossmann W, Tillack F. 2003. On the taxonomic status of *Asthenodipsas tropidonotus* (Van Lidth de Jeude, 1923) and *Pareas vertebralis* (Boulenger, 1900) (Serpentes: Colubridae: Pareatinae). *Russian Journal of Herpetology* **10**:175–190.

Groth JG, Barrowclough GF. 1999. Basal divergences in birds and the phylogenetic utility of the nuclear RAG-1 gene. *Molecular Phylogenetics and Evolution* 12:115–123. DOI10.1006/mpev.1998.0603.

Guo K, Deng X. 2009. A new species of *Pareas* (Serpentes: Colubridae: Pareatinae) from the Gaoligong Mountains, southwestern China. *Zootaxa* **2008**:53–60.

Guo P, Zhao E-M. 2004. *Pareas stanleyi* - A record new to Sichuan, China and a Key to the Chinese species. *Asiatic Herpetological Research* **10**:280–281.

Guo Y, Wang G, Rao D–Q. 2020. Scale microornamentation of five species of *Pareas* (Serpentes, Pareidae) from China. *Zootaxa* **4742(3)**:565-572. DOI 10.11646/zootaxa.4742.3.10.

2812   **Guo Y, Wu Y, He S, Zhao E.** 2011. Systematics and molecular phylogenetics of Asian
2813 snail-eating snakes (Pareatidae). *Zootaxa*, **3001**:57–64.

2814   **Haas, C.P.J, de.** 1950. Checklist of the snakes of the Indo-Australian Archipelago
2815 (Reptilia, Ophidia). *Treubia*, Bogor **20(3)**:511–625.

2816   **Hall R.** 2012. Late Jurassic-Cenozoic reconstructions of the Indonesian region and the
2817 Indian Ocean. *Tectonophysics* **570**:1–41. DOI 10.1016/j.tecto.2012.04.021.

2818   **Hall TA. 1999.** BioEdit: a user-friendly biological sequence alignment editor and analysis
2819 program for Windows 95/98/NT. In: *Nucleic acids symposium series*. London: Information
2820 Retrieval Ltd c1979-c2000, 95–98.

2821   **Hauser S.** 2017. On the validity of *Pareas macularius* Theobald, 1868 (Squamata:
2822 Pareidae) as a species distinct from *Pareas margaritophorus* (Jan in Bocourt, 1866). *Tropical*
2823 *Natural History* **17**:147–174.

2824   **He M.** (2009) *Discussion on taxonomy of colubrid snakes based on scale micro-*
2825 *ornamentations*—Unpubl. Ph.D. thesis, Sichuan University (in Chinese).

2826   **Hennig W.** 1966. Phylogenetic systematics. University of Illinois Press, Urbana, Illinois
2827 USA.

2828   **Hillis DM**. 2020. The detection and naming of geographic variation within species.
2829 *Herpetological Review* 51:52–56. DOI10.1016/S0022-3182(70)80093-0.

2830   **Hillis DM.** 2021. New and not-so-new conceptualizations of species and subspecies: A
2831 reply to the "It's species all the way down" view. *Herpetological Review* **52**:49–50.

2832   **Hoang DT, Chernomor O, von Haeseler A, Minh BQ, Vinh LS**. 2018. UFBoot2:
2833 Improving the ultrafast bootstrap approximation. *Molecular Biology and Evolution* **35**:518–522.
2834 DOI 10.1093/molbev/msx281.

2835   **Hoso M, Asami T, Hori M.** 2007. Right-handed snakes: convergent evolution of
2836 asymmetry for functional specialization. *Biology Letters* **3**:169–172. DOI
2837 10.1098/rsbl.2006.0600.

2838   **Hoso M, Hori M.** 2006. Identification of molluscan prey from feces of Iwasaki's slug
2839 snake, *Pareas iwasakii*. *Herpetological Review*, **37**:174–176.

2840   **Hoso M, Hori M.** 2008. Divergent shell shape as an antipredator adaptation in tropical
2841 land snails. *The American Naturalist* 172:726–732. DOI 10.1086/591681.

2842 **Hoso M, Kameda Y, Wu S.P, Asami T, Kato M, Hori M.** 2010. A speciation gene for
2843 left–right reversal in snails results in anti-predator adaptation. *Nature Communications* **1**:133.
2844 DOI 10.1038/ncomms1133.

2845 **Hoso M.** 2007. Oviposition and hatchling diet of a snail-eating snake *Pareas iwasakii*
2846 (Colubridae: Pareatinae). *Current Herpetology* **26**:41–43. DOI 10.3105/1345-
2847 5834(2007)26[41:OAHDOA]2.0.CO;2.

2848 **Huelsenbeck JP, Ronquist F.** 2001. MrBayes: Bayesian inference of phylogenetic trees.
2849 *Bioinformatics* **17(8)**:754–755. DOI 10.1093/bioinformatics/17.8.754.

2850 **ICZN.** 1999. *International Code of Zoological Nomenclature*. Fourth edition. London,
2851 U.K. [available online at https://www.iczn.org/the-code/the-code-online/]: International Trust for
2852 Zoological Nomenclature.

2853 **Isaac NJ, Mallet J, Mace GM**. 2004. Taxonomic inflation: its influence on macroecology
2854 and conservation. *Trends in ecology & evolution* **19(9)**:464–9.

2855 **Iskandar DT. Colijn E.** 2002"2001". *A checklist of Southeast Asian and New Guinean
2856 Reptiles. Part I. Serpentes*, Biodiversity Conservation Project, Jakarta.

2857 **IUCN Standards and Petitions Committee** 2019. *Guidelines for Using the IUCN Red
2858 List Categories and Criteria. Ver. 14. Prepared by the Standards and Petitions Committee*.
2859 http:www.iucnredlist.orgdocumentsRedListGuidelines.pdf (accessed 2021-01-30).

2860 **Jan G.** 1863. *Elenco sistematico degli ofidi descritti e disegnati per l'iconografia generale*,
2861 A. Lombardi, Milano. 143 pp.

2862 **Jobb G.** 2011. TREEFINDER: March 2011 www.treefinder.de.

2863 **Jønsson KU, Fabre FH, Ricklefs RE, Fjeldså J**. 2011. Major global radiation of corvoid
2864 birds originated in the proto-Papuan archipelago. *Proceedings of the National Academy of
2865 Sciences* **108(6)**:2328–33. DOI 10.1073/pnas.1018956108/

2866 **Kaiser H, Crother BI, Kelly CM, Luiselli L, O'Shea M, Ota H, Passos P, Schleip WD,
2867 Wüster W.** 2013. Best practices: in the 21st century, taxonomic decisions in herpetology are
2868 acceptable only when supported by a body of evidence and published via peer-review.
2869 *Herpetological Review* **44(1)**:8–23.

2870 **Katoh K, Misawa K, Kuma K, Miyata T.** 2002. MAFFT:a novel method for rapid
2871 multiple sequence alignment based on fast Fourier transform. *Nucleic Acids Research* **30**:3059–
2872 3066. DOI 10.1093/nar/gkf436.

2873 **Keogh JS.** 1999. Evolutionary implications of hemipenial morphology in the terrestrial
2874 Australian elapid snakes. *Zoological Journal of the Linnean Society* **125**:239–278. DOI
2875 10.1111/j.1096-3642.1999.tb00592.x.

2876 **Kindler C, Fritz U.** 2018. Phylogeography and taxonomy of the barred grass snake (*Natrix*
2877 *helvetica*), with a discussion of the subspecies category in zoology. *Vertebrate Zoology*
2878 **68(3)**:269–281.

2879 **Knowles LL, Carstens BC**. 2007. Delimiting species without monophyletic gene trees,
2880 *Systematic Biology* **56(6)**:887–895. DOI 10.1080/10635150701701091.

2881 **Kojima, Y, Fukuyama, I, Kurita, T. Hossman, Nishikawa K**. 2020. Mandibular sawing
2882 in a snail-eating snake. *Scientific Reports* **10**:12670. DOI 10.1038/s41598-020-69436-7.

2883 **Kopstein F.** 1936. Herpetologische Notizen. XIII. Ueber *Vipera russellii* von Java. *Treubia*
2884 15(3):259–264.

2885 **Kumar S, Stecher G, Tamura K**. 2016. MEGA7: Molecular evolutionary genetics
2886 analysis Version 7.0 for Bigger Datasets. *Molecular Biology and Evolution* **33(7)**:1870–1874.
2887 DOI 10.1093/molbev/msw054.

2888 **Lanfear R, Calcott B, Ho SYW, Guindon S.** 2012. PartitionFinder: combined selection
2889 of partitioning schemes and substitution models for phylogenetic analyses. *Molecular Biology*
2890 *and Evolution* **29(6)**:1695–1701. DOI 10.1093/molbev/mss020.

2891 **Lang C. 2001**. Deforestation in Vietnam, Laos and Cambodia. Deforestation, environment,
2892 and sustainable development: *A comparative analysis* **2001**:111–37.

2893 **Le DT, Nguyen SHL, Pham CT, Nguyen TQ.** 2014. New records of snakes (Squamata:
2894 Serpentes) from Dien Bien Province. *Journal of Biology* **36**:460–470. DOI 10.15625/0866-
2895 7160/v36n4.6175.

2896 **Le DTT, Tran TG, Hoang HD, Stuart BL.** 2021. A new species of *Pareas* (Squamata,
2897 Pareidae) from southern Vietnam. *Vertebrate Zoology* **71**:439–451. DOI 10.3897/vz.71.e70438.

2898 **Li J-N, Liang D, Wang Y-Y, Guo P, Huang S, Zhang P.** 2020. A large-scale systematic
2899 framework of Chinese snakes based on a unified multilocus marker system. *Molecular*
2900 *Phylogenetics and Evolution* **148**:106807. DOI 10.1016/j.ympev.2020.106807.

2901 **Liu S, Rao D-Q.** 2021. A new species of the genus *Pareas* (Squamata, Pareidae) from
2902 Yunnan, China. *ZooKeys* **1011**:121–138. DOI 10.3897/zookeys.1011.59029.

2903   **Loredo AI, Wood PL, Quah ESH, Anuar S, Greer LF, Ahmad N, Grismer L.** 2013.
2904   Cryptic speciation within *Asthenodipsas vertebralis* (Boulenger, 1900) (Squamata: Pareatidae),
2905   the description of a new species from Peninsular Malaysia, and the resurrection of *A.*
2906   *tropidonotus* (Lidth de Jude, 1923) from Sumatra: an integrative taxonomic analysis. *Zootaxa*
2907   **3664**:505–524. DOI 10.11646/zootaxa.3664.4.5.

2908   **Malkmus R, Manthey U, Vogel G. Hoffmann P. Kosuch J.** 2002. *Amphibians and*
2909   *reptiles of Mount Kinabalu (North Borneo)*. A.R.G. Gantner Verlag, Rugell, 404 pp.

2910   **Malkmus R, Sauer H.** 1996. Ruhestellung von *Pareas nuchalis* und Erstnachweis dieser
2911   Art im Nationalpark Mount Kinabalu/Malaysia. *Salamandra* **32(1)**:55–58.

2912   **Manthey U. Grossmann W.** (1997), *Amphibien and Reptilien Südostasiens*, Natur- und
2913   Tier Verlag, Münster, 512 pp.

2914   **Marshall TL, Chambers EA, Matz MV, Hillis DM.** 2021. How mitonuclear discordance
2915   and geographic variation have confounded species boundaries in a widely studied snake.
2916   *Molecular Phylogenetics and Evolution*, **162**:107194. DOI 10.1016/j.ympev.2021.107194.

2917   **Matzke NJ.** 2013. Probabilistic historical biogeography: new models for founder-event
2918   speciation, imperfect detection, and fossils allow improved accuracy and model-testing.
2919   *Frontiers of Biogeography* **5**(4):242–248. DOI 10.21425/F5FBG19694.

2920   **Mertens, R.** 1930. Die Amphibien und Reptilien der Inseln Bali, Lombok, Sumbawa und
2921   Flores. *Abhandlungen der Senckenbergischen Naturforschenden Gesellschaft* **42**(3):117–344.

2922   **Meyfroidt P, Lambin EF**. 2009. Forest transition in Vietnam and displacement of
2923   deforestation abroad. *Proceedings of the National Academy of Sciences* **106**(38):16139–16144.

2924   **Milne RI, Abbot RJ.** 2002. The origin and evolution of Tertiary relict floras. *Advances in*
2925   *Botanical Research* **38**:281–314. DOI 10.1016/S0065-2296(02)38033-9.

2926   **Minh BQ, Nguyen MAT, von Haeseler A**. 2013. Ultrafast approximation for
2927   phylogenetic   bootstrap.   *Molecular   Biology   and   Evolution*   **30**:1188–1195.   DOI
2928   10.1093/molbev/mst024.

2929   **Monastyrskii AL, Holloway JD.** 2013. The biogeography of the butterfly fauna of
2930   Vietnam with a focus on the endemic species (Lepidoptera). In: Silva-Opps M (Ed.). *Current*
2931   *Progress in Biological Research*. Rijeka, Croatia, InTech, pp. 95–123.

Morley RJ. 2018. Assembly and division of the South and South-East Asian flora in relation to tectonics and climate change. *Journal of Tropical Ecology* **34(4)**:209–234 DOI 10.1017/S0266467418000202.

Mulcahy DG, Lee JL, Miller AH, Chand M, Thura MK, Zug GR. 2018. Filling the BINs of life: Report of an amphibian and reptile survey of the Tanintharyi (Tenasserim) Region of Myanmar, with DNA barcode data. *ZooKeys* **757**:85–152. DOI 10.3897/zookeys.757.24453.

Murphy RW, Crawford AJ, Bauer AM, Che J, Donnellan SC, Fritz U, Haddad CFB, Nagy ZT, Poyarkov NA, Vences M, Wang W-Z, Zhang Y. 2013. Cold Code: the global initiative to DNA barcode amphibians and nonavian reptiles. *Molecular Ecology Resources* **13:**161–167. DOI 10.1111/1755-0998.12050.

Nguyen HN, Tran BV, Nguyen LH, Neang T, Yushchenko PV, Poyarkov NA. 2020. A new species of *Oligodon* Fitzinger, 1826 from Langbian Plateau, southern Vietnam, with additional information on *Oligodon annamensis* Leviton, 1953 (Squamata: Colubridae). *PeerJ*, **8**:e8332. DOI 10.7717/peerj.8332.

Nguyen LT, Poyarkov NA, Le DV, Vo BD, Phan HT, Duong TV, Murphy RW, Nguyen SN. 2018. A new species of *Leptolalax* (Anura: Megophryidae) from Son Tra Peninsula, central Vietnam. *Zootaxa* **4388**:1–21. DOI 10.11646/zootaxa.4388.1.1.

Nguyen LT, Poyarkov NA, Nguyen TT, Nguyen TA, Tran VH, Gorin VA, Murphy RW, Nguyen SN. 2019. A new species of the genus *Microhyla* Tschudi, 1838 (Amphibia: Anura: Microhylidae) from Tay Nguyen Plateau, central Vietnam. *Zootaxa* **4543**:549–580. DOI 10.11646/zootaxa.4543.4.4.

Nguyen LT, Schmidt HA, von Haeseler A, Minh BQ. 2015. IQ-TREE: A fast and effective stochastic algorithm for estimating maximum likelihood phylogenies. *Molecular Biology and Evolution* **32(1)**:268–274. DOI 10.1093/molbev/msu300.

Nguyen SV & Ho CT. 1996. *A checklist of reptiles and amphibians in Vietnam*. Science and Technology Publishing House, Hanoi, 264 pp. (in Vietnamese).

Nguyen SV, Ho CT, Nguyen TQ. 2009. *Herpetofauna of Vietnam*. Frankfurt: Edition Chimaira.

Nguyen TV, Brakels P, Maury N, Sudavanh S, Pawangkhanant P, Idiiatullina S, Lorphengsy S, Inkhavilay K, Suwannapoom C, Poyarkov NA. 2020b. New herpetofaunal

observations from Laos based on photo records. *Amphibian & Reptile Conservation* **14**:218–249 (e248).

Nguyen TV, Duong TV, Luu KT, Poyarkov NA. 2020a. A new species of *Kurixalus* (Anura: Rhacophoridae) from northern Vietnam with comments on the biogeography of the genus. *Journal of Natural History* **54**:195–223. DOI 10.1080/00222933.2020.1728411.

Okamiya H, Sugawara H, Nagano M, Poyarkov NA. 2018. An integrative taxonomic analysis reveals a new species of lotic *Hynobius* salamander from Japan. *PeerJ* **6**:e5084. DOI 10.7717/peerj.5084.

Padial JM, Miralles A, De la Riva I, Vences M. 2010. The integrative future of taxonomy. *Frontiers in Zoology* **7**:16(2010). DOI 10.1186/1742-9994-7-16.

Peters WCH. 1864. Über neue Amphibien (*Typhloscincus*, *Typhlops*, *Asthenodipsas*, *Ogmodon*). *Monatsberichte der königlich Akademie der Wissenschaften zu Berlin* **1864(4)**:271–276.

Pham AV, Nguyen TQ. 2019. New records of snakes (Reptilia: Squamata: Serpentes) from Lai Chau Province, Vietnam. *VNU Journal of Science:Natural Sciences and Technology* **35**:1–7. DOI 10.25073/2588-1140/vnunst.4854.

Pope CH. 1935. *The reptiles of China. Turtles, Crocodilians, Snakes, Lizards. Natural History of Central Asia Vol. X*. The American Museum of Natural History, New York, 604 pp.

Poyarkov NA, Geissler P, Gorin VA, Dunayev EA, Hartmann T, Suwannapoom C. 2019. Counting stripes: revision of the *Lipinia vittigera* complex (Reptilia, Squamata, Scincidae) with description of two new species from Indochina. *Zoological Research* **40**(5):358–393. DOI 10.24272/j.issn.2095-8137.2019.052.

Poyarkov NA, Nguyen TV, Duong TV, Gorin VA, Yang J-H. 2018a. A new limestone-dwelling species of *Micryletta* (Amphibia: Anura: Microhylidae) from northern Vietnam. *PeerJ* **6**:e5771. DOI 10.7717/peerj.5771.

Poyarkov NA, Nguyen TV, Popov ES, Geissler P, Paawangkhanant P, Neang T, Suwannapoom C, Orlov NL. 2021. Recent progress in taxonomic studies, biogeographic analysis and revised checklist of Amphibians in Indochina. *Russian Journal of Herpetology* **28**:1–110. DOI 10.30906/1026-2296-2021-28-3A-1-110.

Poyarkov NA, Suwannapoom C, Pawangkhanant P, Aksornneam A, Duong TV, Korost DV, Che J. 2018b. A new genus and three new species of miniaturized microhylid frogs

from Indochina (Amphibia: Anura: Microhylidae: Asterophryinae). *Zoological Research* **39**:130–157. DOI 10.24272/j.issn.2095-8137.2018.019.

Poyarkov NA, Vassilieva AB, Orlov NL, Galoyan EA, Tran DTA, Le DTT, Kretova VD, Geissler P. 2014. Taxonomy and distribution of narrow-mouth frogs of the genus *Microhyla* Tschudi, 1838 (Anura: Microhylidae) from Vietnam with descriptions of five new species. *Russian Journal of Herpetology* 21:89–148.

Pyron RA, Burbrink FT, Colli GR, de Oca ANM, Vitt LJ, Kuczynski CA, Wiens JJ. 2011. The phylogeny of advanced snakes (Colubroidea), with discovery of a new subfamily and comparison of support methods for likelihood trees. *Molecular Phylogenetics and Evolution* **58**:329–342. DOI 10.1016/j.ympev.2010.11.006.

Pyron RA, Burbrink FT, Wiens JJ. 2013. A phylogeny and revised classification of Squamata, including 4161 species of lizards and snakes. *BMC Evolutionary Biology* **13**:93. DOI 10.1186/1471-2148-13-93.

Quah ESH, Grismer LL, Lim KKP, Anuar M. S. S, Chan KO. 2020. A taxonomic revision of *Asthenodipsas malaccana* Peters, 1864 (Squamata: Pareidae) with a description of a new species from Borneo. *Zootaxa* **4729**:001–024. DOI 10.11646/zootaxa.4729.1.1.

Quah ESH, Grismer LL, Lim KKP, Anuar M. S. S, Imbun AY. 2019. A taxonomic reappraisal of the Smooth slug snake *Asthenodipsas laevis* (Boie, 1827) (Squamata: Pareidae) in Borneo with the description of two new species. *Zootaxa* **4646**:501–526. DOI 10.11646/zootaxa.4646.3.4.

Quah ESH, Lim KKP, Grismer LL. 2021. On the taxonomic status of *Asthenodipsas vertebralis* (Boulenger, 1900) (Squamata: Pareidae) in Borneo with the description of a new species. *Zootaxa* **4949**:24–44. DOI 10.11646/zootaxa.4949.1.2.

Rambaut A, Drummond AJ. 2007. Tracer. Version 1.5. Available at http://beast.bio.ed.ac.uk/Tracer.

Rao D-Q, Yang D-T. 1992. Phylogenetic systematics of Pareatinae (Serpentes) of Southeastern Asia and adjacent islands with relationship between it and the geology changes. *Acta Zoologica Sinica* **38**:139–150 (in Chinese).

Ree RH, Moore BR, Webb CO, Donoghue MJ. 2005. A likelihood framework for inferring the evolution of geographic range on phylogenetic trees. *Evolution* **59(11)**:2299–2311. DOI 10.1111/j.0014-3820.2005.tb00940.x.

3024   **Ree RH, Smith SA**. 2008. Maximum likelihood inference of geographic range evolution
3025 by dispersal, local extinction, and cladogenesis. *Systematic Biology* **57(1)**:4–14. DOI
3026 10.1080/10635150701883881.

3027   **Ronquist F, Huelsenbeck JP.** 2003. MrBayes 3: Bayesian phylogenetic inference under
3028 mixed models. *Bioinformatics* **19(12)**:1572–1574. DOI 10.1093/bioinformatics/btg180.

3029   **Ronquist F.** 1997. Dispersal-vicariance analysis: a new approach to the quantification of
3030 historical biogeography. *Systematic Biology* **46(1)**:195–203 DOI 10.1093/sysbio/46.1.195.

3031   **Russell DW, Sambrook J.** 2001. Molecular cloning: a laboratory manual. Cold Spring
3032 Harbor:Cold Spring Harbor Laboratory.

3033   **Salvi D, Harris DJ, Kaliontzopoulou A, Carretero MA, Pinho C**. 2013. Persistence
3034 across Pleistocene ice ages in Mediterranean and extra-Mediterranean refugia: Phylogeographic
3035 insights from the common wall lizard. *BMC Evolutionary Biology* 13:147. DOI 10.1186/1471-
3036 2148-13-147.

3037   **Schlegel H.** 1826. Notice sur l'Erpétologie de l'ile de Java; par M. Böié (Ouvrage
3038 manuscrit). *Bulletin des Sciences Naturelles et de Géologie (Section II du Bulletin Universel des*
3039 *Sciences naturelles de Férussac)* **9(2)**:233–240.

3040   **Schlegel H.** 1837. *Essai sur la physionomie des serpens. I. Partie générale. II. Partie*
3041 *descriptive. Atlas, 21 planches et 3 cartes.* Arnz Arnz & Comp, Leiden, 606 pp.

3042   **Schmidt D, Kunz K.** 2005. *Ernährung von Schlangen*. Natur und Tier Verlag, Münster,
3043 159 pp (in German).

3044   **Shaffer, H.B, Gidis, M, McCartney-Melstad, E, Neal, K.M, Oyamaguchi, H.M, Tellez,**
3045 **M. & Toffelmeir, E.M.** 2015. Conservation genetics and genomics of amphibians and reptiles.
3046 *Annual Review of Animal Biosciensces* **3**:23.1–23.26. DOI 10.1146/annurev-animal-022114-
3047 110920.

3048   **Shimodaira H.** 2002. An approximately unbiased test of phylogenetic tree selection.
3049 *Systematic Biology* **51(3)**:492–508.

3050   **Slowinski JB, Lawson R.** 2002. Snake phylogeny: evidence from nuclear and
3051 mitochondrial genes. *Molecular Phylogenetics & Evolution* **24(2)**:194–202. DOI 10.1016/S1055-
3052 7903(02)00239-7.

3053   **Smedley N.** 1931. Amphibiens and Reptiles from the Cameron Highlands, Malay
3054 Peninsular. *The Raffles Bulletin of Zoology* **6**:105–123.

3055   **Smith AM, Poyarkov NA, Hebert PDN.** 2008. CO1 DNA barcoding amphibians:take the
3056   chance, meet the challenge. *Molecular Ecology Notes* **8**:235–246. DOI 10.1146/annurev-animal-
3057   022114-110920.

3058   **Smith MA**. 1943. *The fauna of British India Ceylon and Burma, including the whole of the*
3059   *Indo-Chinese Sub-region. Reptilia and Amphibia. Vol. III. Serpentes*. Taylor and Francis,
3060   London, 583 pp.

3061   **Stephens M, Smith NJ, Donnelly P**. 2001. A new statistical method for haplotype
3062   reconstruction from population data. *The American Journal of Human Genetics* **68(4)**:978–989.
3063   DOI 10.1086/319501.

3064   **Stuebing RB, Inger RF, Lardner B**. 2014. *A field guide to the snakes of Borneo* (2nd
3065   edition). Natural History Publications (Borneo), Kota Kinabalu, 310 pp.

3066   **Suntrarachun S, Chanhome L, Hauser S, Sumontha M, Kanya K**. 2020. Molecular
3067   phylogenetic support to the resurrection of *Pareas macularius* from the synonymy of *Pareas*
3068   *margaritophorus* (Squamata: Pareidae). *Tropical Natural History* **20**:182–190.

3069   **Suwannapoom C, Sumontha M, Tunprasert J, Ruangsuwan T, Pawangkhanant P,**
3070   **Korost DV, Poyarkov NA.** 2018. A striking new genus and species of cave-dwelling frog
3071   (Amphibia: Anura: Microhylidae: Asterophryinae) from Thailand. *PeerJ* **6**:e4422. DOI
3072   10.7717/peerj.4422.

3073   **Taylor EH.** 1965. The serpents of Thailand and adjacent waters. *University of Kansas*
3074   *Science Bulletin* **45(9)**:609–1096.

3075   **Teynié A, David P.** 2010. *Voyages naturalistes au Laos. Les Reptiles*. Editions Revoir,
3076   Nohanent (France), 315 pp.

3077   **Teynié A, David P, Ohler, Luanglath, K.** 2004. Note on a collection of Amphibians and
3078   Reptiles from South Laos, with a discussion of the occurrence of Indo-Malayan species.
3079   *Hamadryad* **29(1)**:33–62.

3080   **Theobald W.** 1868a. Catalogue of the Reptiles of British Birma, embracing the Provinces
3081   of Pegu, Martaban, and Tenasserim; with descriptions of new or little-known species. *Journal of*
3082   *the Linnean Society*, London, (Zoology), **10(1)**:4–67.

3083   **Theobald W.** 1868b. Catalogue of Reptiles in the Museum of the Asiatic Society of
3084   Bengal. *Journal of the Asiatic Society of Bengal (Extra number)* 37: vi + 88 + iii pp, 4 pls.

3085   **Trifnopoulos J, Nguyen TL, von Haeseler A, Bui MQ**. 2016. W-IQTREE: a fast online
3086   phylogenetic tool for maximum likelihood analysis. *Nucleic Acids Research* **44(W1)**:W232–
3087   W235. DOI 10.1093/nar/gkw256.

3088   **Uetz P, Freed P, Hošek J.** 2021. *The Reptile Database*, http:reptiledatabase.reptarium.cz
3089   (accessed in March 2021).

3090   **Vences M, Guayasamin JM, Miralles A, de la Riva I**. 2013. To name or not to name:
3091   Criteria to promote economy of change in Linnaean *classifcation* schemes. *Zootaxa*
3092   **3636(2)**:201–244. DOI 10.11646/zootaxa.3636.2.1.

3093   **Vogel G, Nguyen TV, Lalremsanga HT, Biakzuala L, Hrima V, Poyarkov NA.** 2020.
3094   Taxonomic reassessment of the *Pareas margaritophorus-macularius* species complex
3095   (Squamata, Pareidae). *Vertebrate Zoology* **70**:547–569. DOI 10.26049/VZ70-4-2020-02.

3096   **Vogel G, Nguyen TV, Than Zaw, Poyarkov NA**. 2021. A new species of the *Pareas*
3097   *monticola* complex (Squamata, Serpentes, Pareidae) from Chin Mountains with additions to the
3098   *Pareas* fauna of Myanmar. *Journal of Natural History* **54(39-40):**2577–2612. DOI
3099   10.1080/00222933.2020.1856953.

3100   **Vogel G.** 2015. New montane species of the genus *Pareas* Wagler, 1830 (Squamata:
3101   Pareatidae) from Northern Myanmar. *Taprobanica* **7(1)**:1–7.

3102   **Wagler JG.** 1830. *Natürliches System der Amphibien, mit vorangehender Classification*
3103   *der Säugetiere und Vögel*. Ein Beitrag zur vergleichenden Zoologie. 1.0. Cotta, München,
3104   Stuttgart, and Tübingen, 354 pp.

3105   **Wallach V, Wuester W, Broadley DG.** 2009. In praise of subgenera: taxonomic status of
3106   cobras of the genus *Naja* Laurenti (Serpentes: Elapidae). *Zootaxa*, **2236**(1):26–36.

3107   **Wallach V, Williams KL, Boundy J.** 2014. *Snakes of the world*: *a catalogue of living and*
3108   *extinct species*. CRC press, Boca Raton:1237pp.

3109   **Wang P, Che J, Liu Q, Li K, Jin JQ, Jiang K, Shi L, Guo P.** 2020. A revised taxonomy
3110   of Asia snail-eating snakes *Pareas* (Squamata, Pareidae): evidence from morphological
3111   comparison and molecular phylogeny. *ZooKeys* **939**:45–64. DOI 10.3897/zookeys.939.49309.

3112   **Wilcox TP, Zwickl DJ, Heath TA, Hillis DM**. 2002. Phylogenetic relationships of the
3113   Dwarf Boas and a comparison of Bayesian and bootstrap measures of phylogenetic support.
3114   *Molecular Phylogenetics and Evolution* **25(2)**:361–371. DOI 10.1016/S1055-7903(02)00244-0.

3115   **Williams EW, Gardner EM, Harris R, Chaveerach A, Pereira JT, Zerega NJC.** 2017.

3116   Out of Borneo: biogeography, phylogeny and divergence date estimates of *Artocarpus*

3117   (Moraceae). *Annals of Botany* **119**:611–627. DOI 10.1093/aob/mcw249.

3118   **Wilson EO, Brown WL. 1953.** The subspecies concept and its taxonomic application.

3119   *Systematic Zoology* 2(3):967–111. DOI 10.2307/2411818.

3120   **Wood PL, Guo X-G, Travers SL, Su Y-C, Olson KV, Bauer AM, Grismer LL, Siler**

3121   **CD, Moyle RG, Andersen MJ, Brown RM.** 2020. Parachute geckos free fall into synonymy:

3122   *Gekko* phylogeny, and a new subgeneric classification, inferred from thousands of ultraconserved

3123   elements. *Molecular Biology and Evolution* **146**:106731. DOI 10.1016/j.ympev.2020.106731.

3124   **Wood PL, Heinicke MP, Jackman TR, Bauer AM.** 2012. Phylogeny of bent-toed geckos

3125   (*Cyrtodactylus*) reveals a west to east pattern of diversification. *Molecular Phylogenetics and*

3126   *Evolution* **65**(3):992–1003. DOI 10.1016/j.ympev.2012.08.025.

3127   **Wüster W, Scott T, O'Shea M, Kaiser H.** 2021. Confronting taxonomic vandalism in

3128   biology: conscientious community self-organization can preserve nomenclatural stability.

3129   *Biological Journal of the Linnean Society* **133(3)**:645–670. DOI 10.1093/biolinnean/blab009.

3130   **Xu W, Dong WJ, Fu TT, Gao W, Lu CQ, Yan F, Wu YH, Jiang K, Jin JQ, Chen HM,**

3131   **Zhang YP.** 2020. Herpetological phylogeographic analyses support a Miocene focal point of

3132   Himalayan uplift and biological diversification. *National Science Review*: nwaa263. DOI

3133   10.1093/nsr/nwaa263/5934401.

3134   **Yang D–T, Rao D–Q.** 2008. *Amphibia and Reptilia of Yunnan*, Kunming, Yunnan

3135   Publishing Group Corporation, Yunnan Science (in Chinese), 411 pp.

3136   **Yang J-H, Poyarkov NA**. 2021. A new species of the genus *Micryletta* (Anura,

3137   Microhylidae) from Hainan Island, China. *Zoological Research* **42**:234–240. DOI

3138   10.24272/j.issn.2095-8137.2020.333.

3139   **Yang J-H, Yeung HY, Huang X-Y, Yang S-P.** 2021. First record of *Pareas vindumi*

3140   Vogel, 2015 (Reptilia: Pareidae) from China with a revision to morphology. *Taprobanica* **10**:39–

3141   46. DOI 10.47605/tapro.v10i1.246.

3142   **Yang Z.** 2007. PAML 4: phylogenetic analysis by maximum likelihood. *Molecular*

3143   *Biology and Evolution* **24(8)**:1586–1591. DOI10.1093/molbev/msm088.

3144   **You CW, Poyarkov NA, Lin SM.** 2015. Diversity of the snail-eating snakes *Pareas*

3145   (Serpentes, Pareatidae) from Taiwan. *Zoologica Scripta* **44(4)**:349–361. DOI 10.1111/zsc.12111.

3146 **Yu Y, Harris AJ, Blair C, He X.** 2015. RASP (Reconstruct Ancestral State in
3147 Phylogenies): a tool for historical biogeography. *Molecular Phylogenetics and Evolution* **87**:46–
3148 49 DOI 10.1016/j.ympev.2015.03.008.

3149 **Yuan ZY, Zhou WW, Chen X, Poyarkov NA, Chen HM, Jang-Liaw NL, Chou WH,**
3150 **Matzke NJ, Iizuka K, Min MS, Kuzmin SL, Zhang YP, Cannatella DC, Hillis DM, Che J.**
3151 2016. Spatiotemporal diversification of the true frogs (genus *Rana*): an historical framework for
3152 a widely studied group of model organisms. *Systematic Biology* **65**(5):824–842;
3153 DOI10.1093/sysbio/syw055.

3154 **Zachos J, Pagani M, Sloan L, Thomas E, Billups K.** 2001. Trends, rhythms, and
3155 aberrations in global climate 65 Ma to present. *Science* **292**:686–693. DOI
3156 10.1126/science.1059412.

3157 **Zaher H, Murphy RW, Arredondo JC, Graboski R, Machado-Filho PR, Mahlow K,**
3158 **Montingelli GG, Quadros AB, Orlov NL, Wilkinson M, Zhang Y-P, Grazziotin FG**. 2019.
3159 Large-scale molecular phylogeny, morphology, divergence-time estimation, and the fossil record
3160 of advanced caenophidian snakes (Squamata: Serpentes). *PLoS ONE* 14:e0216148. DOI
3161 10.1371/journal.pone.0216148.

3162 **Ziegler T, Ohler A, Vu NT, Le KQ, Nguyen XT, Dinh HT, Bui NT.** 2006. Review of
3163 the amphibian and reptile diversity of Phong Nha – Ke Bang National Park and adjacent areas,
3164 central Truong Son, Vietnam. In: Vences M, Köhler J, Ziegler T, Böhme W (Eds.): *Herpetologia*
3165 *Bonnensis II*; Proceedings of the 13th Ordinary General Meeting of the Societas Europaea
3166 Herpetologica, Bonn: 247–262.

Table 1. Species-level scientific names erected for the members of the subgenus *Pareas*.

1   **Table 1.** Species-level scientific names erected for the members of the subgenus *Pareas*.

No.	Authority	Original taxon name	Type locality	Previous taxonomy	New taxonomy
1	*Wagler, 1830*	*Pareas carinata*	Java, Indonesia	*Pareas carinatus*	*Pareas carinatus*
2	*Theobald, 1868*	*Pareas berdmorei*	Mon State, Myanmar	synonym of *Pareas carinatus*	*Pareas berdmorei*
3	*Boulenger, 1900*	*Amblycephalus nuchalis*	Matang, Kidi District, Sarawak, Malaysia	*Pareas nuchalis*	*Pareas nuchalis*
4	*Bourret, 1934*	*Amblycephalus carinatus unicolor*	Kampong Speu Province, Cambodia	synonym of *Pareas carinatus*	*Pareas berdmorei unicolor* **comb. nov.**
5	*Wang et al., 2020*	*Pareas menglaensis*	Mengla County, Yunnan Province, China	*Pareas menglaensis*	synonym of *Pareas berdmorei*
6	*Le et al., 2021*	*Pareas temporalis*	Doan Ket Commune, Da Huoai District, Lam Dong Province, Vietnam	*Pareas temporalis*	*Pareas temporalis*
7	*this paper*	*Pareas carinatus tenasserimicus*	Suan Phueng District, Ratchaburi Province, Thailand	-	*Pareas carinatus tenasserimicus* **ssp. nov.**
8	*this paper*	*Pareas berdmorei annamiticus*	Nahin District, Khammouan Province, Laos	-	*Pareas berdmorei annamiticus* **ssp. nov.**
9	*this paper*	*Pareas kuznetsovorum*	Song Hinh District, Phu Yen Province, Vietnam	-	*Pareas kuznetsovorum* **sp. nov.**
10	*this paper*	*Pareas abros*	Song Thanh N.P., Quang Nam Province, Vietnam	-	*Pareas abros* **sp. nov.**

Table 2. Measurements and meristic characters of members of the subgenus *Pareas*: *Pareas abros* sp. nov., *P. kuznetsovorum* sp. nov., *P. carinatus*, *P. berdmorei*, *P. nuchalis* and *P. temporalis*.

Abbreviations are listed in the Materials and methods.

1 **Table 2.** Measurements and meristic characters of members of the subgenus *Pareas*: *Pareas abros* **sp. nov.**, *P. kuznetsovorum* **sp.**
2 **nov.**, *P. carinatus*, *P. berdmorei*, *P. nuchalis* and *P. temporalis*.

Characters		*P. abros*	*P. kuznetsovorum*	*P. carinatus*	*P. berdmorei*	*P. nuchalis*	*P. temporali*
TL	Min–Max	434–565	638.5	337–702	421–770	555–665	555–665
	Mean±SD	506.7±66.7		494.3±73.3	554.9±73.3	577.1±34.5	577.1±34.5
	n	3	1	24	34	7	7
TaL/TL	Min–Max	0.26–0.29	0.25	0.18–0.25	0.17–0.27	0.20–0.26	0.20–0.26
	Mean±SD	0.28±0.01		0.22±0.02	0.21±0.02	0.24±0.02	0.24±0.02
	n	3	1	24	32	7	7
VEN	Min–Max	180–184	167	158–194	162–187	185–198	185–198
	Mean±SD	182.7±2.3		171.4±9.3	176.9±5.8	189.0±4.4	189.0±4.4
	n	3	1	26	38	7	7
SC	Min–Max	83–95	87	54–96	57–89	86–92	86–92
	Mean±SD	90.0±6.2		69.3±9.0	71.6±7.3	88.7±2.4	88.7±2.4
	n	3	1	26	34	7	7
KMD	Min–Max	9–11	0	0–11	3–13	15	15
	Mean±SD	10.3±1.1		6.5±2.9	8.83±2.76	15.0±0.0	15.0±0.0
	n	3	1	19	33	7	7
VSC	Min–Max	1	1	3	1–3	3	3
	Mean±SD	1.0±0.0		3.0±0.0	2.83±0.56	3.0±0.0	3.0±0.0
	n	3	1	26	38	7	7

5

Figure 1

Figure 1. Map showing distribution of the subgenus *Pareas* and location of studied populations.

Circles denote localities for which both DNA and morphological data were examined; triangles denote populations for which only DNA data were available; filled diamonds denote localities for which only morphological data were available; empty diamonds denote localities for which only photo data was available and therefore the species identification is tentative (a–c); dot in the center of an icon indicates the type locality. **Confirmed localities:** (1) Indonesia, Java; (2) Indonesia, West Java, Bogor; (3) Indonesia, West Java; (4) Indonesia, Central Java, Karimundjava Isl.; (5) Indonesia, East Java; (6) Indonesia, Sumatra, Ranau Lake; (7) Indonesia, North Sumatra; (8) Indonesia, Borneo, Central Kalimantan, Moara Terweh; (9) Indonesia, Borneo, East Kalimantan, Kutai N.P.; (10) Malaysia, Borneo, Sarawak; (11) Malaysia, Pahang, Frazers Hills; (12) Malaysia, Terengganu; (13) Malaysia, Kedah, Sungai Sedim; (14) Thailand, Ratchaburi, Suan Phueng; (15) Myanmar, Tanintharyi, Yaephyu; (16) Myanmar, Mon; (17) Myanmar, Mon, Kyaikhto, Kinpon Chaung; (18) Thailand, Chiang Mai, Doi Inthanon N.P.; (19) Thailand, Phitsanulok, Phu Hin Rong Kla N.P.; (20) Laos, Luangphrabang; (21) Laos, Phongsaly; (22) China, Yunnan, Mengla; (23) China, Yunnan, Xishuangbannna; (24) China, Yunnan, Pu'er; (25) Vietnam, Dien Bien, Muong Nhe N.R.; (26) Vietnam, Vinh Phuc, Tam Dao N.P.; (27) Laos, Khammouan, Nahin; (28) Vietnam, Quang Binh, Thanh Thach; (29) Cambodia, Kampong Speu; (30) Vietnam, An Giang, Bay Nui Mt.; (31) Vietnam, Dong Nai, Trang Bom; (32) Vietnam, Dong Nai, Ma Da N.R. (Vinh Cuu); (33) Vietnam, Dong Nai, Cat Tien N.P.; (34) Vietnam, Tay Ninh, Lo Go - Xa Mat N.P.; (35) Vietnam, Binh Phuoc, Bu Gia Map N.P.; (36) Vietnam, Lam Dong, Loc Bao; (37) Vietnam, Lam Dong, Di Linh; (38) Vietnam, Lam Dong, Cat Loc; (39) Vietnam, Lam Dong, Da Huoai; (40) Vietnam, Lam Dong, Bidoup - Nui Ba N.P.; (41) Vietnam, Phu Yen, Song Hinh; (42) Vietnam, Quang Nam, Song Thanh N.P.; (43)

Vietnam, Thua Thien-Hue, A Roang, Sao La N.R.; (44) Malaysia, Sarawak, Betong, Saribas; (45) Malaysia, Sarawak, Niah N.P.; (46) Malaysia, Sarawak, Bintulu; (47) Brunei, *Brunei Darussalam*; (48) Malaysia, Sabah, Tenom; (49) Indonesia, Sumatra, Riau, Indragiri; (50) Indonesia, Sumatra, Bengkulu, Kepahiang. **Unconfirmed localities:** (a) Thailand, Phetchaburi, Kaeng Krachan N.P.; (b) Laos, Champasak, Xe Pian N.P.A.; (c) Vietnam, Quang Binh, Phong Nha - Ke Bang N.P.. Base Map created using simplemappr.net.
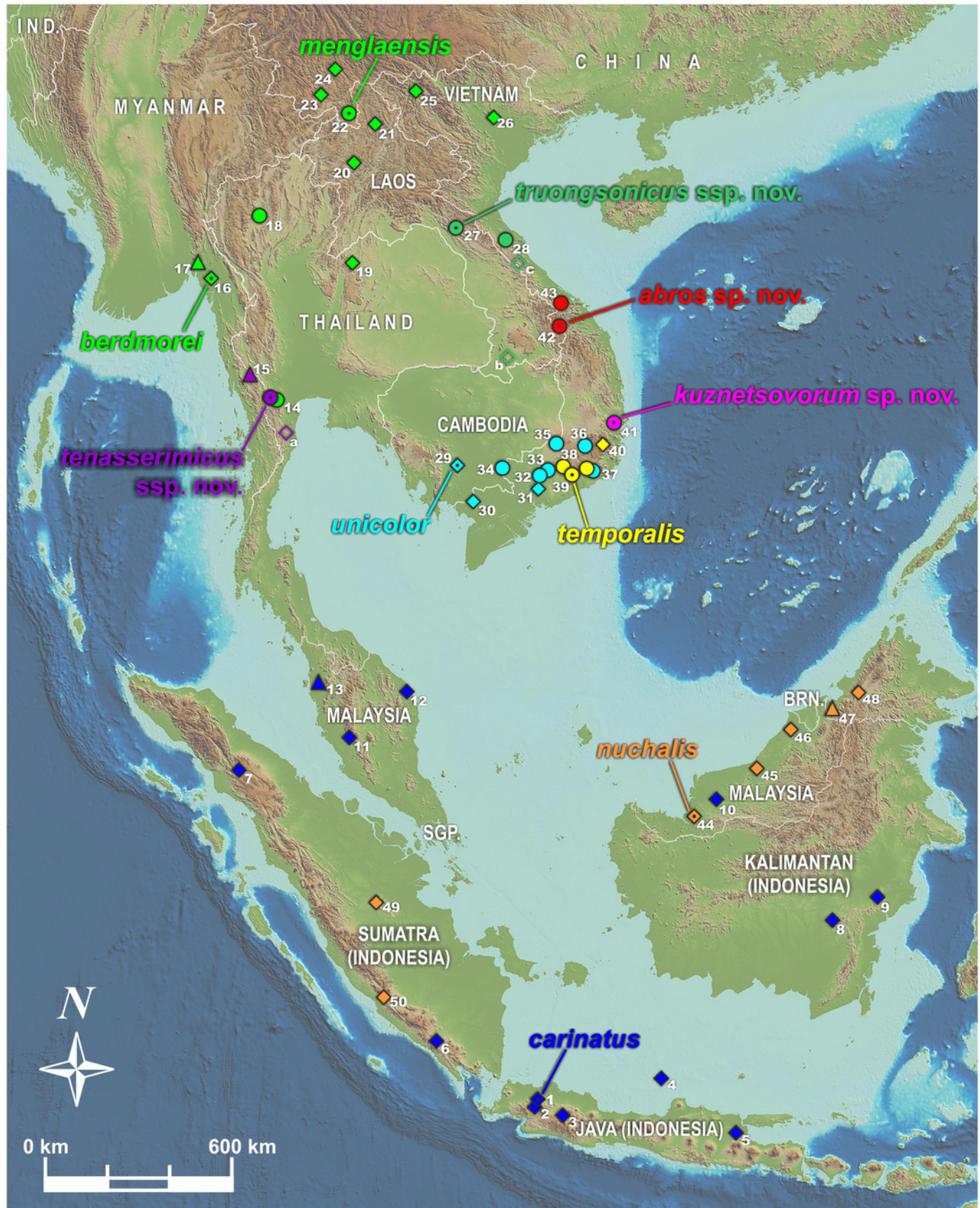
Figure 2

Figure 2. Time tree and biogeographic history of the subfamily Pareinae.

(A) Biogeographic regions used in the present study; (B) BEAST chronogram on the base of 3588 bp–long mtDNA + nuDNA dataset with the results of ancestral area reconstruction using Langrange Dispersal-Extinction-Cladogenesis (DEC) model in RASP. For biogeographic areas definitions, species occurrence data and transition matrices see Supplementary Tables S5 and S6. Information at tree tips corresponds to biogeographic area code (see Fig. 2A), sample number (summarized in Supplementary Table S1), and species name, respectively. Node colors correspond to the respective biogeographic areas; values inside node icons correspond to node numbers (see Supplementary Table S9 and Supplementary Figure S1 for divergence time estimates); values in grey near nodes indicate marginal probabilities for ancestral ranges (S–DIVA analysis), values in blue near nodes correspond to median time of divergence (see Supplementary Table S9); icons illustrate vicariant and dispersal events (see Legend). Base Map created using simplemappr.net.
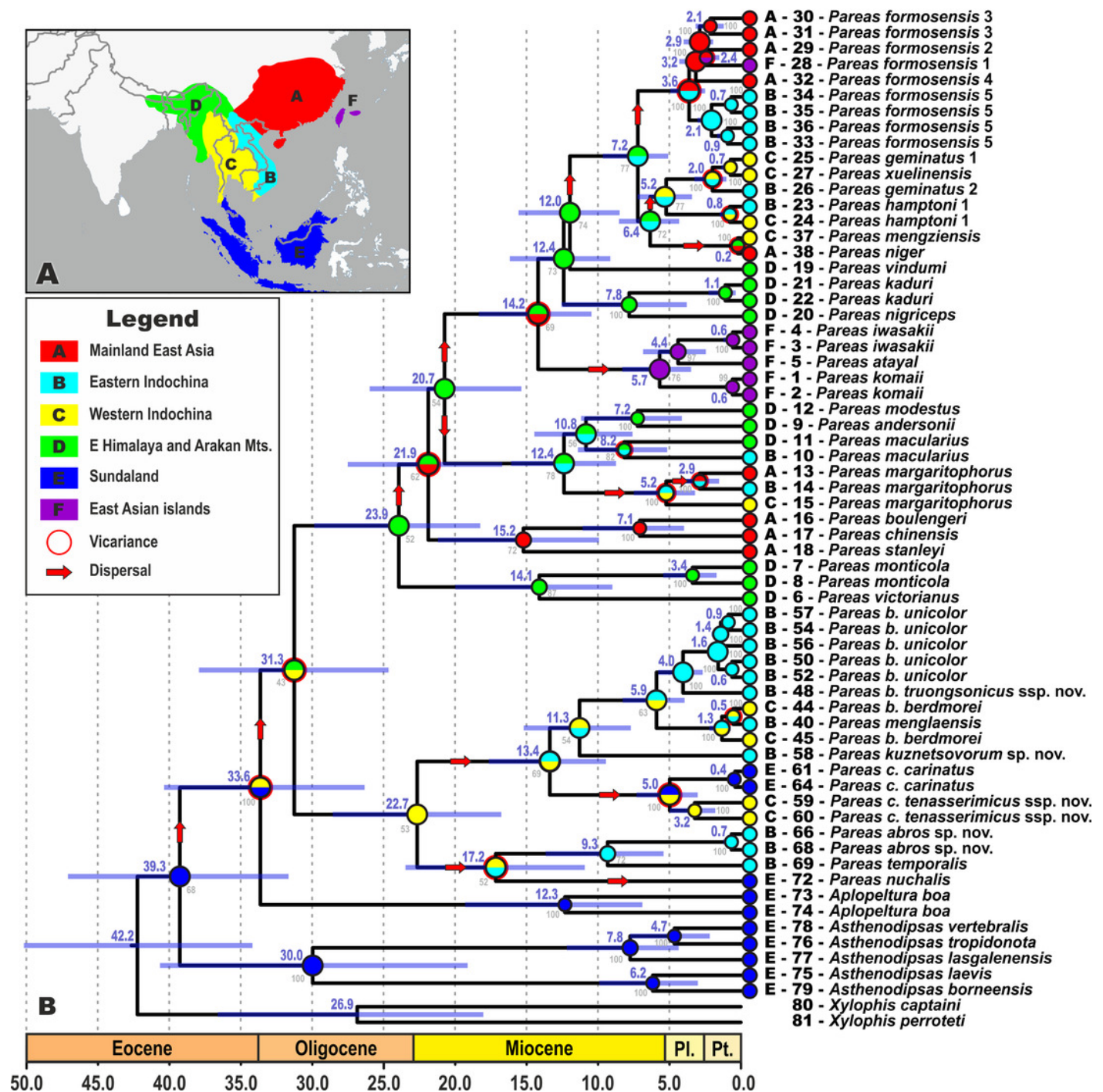
Figure 3

Figure 3. Bayesian inference tree of the subfamily Pareinae derived from the analysis of 1,126 bp of cyt *b*, 681 bp of *ND4*, 737 bp of *cmos*, and 1,026 bp of *RAG1* gene fragments.

For voucher specimen information and GenBank accession numbers see Supplementary Table S1. Colors denote the taxa of the subgenus *Pareas* and correspond to the color of icons in Figures 1 and 4. Numbers at tree nodes correspond to PP/UFBS support values, respectively. Photos on thumbnails by N. A. Poyarkov (*Pareas abros* **sp. nov.**, *P. temporalis*, and *P. kuznetsovorum* **sp. nov.**), and P. Pawangkhanant (*P. berdmorei truongsonicus* **ssp. nov.** and *P. carinatus tenasserimicus* **ssp. nov.**).

P. kuznetsovorum sp. nov.

P. b. truongsonicus ssp. nov.

P. c. tenasserimicus ssp. nov.

P. abros sp. nov.

P. temporalis

Pareas carinatus
species group

Pareas nuchalis
species group

A1

A2

A

0.97/88	53 - *Pareas carinatus* - Lam Dong (Loc. 36)
1.0/88	55 - *Pareas carinatus* - Dong Nai (Loc. 33)
0.96/85	52 - *Pareas carinatus* - Tay Ninh (Loc. 34)
1.0/100	49 - *Pareas carinatus* - Dong Nai (Loc. 32)
1.0/96	51 - *Pareas carinatus* - Dong Nai (Loc. 32)
1.0/100	50 - *Pareas carinatus* - Dong Nai (Loc. 32)
1.0/99	54 - *Pareas carinatus* - Lam Dong (Loc. 37)
	57 - *Pareas carinatus* - Binh Phuoc (Loc. 35)
0.97/91	56 - *Pareas carinatus* - Dong Nai (Loc. 33)
1.0/100	47 - *Pareas carinatus* - Khammoun (Loc. 27)
1.0/98	48 - *Pareas carinatus* - Quang Binh (Loc. 28)
1.0/97	42 - *Pareas menglaensis* - Yunnan (Loc. 22)
1.0/95	43 - *Pareas menglaensis* - Yunnan (Loc. 22)
1.0/100	41 - *Pareas menglaensis* - Yunnan (Loc. 22)
	40 - *Pareas menglaensis* - Yunnan (Loc. 22)
	39 - *Pareas menglaensis* - Yunnan (Loc. 22)
1.0/100	44 - *Pareas carinatus* - Chiang Mai (Loc. 18)
1.0/100	45 - *Pareas berdmorei* - Mon (Loc. 17)
	46 - *Pareas carinatus* - Ratchaburi (Loc. 14)
	58 - *Pareas* cf. *carinatus* - Phu Yen (Loc. 41)

1. *Pareas berdmorei unicolor* comb. nov.

2. *Pareas berdmorei truongsonicus* ssp. nov.

3. *Pareas berdmorei berdmorei*

4. *Pareas kuznetsovorum* sp. nov.

1.0/100	63 - *Pareas carinatus* - Peninsular Malaysia
1.0/100	64 - *Pareas carinatus* - Peninsular Malaysia
0.94/99	65 - *Pareas carinatus* - Peninsular Malaysia
1.0/100	62 - *Pareas carinatus* - Peninsular Malaysia
	61 - *Pareas carinatus* - Kedah (Loc. 13)
1.0/100	60 - *Pareas carinatus* - Ratchaburi (Loc. 14)
	59 - *Pareas carinatus* - Tanintharyi (Loc. 15)
1.0/100	67 - *Pareas* cf. *carinatus* - Thua Thien-Hue (Loc. 43)
1.0/100	68 - *Pareas* cf. *carinatus* - Thua Thien-Hue (Loc. 43)
	66 - *Pareas* cf. *carinatus* - Quang Nam (Loc. 42)
1.0/100	69 - *Pareas temporalis* - Lam Dong (Loc. 38)
1.0/100	71 - *Pareas temporalis* - Lam Dong (Loc. 39)
	71 - *Pareas nuchalis* - Brunei (Loc. 47)

5. *Pareas carinatus carinatus* stat. nov.

6. *Pareas carinatus tenasserimicus* ssp. nov.

7. *Pareas abros* sp. nov.

8. *Pareas temporalis*

9. *Pareas nuchalis*

subgenus *Pareas*

genus *Pareas*

Pareas hamptoni
species group

1.0/100	36 - *Pareas formosensis* 5
1.0/99	33 - *Pareas formosensis* 5
0.99/98	35 - *Pareas formosensis* 5
1.0/100	34 - *Pareas formosensis* 5
0.75/74	32 - *Pareas formosensis* 4 (= *P. tonkinensis*)
1.0/94	31 - *Pareas formosensis* 3
	30 - *Pareas formosensis* 3
	29 - *Pareas formosensis* 2
	28 - *Pareas formosensis* 1
1.0/100	27 - *Pareas xuelinensis*
1.0/100	25 - *Pareas geminatus* 1
1.0/98	26 - *Pareas geminatus* 2
1.0/100	23 - *Pareas hamptoni*
	24 - *Pareas hamptoni*
	38 - *Pareas niger*
	37 - *Pareas mengziensis*
0.56/88	3 - *Pareas iwasakii*
1.0/100	4 - *Pareas iwasakii*
	5 - *Pareas atayal*
1.0/100	1 - *Pareas komaii*
	2 - *Pareas komaii*
	19 - *Pareas vindumi*
1.0/100	21 - *Pareas kaduri*
1.0/99	22 - *Pareas kaduri*
	20 - *Pareas nigriceps*

0.97/79

0.53/54

0.60/-

B1

subgenus *Eberhardtia* stat. nov.

Pareas margaritophorus
species group

1.0/100	9 - *Pareas andersonii*
0.90/97	12 - *Pareas modestus*
1.0/100	10 - *Pareas macularius*
1.0/100	11 - *Pareas macularius*
1.0/100	13 - *Pareas margaritophorus*
1.0/100	14 - *Pareas margaritophorus*
	15 - *Pareas margaritophorus*

B2

Pareas chinensis species group

1.0/100	16 - *Pareas boulengeri*
1.0/100	17 - *Pareas chinensis*
	18 - *Pareas stanleyi*

B3

Pareas monticola species group

1.0/100	7 - *Pareas monticola*
1.0/100	8 - *Pareas monticola*
	6 - *Pareas victorianus*

B4

0.99/89

1.0/92

B 1.0/100

Pareinae 1.0/100

C 1.0/100

1.0/100	72 - *Aplopeltura boa*
	73 - *Aplopeltura boa*

genus *Aplopeltura*

D 1.0/100

1.0/98	75 - *Asthenodipsas tropidonota*
1.0/100	77 - *Asthenodipsas vertebralis*
	76 - *Asthenodipsas lasgalenensis*

subgenus *Spondylodipsas* subgen. nov.

genus *Asthenodipsas*

E

1.0/100	74 - *Asthenodipsas laevis*
	78 - *Asthenodipsas borneensis*

subgenus *Asthenodipsas*

Xylophiinae

79 - *Xylophis captaini*

0.07

Figure 4

Figure 4. Principal component analysis (PCA) of the species of the subgenus *Pareas* showing ordination along the first two (A) and the first and the third (B) principal components.

Colors denote the taxa of the subgenus *Pareas* and correspond to the color of icons in Figures 1 and 3; dot in the center of an icon indicates the holotype or lectotype of a taxon.
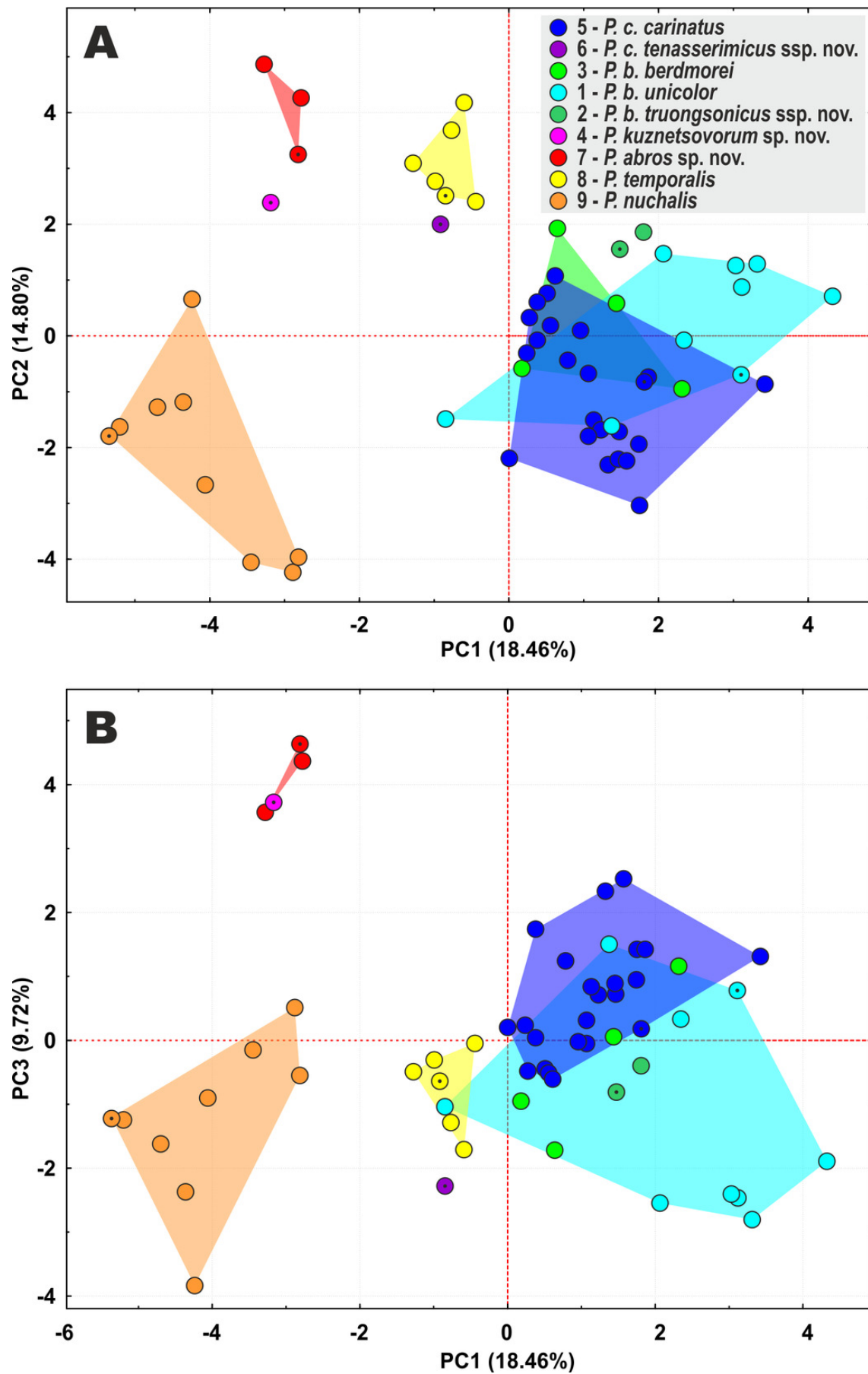
Figure 5

Figure 5. Head scalation of the genera of the subfamily Pareinae.

Dorsal aspect: A – *Pareas (Eberhardtia) formosensis* (FMNH 2555567); B – *Pareas (Pareas) carinatus* (RMNH 954C, lectotype); Ventral aspect: C – *Asthenodipsas (Asthenodipsas) malaccana* (SMF 32580); D – *Asthenodipsas (Asthenodipsas) laevis* (SMF 81195); E – *Asthenodipsas (Spondylodipsas* **subgen. nov.***)* *vertebralis* (ZMB 65285); F – *Asthenodipsas (Spondylodipsas* **subgen. nov.***)* *tropidonota* (RMNH 4902B, lectotype); G – *Aplopeltura boa* (ZMB 5397); H – *Pareas (Pareas) carinatus* (ZMB 5397); I – *Pareas (Eberhardtia) formosensis* (ZMB 30585); J – *Pareas (Eberhardtia) margaritophorus* (ZMB 6339). Not to scale. Magenta, cyan, blue, red, green and yellow denote frontal, parietals, mental, inframaxillary, infralabials, and chin shields, respectively. Drawings by N. A. Poyarkov (A–B) and L. B. Salamakha (C–J).
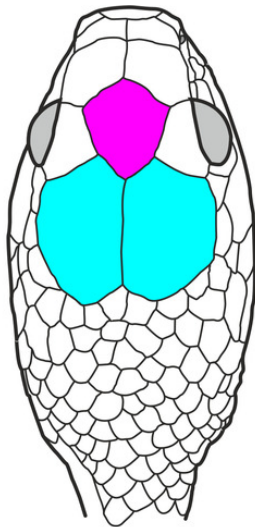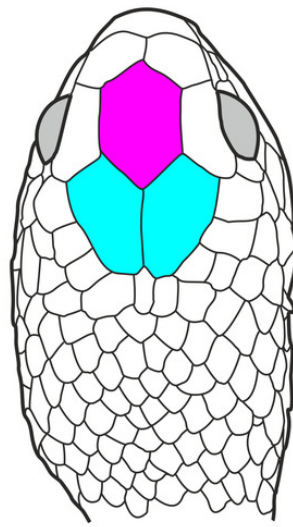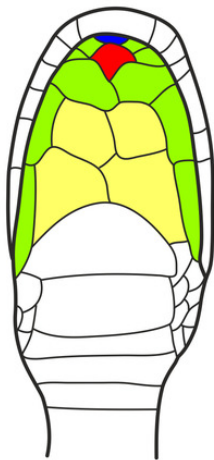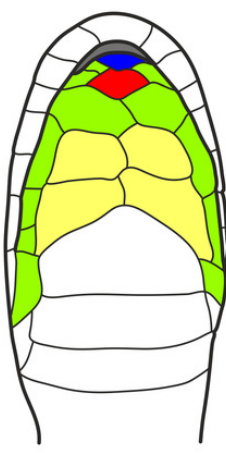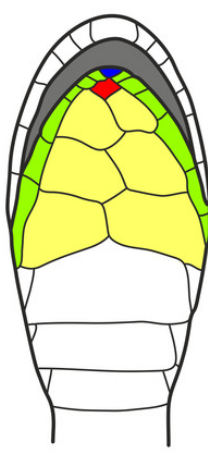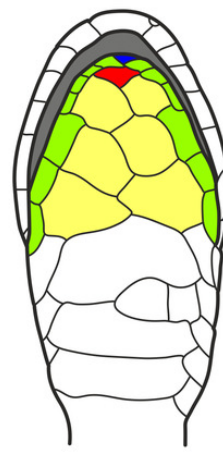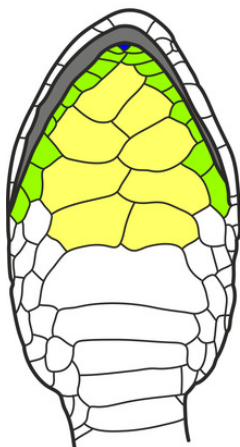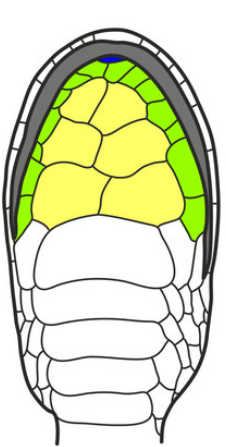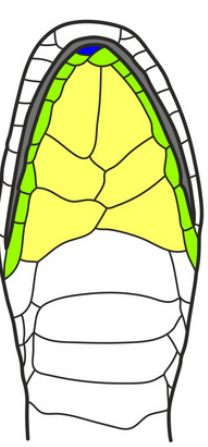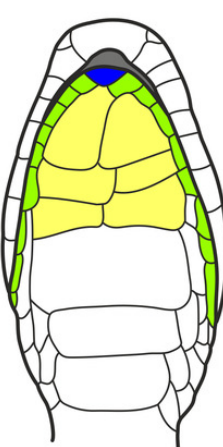
frontal   parietals   chin shields
mental   inframaxillary   infralabials

Figure 6

Figure 6. Lateral views of head scalation of taxa of the subgenus *Pareas*.

A – lectotype of *Pareas carinatus* Wagler, 1830 (RMNH 954 C); B – holotype of *P. carinatus tenasserimicus* **ssp. nov.** (ZMMU R-16800); C – lectotype of *Pareas berdmorei* Theobald, 1868 (ZSI 8022); D – holotype of *Pareas menglaensis* Wang, Che, Liu, Ki, Jin, Jiang, Shi & Guo, 2020 (YBU 14124); E – holotype of *P. berdmorei truongsonicus* **ssp. nov.** (ZMMU R-16801); F – holotype of *Amblycephalus carinatus unicolor* Bourret, 1934 (MNHN 1938.0149); G – holotype of *Pareas kuznetsovorum* **sp. nov.** (ZMMU R-16802); H – *Pareas nuchalis* (Boulenger, 1900) (FMNH 131635); I – holotype of *Pareas abros* **sp. nov.** (ZMMU R-16393); J – male of *Pareas temporalis* Le, Tran, Hoang & Stuart, 2021 (ZMMU R-13656). Not to scale. Drawings by L. B. Salamakha.
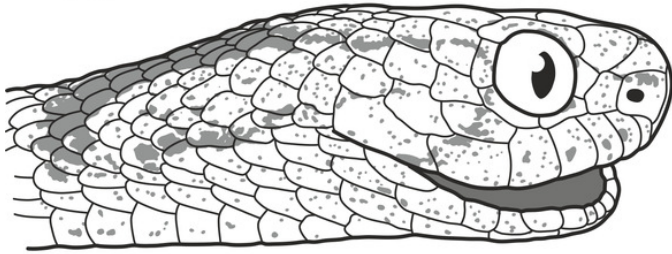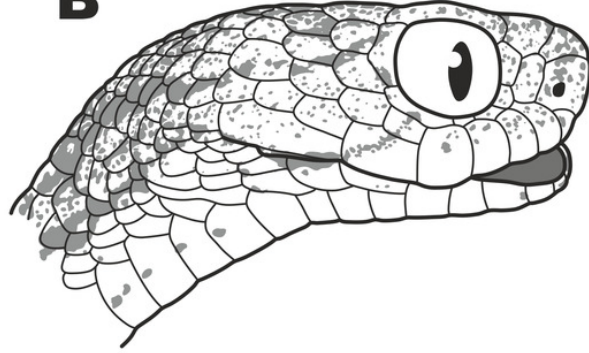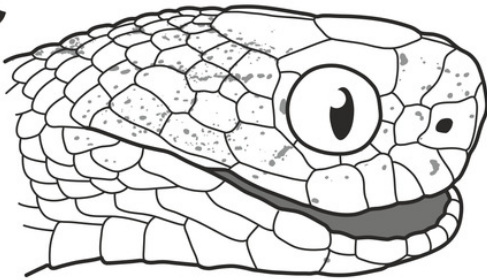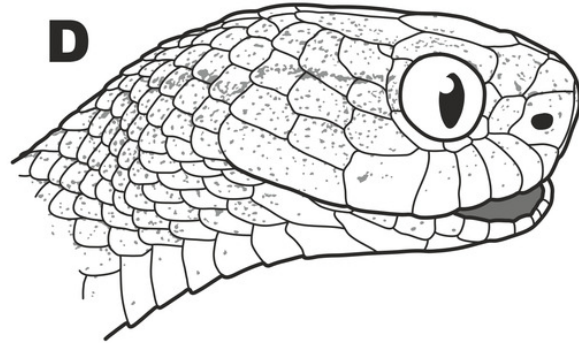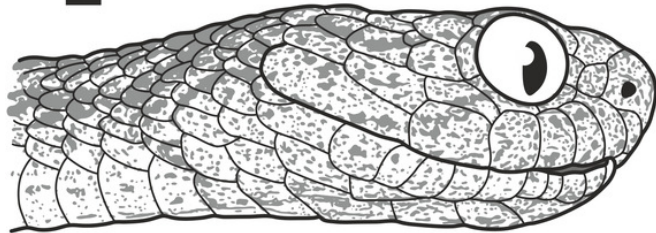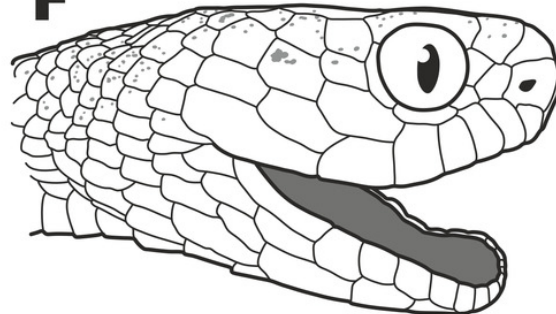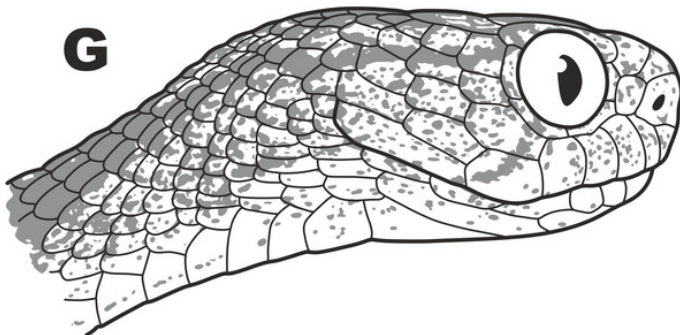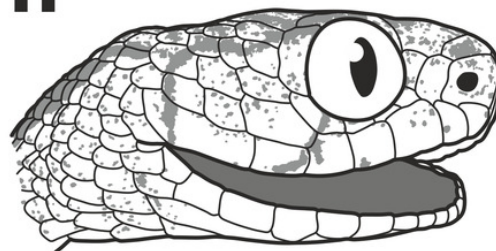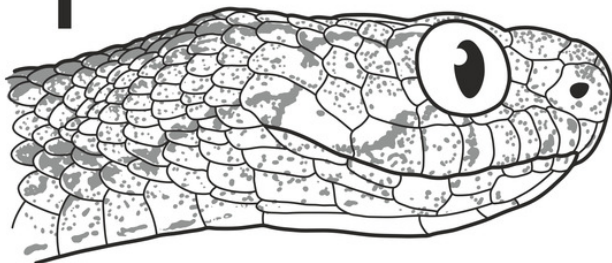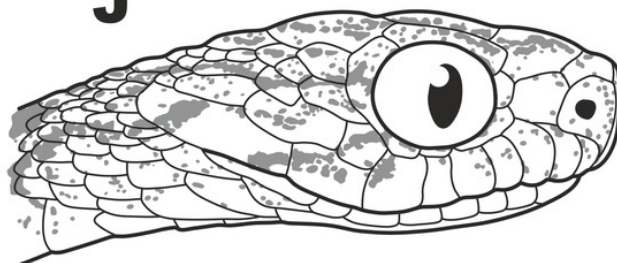
Figure 7

Figure 7. Lectotype of *Pareas carinatus* Wagler, 1830 in preservative (RMNH 954 C, adult male).

A – dorsal view of body; B – ventral view of body; C–F – head in lateral right, lateral left, dorsal, and ventral aspects, respectively. Photos by G. Vogel.
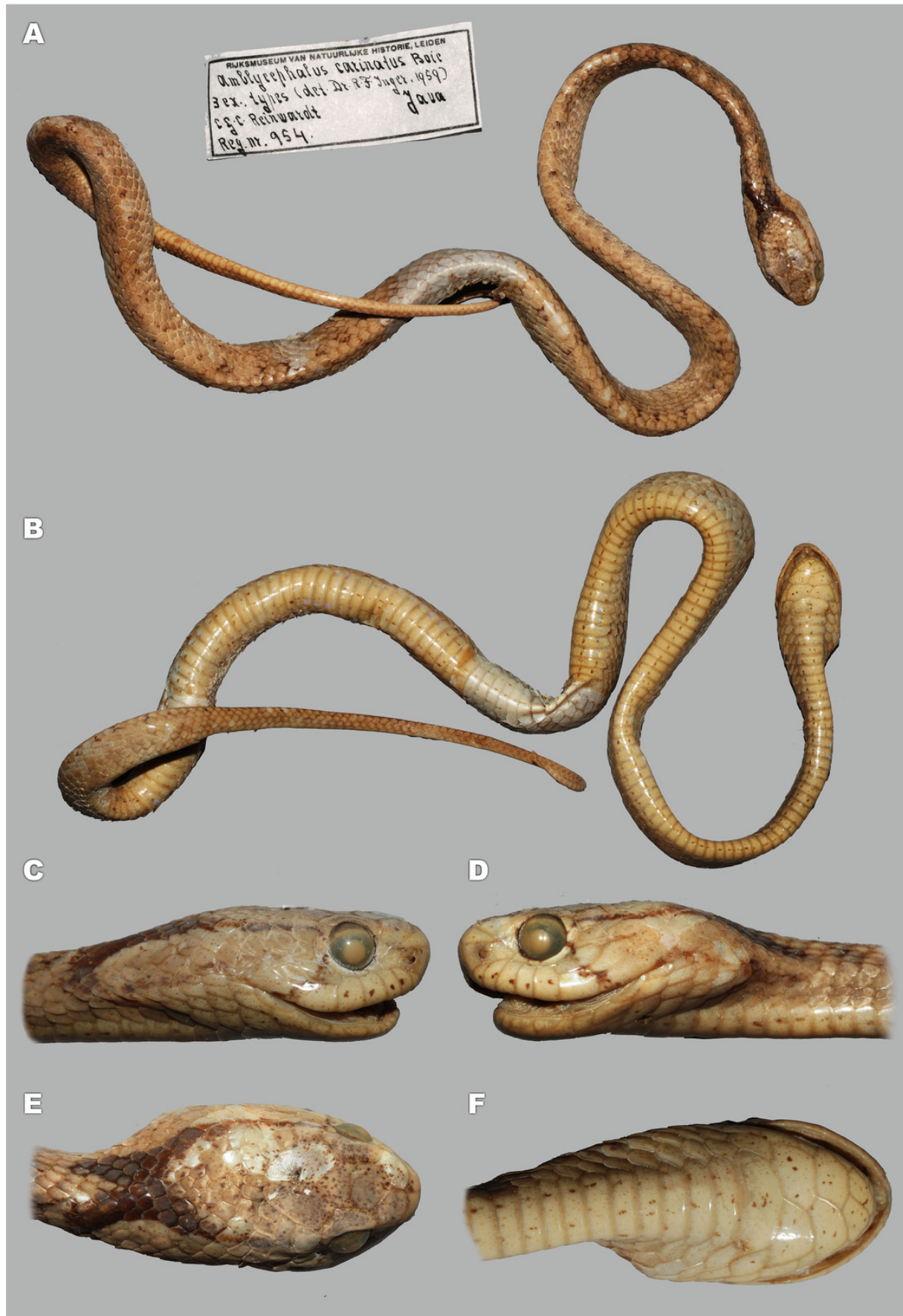
Figure 8

Figure 8. Holotype of *P. carinatus tenasserimicus* ssp. nov. in preservative (ZMMU
R-16800, adult male).

A – dorsal view of body; B – ventral view of body; C–F – head in lateral right, lateral left,
dorsal, and ventral aspects, respectively. Photos by N. A. Poyarkov.
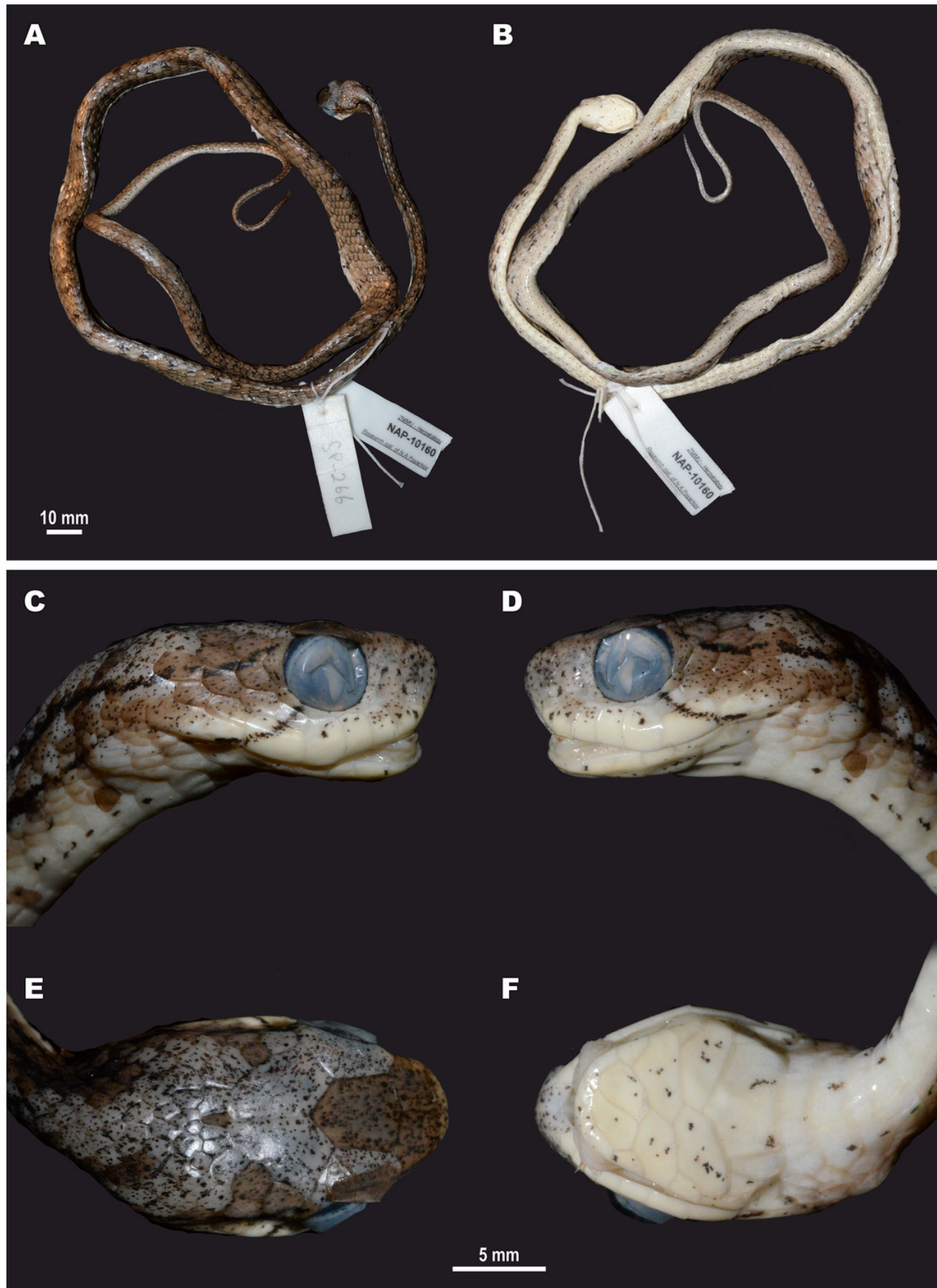
Figure 9

Figure 9. Members of the *Pareas carinatus* complex in life.

A – *P. c. carinatus* from Hala-Bala W.S., Narathiwat Province, Thailand; B, C – *P. c. carinatus* from Gunung Leuser N.P., Bukit Lawang Province, Sumatra, Indonesia; D – *P. c.* cf. *tenasserimicus* **ssp. nov.** from Kaeng Krachan N.P., Phetchaburi Province, Thailand; E – *P. c. tenasserimicus* **ssp. nov.** from Suan Phueng, Ratchaburi Province, Thailand. Photos by L.A. Neimark (A), Guek Hock Ping aka Kurt Orion (B), H.X.N. Nguyen (C), P. Pawangkhanant (D), and M. Naiduangchan (E).

Figure 10

Figure 10. Lectotype of *Pareas berdmorei* Theobald, 1868 in preservative (ZSI 8022, adult male).

A – general dorsolateral view of body; B – lateral left aspect of head. Photos by I. Das.

Figure 11

Figure 11. Holotype of *Amblycephalus carinatus unicolor* Bourret, 1934 in preservative (MNHN 1938.0149, adult female).

A – dorsal view of body; B – ventral view of body; C–F – head in lateral right, lateral left, dorsal, and ventral aspects, respectively. Photos by G. Vogel.
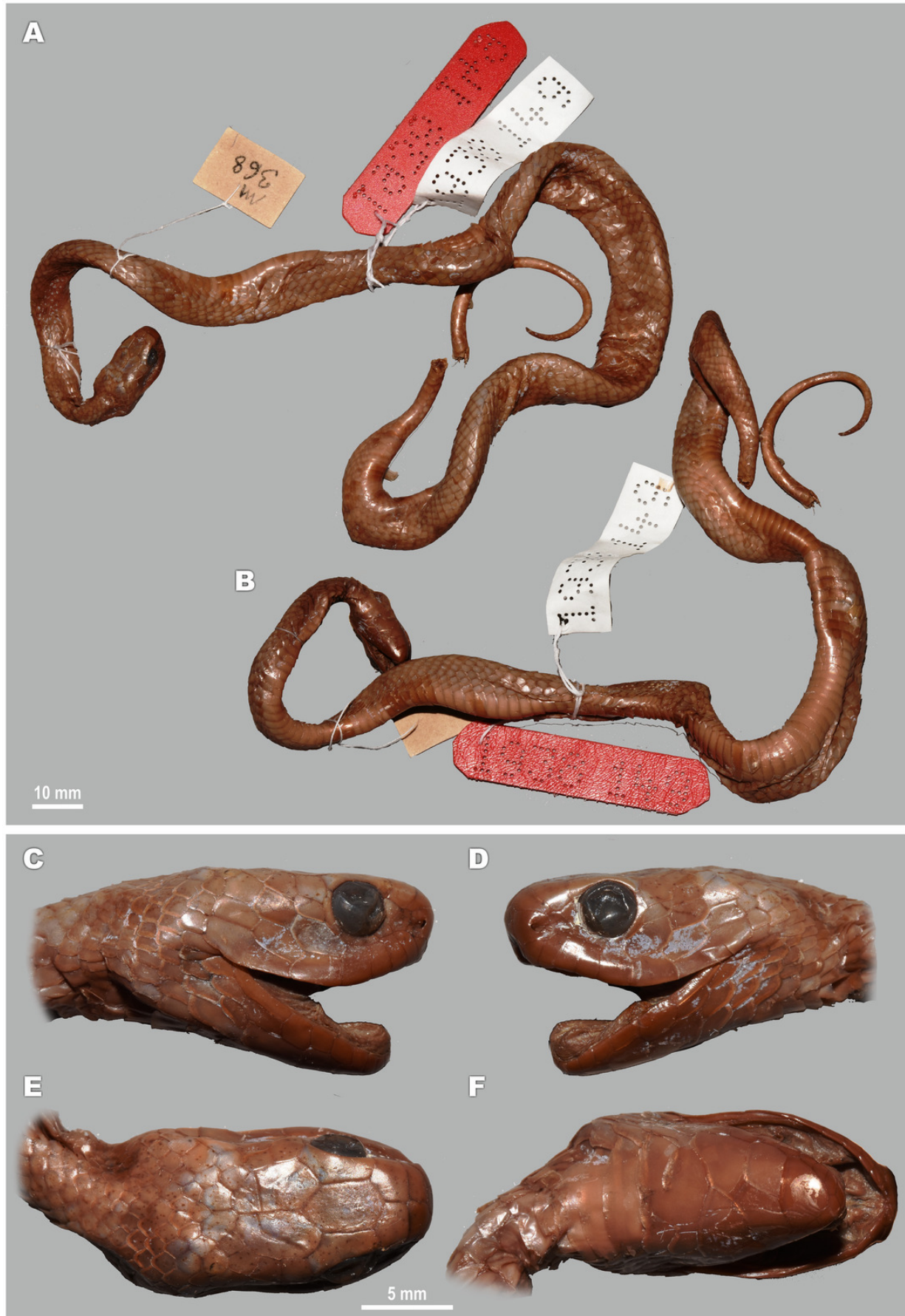
Figure 12

Figure 12. Holotype of *P. berdmorei truongsonicus* ssp. nov. in preservative (ZMMU R-16801, adult female).

A – dorsal view of body; B – ventral view of body; C–F – head in lateral right, lateral left, dorsal, and ventral aspects, respectively. Photos by N. A. Poyarkov.
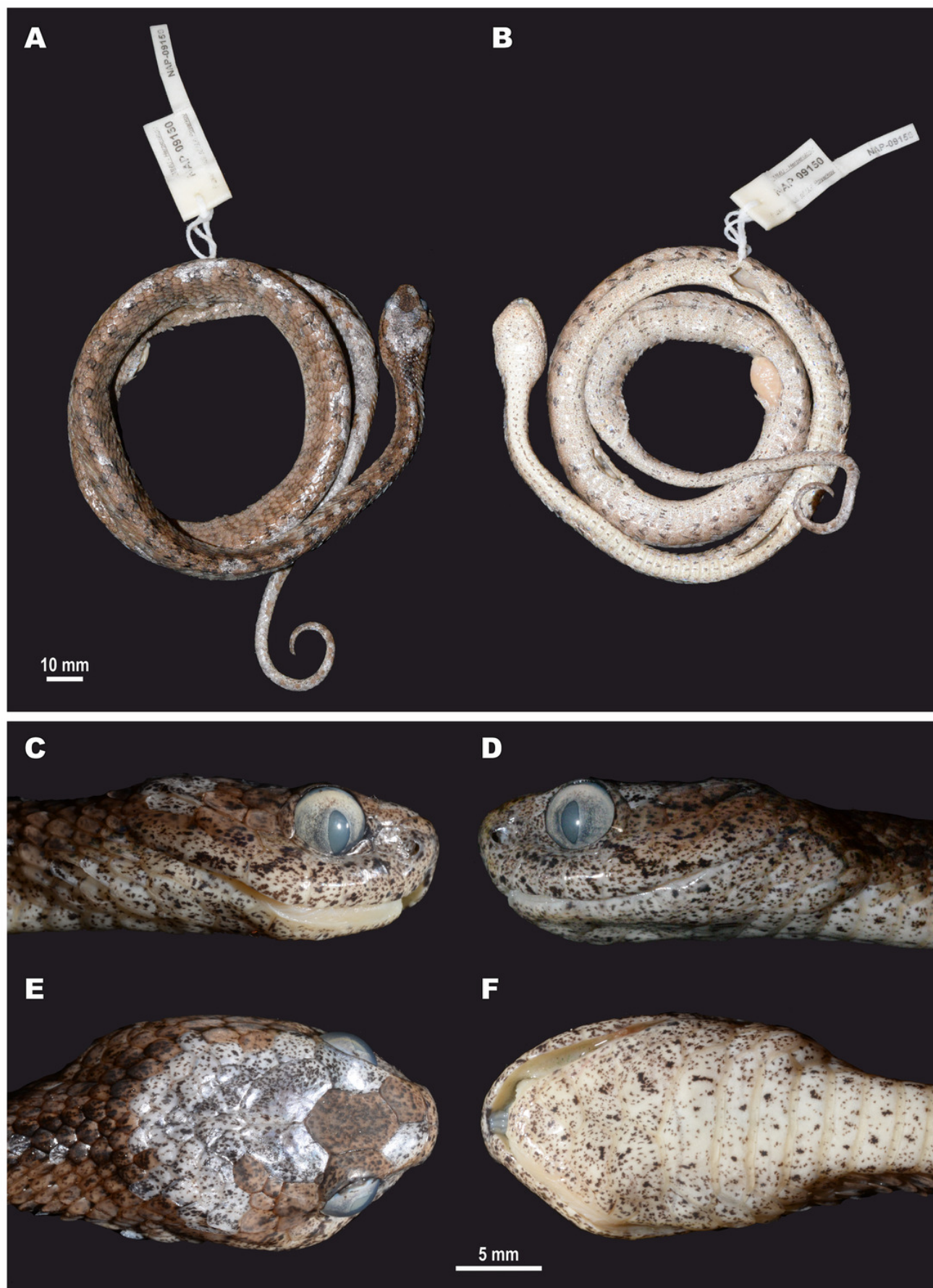
Figure 13

Figure 13. Members of the *Pareas berdmorei* complex in life.

A – *P. b. berdmorei* from Thung Yai Naresuan W.S., Kanchanaburi Province, Thailand; B – *P. b. berdmorei* from Huai Kha Khaeng W.S., Uthai Thani Province, Thailand; C – *P. b. berdmorei* from Phu Hin Rong Kla N.P., Phitsanulok Province, Thailand; D – *P. b. berdmorei* from Jiangcheng, Pu'er City, Yunnan Province, China (close to the type locality of *P. menglaensis*); E – *P. b. unicolor* from Cat Tien N.P., Dong Nai Province, Vietnam; F – *P. b. unicolor* from Loc Bac Forest, Lam Dong Province, Vietnam; G – *P. berdmorei* cf. *truongsonicus* **ssp. nov.** from Xe Pian N.P.A., Champasak Province, Laos; H – *P. berdmorei truongsonicus* **ssp. nov.** from Nahin District, Khammouan Province, Laos (ZMMU R-16801, holotype in life). Photos by P. Pawangkhanant (A–B, H), N.A. Poyarkov (C, E–F), and G. Vogel (D, G).

Figure 14

Figure 14. Holotype of *Pareas kuznetsovorum* sp. nov. in life (ZMMU R-16802, adult male).

A – dorsal view of body; B – ventral view of body; C–F – head in lateral right, lateral left, dorsal, and ventral aspects, respectively. Photos by N. A. Poyarkov.
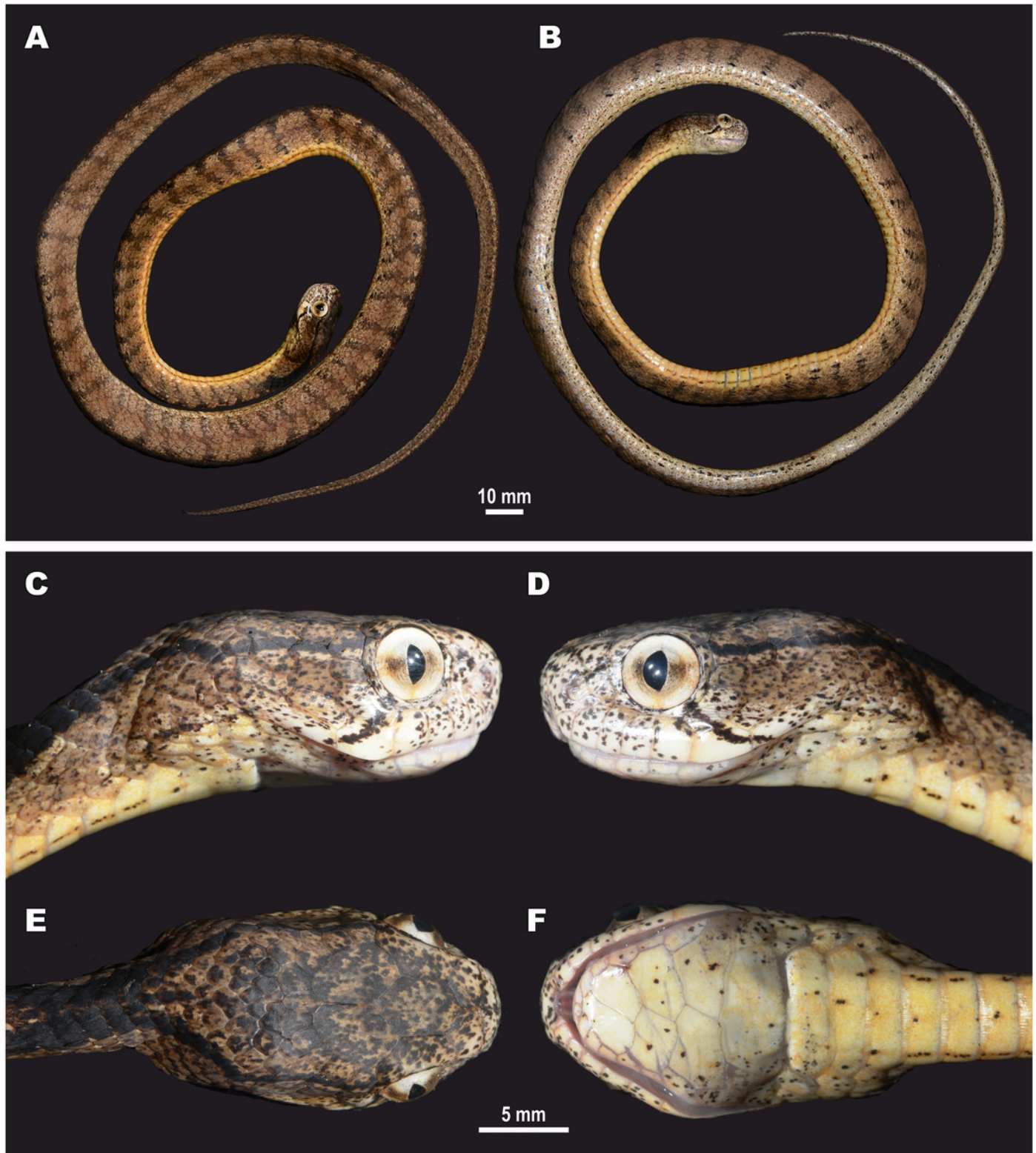
Figure 15

Figure 15. Holotype of *Pareas kuznetsovorum* sp. nov. in life (ZMMU R-16802, adult male) from Song Hinh, Phu Yen Province, Vietnam.

A – general view; B–C – sulcal and asulcal aspects of fully everted hemipenis; D – close-up of midbody showing smooth dorsal scales. Photos by N. A. Poyarkov.

Figure 16

Figure 16. Holotype of *Amblycephalus nuchalis* Boulenger, 1900 in preservative (NHMUK 1901.5.14.2, adult male).

A – dorsolateral view of body; B – ventrolateral view of body; C–F – head in lateral right,

lateral left, dorsal, and ventral aspects, respectively. Photos by G. Vogel.

Figure 17

Figure 17. *Pareas nuchalis* in life, adult male from Kota Kinabalu N.P., Kundasang, Sabah, Borneo, Malaysia.

Photo by L.A. Neimark.

Figure 18

Figure 18. Holotype of *Pareas abros* sp. nov. in life (ZMMU R-16393, adult male).

A – lateral left view of body; B – later right view of body; C–E – head in lateral right, ventral, and dorsal aspects, respectively; F – close-up of midbody showing keeled dorsal scales (in eleven rows, five to six of them seen on one side of the body). Photos by N. A. Poyarkov.
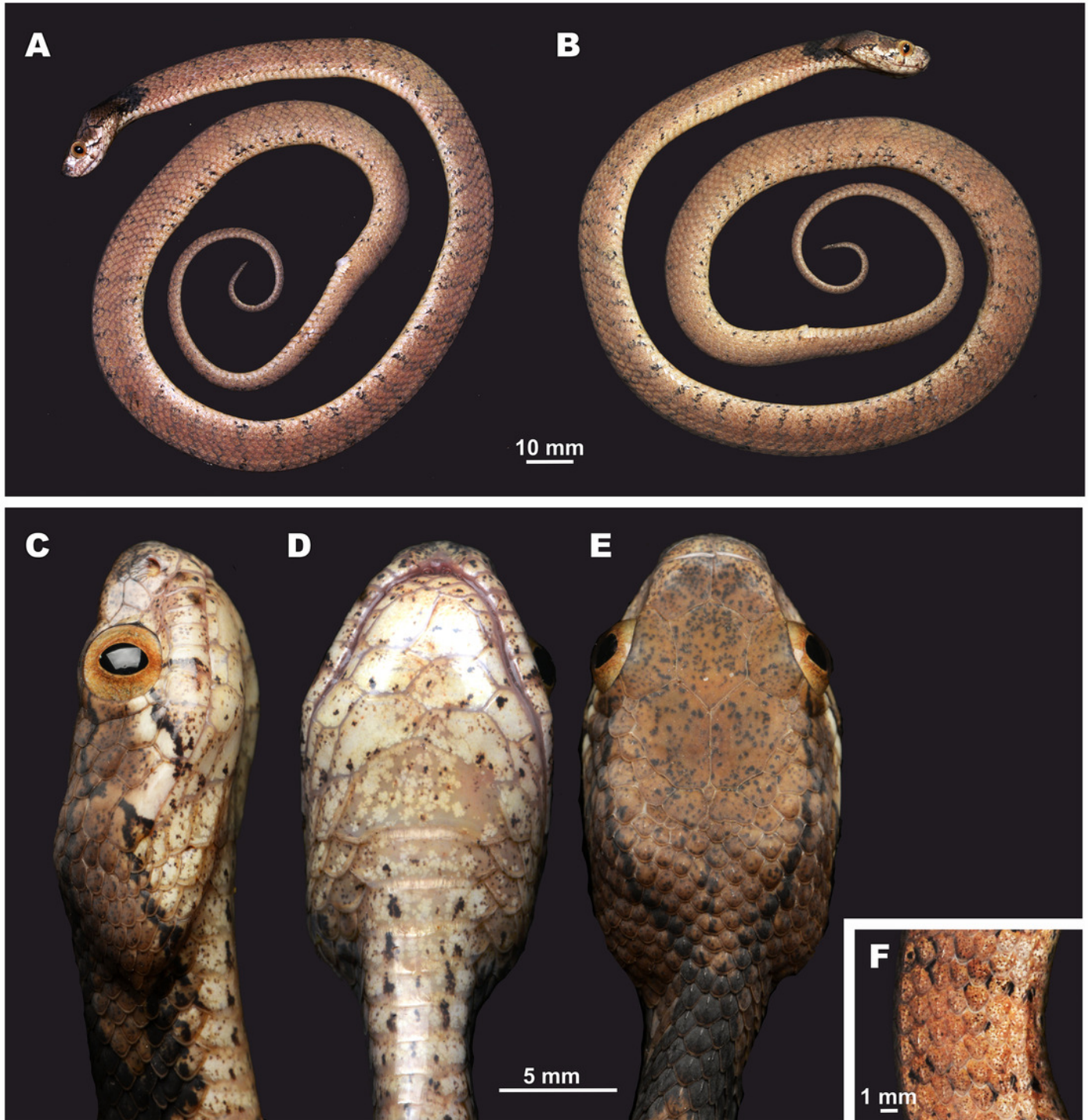
Figure 19

Figure 19. *Pareas abros* sp. nov. in life.

A – male holotype from Song Thanh N.P., Quang Nam Province, Vietnam (ZMMU R-16393); B – male paratype from A Roang, Sao La N.R., Thua Thien – Hue Province, Vietnam (ZMMU R-16392); C – female paratype from A Roang, Sao La N.R., Thua Thien – Hue Province, Vietnam (ZMMU R-14788); D – partially everted hemipenis of ZMMU R-16392 from asulcal (above) and sulcal (below) aspects; E – close-up of midbody of ZMMU R-16392 showing enlarged vertebrals and keeled dorsal scales (in eleven rows). Photos by N. A. Poyarkov.
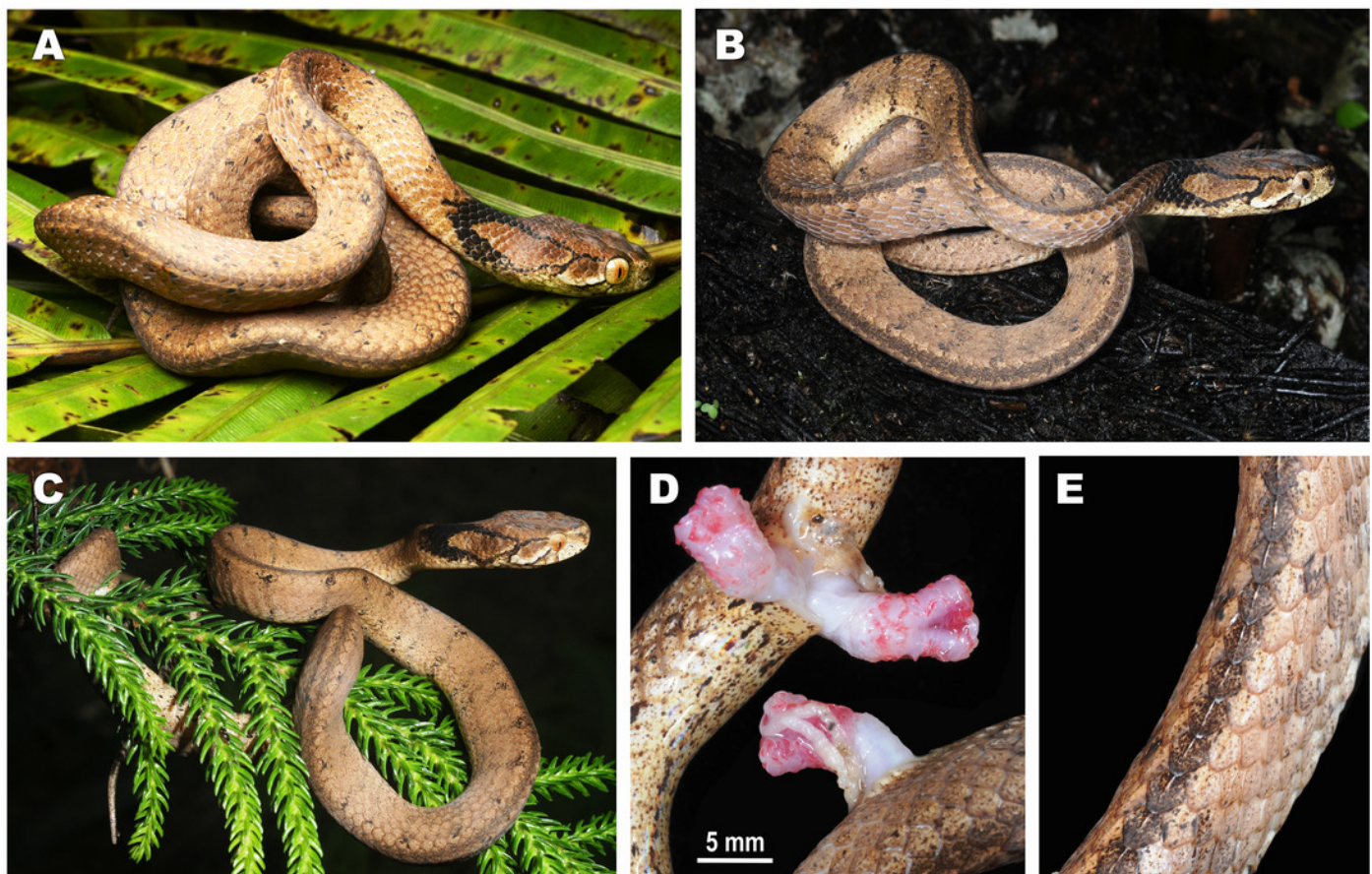
Figure 20

Figure 20. Specimen of *Pareas temporalis* Le, Tran, Hoang & Stuart, 2021 in preservative (ZMMU R-13656, adult male).

A – dorsal view of body; B – ventral view of body; C–E – head in lateral right, ventral, and dorsal aspects, respectively. Photos by G. Vogel.
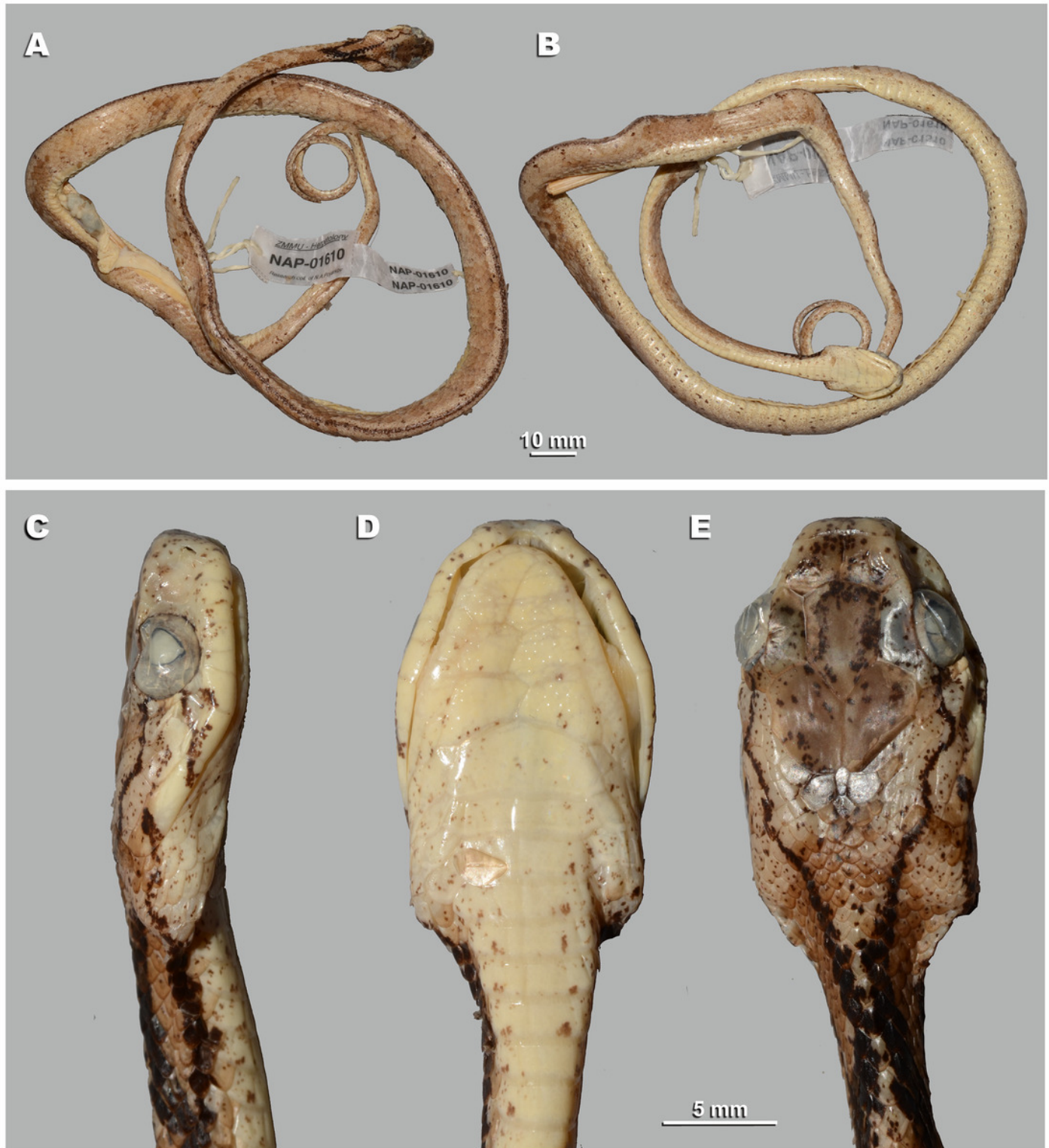
Figure 21

Figure 21. *Pareas temporalis* in life.

A – male specimen from Cat Loc, Lam Dong Province, Vietnam (ZMMU R-13656); B–C – female specimen from Di Linh, Lam Dong Province, Vietnam (SIEZC 20214); D – close-up of midbody of SIEZC 20214 showing all dorsal scales keeled (in 15 rows). Photos by N. A. Poyarkov (A), and L.H. Nguyen (B–D).